

Mechanisms of Glucocorticoids in the modulation of Graft-versus-Host Disease and the Graft-versus-Leukemia Reaction

Dissertation

for the award of the degree
“Doctor rerum naturalium”
of the Georg-August-Universität Göttingen

within the doctoral program GGNB (Göttingen Graduate School for Neurosciences,
Biophysics, and Molecular Biosciences), Molecular Medicine
of the Georg-August University School of Science (GAUSS)

submitted by

Hu Li

from Changzhi, Shanxi, China

Göttingen, May 2020

THESIS COMMITTEE

Prof. Dr. Holger Reichardt

(1st Referee)

Institute for Cellular and Molecular Immunology
University Medical Center, Göttingen

Prof. Dr. Lutz Walter

(2nd Referee)

Department of Primate Genetics
German Primate Center, Göttingen

Prof. Dr. Ralf Dressel

Institute for Cellular and Molecular Immunology
University Medical Center, Göttingen

ADDITIONAL MEMBERS OF THE EXAMINATION BOARD

Prof. Dr. Dieter Kube

Department of Haematology and Oncology
University Medical Center, Göttingen

Prof. Dr. Heidi Hahn

Department of Human Genetics, Section of Developmental Genetics
University Medical Center, Göttingen

Prof. Dr. Thomas Meyer

Department of Psychosomatic Medicine and Psychotherapy
University Medical Center, Göttingen

Date of thesis submission: 26th May, 2020

Date of the oral examination: 14th July, 2020

DECLARATION

I hereby declare that I have written this PhD thesis entitled “Mechanisms of Glucocorticoids in the modulation of Graft-versus-Host Disease and the Graft-versus-Leukemia Reaction” independently and with no other sources and aids than quoted. This thesis has not been submitted elsewhere for any academic degree.

Hu Li

26th May, 2020

Göttingen, Germany

Contents

Abstract..... 5

List of Figures..... 6

List of Tables 8

Abbreviations 9

1. Introduction..... 12

 1.1 Hematopoietic stem cell transplantation..... 12

 1.2 Graft-versus-Host Disease and Graft-versus-Tumor effects..... 13

 1.2.1 Graft-versus-Host Disease 13

 1.2.2 Graft-versus-Tumor Effects 15

 1.2.3 Pathogenesis of aGvHD..... 16

 1.2.4 Prevention and treatment to GvHD..... 19

 1.3 Glucocorticoids 21

 1.3.1 Overview of glucocorticoids..... 21

 1.3.2 Mechanisms of glucocorticoids 22

 1.3.3 Effects of glucocorticoids on immune cells..... 25

 1.3.4 Targeted delivery of glucocorticoids 27

 1.4 Objectives 29

2. Material and Methods 30

 2.1 Material 30

 2.1.1 Instruments..... 30

 2.1.2 Consumables 32

 2.1.3 Reagents and Chemicals 34

 2.1.4 Buffers..... 37

 2.1.5 Primers 38

2.1.6 Fluorochrome-conjugated monoclonal antibodies.....	44
2.1.7 Commercial kits and Enzymes.....	45
2.1.8 Software	46
2.2 Methods.....	47
2.2.1 Mice and housing conditions	47
2.2.2 The acute GvHD mouse model.....	48
2.2.3 Combined aGvHD/GvL mouse model.....	52
2.2.4 Phenotypic analysis of donor T cells	55
2.2.5 Fluidigm [®] gene chip analysis.....	56
2.2.6 Real-time quantitative PCR	60
2.2.7 Enzyme-linked Immunosorbent Assay	63
2.2.8 Histology and Immunohistochemistry.....	63
2.2.9 RNA sequencing analysis	64
2.2.10 Analysis of myeloid cell origin after HSCT in mice	65
2.2.11 Preparation of individual cell population from mice	66
2.2.12 ⁵¹ Chromium release assay.....	67
2.2.13 Statistical analysis.....	68
3. Results	69
3.1 Transplantation of GC-resistant allogeneic T cells as well as GC-resistant myeloid cells into recipients both aggravate aGvHD in mice	69
3.2 GC-resistance does not alter the phenotypes of the transferred allogeneic T cells	71
3.2.1 Lack of the GR in T cells has no impact on cell frequencies	71
3.2.2 GC-resistant T cells show a comparable activation level as GC-responsive T cells.....	72
3.2.3 GC-resistant and GC-responsive T cells show similar levels of adhesion molecules and chemokine receptors on the cell surface	73

3.3 Transplantation of allogeneic GC-resistant T cells results in increased systemic cytokine level and an up-regulation of disease-associated genes in aGvHD target organs.....	74
3.4 GC-resistance of allogeneic T cells but not myeloid cells alters the gene expression profile in the inflamed small intestine in mice undergoing aGvHD.....	77
3.5 Myeloid cells in the inflamed small intestine are partially reconstituted in recipient mice after aGvHD induction.....	82
3.6 Identification of novel candidate genes in murine aGvHD triggered by GC-resistant allogeneic T cells	84
3.7 Histological and immunohistochemical analyses indicate tissue damage and lymphocyte infiltration into the inflamed small intestine in aGvHD mice.....	87
3.8 Serum protein levels of key inflammatory cytokines are elevated during the course of aGvHD in mice transferred with GC-resistant allogeneic T cells	89
3.9 Expression analysis of the genes previously identified by RNA-sequencing.....	90
3.10 Expression analysis of the genes identified by RNA-seq reveals cell-type specificity	93
3.11 Administration of BMP-NPs alleviates aGvHD in mice with the beneficial GvL effect retained.....	95
3.12 Cytolytic ability of CD8 ⁺ T cells after short-term treatment with BMP-NPs.....	99
4. Discussion.....	101
4.1 GC-resistance of allogeneic donor T cells causes aggravated aGvHD in mice....	101
4.1.1 GC-resistant aGvHD in mice	101
4.1.2 Phenotype of mice transferred with GR ^{lck} or GR ^{flox} allogeneic T cells.....	102
4.1.3 Systemic levels of inflammatory cytokines during aGvHD in mice	103
4.1.4 Histological and immunohistochemical analyses of the small intestine of aGvHD mice	104

4.2 GC-resistance in allogeneic T cells alters the gene expression profile of mice suffering from aGvHD	105
4.2.1 Gene expression analysis of mice receiving GR ^{lck} T cells or harboring GR ^{lysM} myeloid cells	106
4.2.2 Expression analysis by RNA-sequencing	108
4.3 Glucocorticoids encapsulated in IOH-NPs sustains GvL activity	112
5. References	115
6. Appendix.....	131
6.1 Acknowledgements.....	131

Abstract

Acute graft-versus-host disease (aGvHD) is a severe complication that frequently occurs after allogeneic hematopoietic stem cell transplantation and results in a high transplant-related morbidity and mortality. Glucocorticoids (GCs) are widely used to treat aGvHD but some patients are refractory to this therapy. Importantly, the mechanisms of GC-resistance remain partially unclear. In our study, we used an aGvHD mouse model based on the transplantation of allogeneic GC-resistant donor T cells derived from cell type-specific GC receptor (GR) knock-out mice. We found that mice transferred with GC-resistant T cells developed a more severe aGvHD than those receiving GC-responsive T cells. We then analyzed the expression of 54 candidate genes in the first full-blown phase of the disease in the inflamed small intestine, an organ that is strongly affected by aGvHD, by using a high-throughput gene chip technology, and found that the majority of genes were significantly up-regulated in mice transplanted with GC-resistant T cells. In addition, we performed RNA-sequencing to identify further GC target genes in the small intestine, and confirmed differential expression of 26 of them by using high-throughput quantitative RT-PCR. Our findings revealed an altered gene expression profile caused by GC-resistance of transplanted allogeneic T cells in aGvHD, which might be helpful to derive biomarkers or develop new therapeutic concepts. Since GCs not only improve aGvHD but also compromise the beneficial graft-versus-lymphoma (GvL) reaction of the allogeneic donor T cells, we also explored whether a specific delivery of GCs may retain the GvL activity but still suppress aGvHD. In our study, we used a nanosized formulation of GCs (BMP-NPs), which are encapsulated in inorganic-organic hybrid nanoparticles that are preferentially taken up by macrophages, to treat mice in a combined aGvHD/GvL mouse model. By detecting the abundance of Bcl₁ lymphoma cells in the blood, we found that treatment with BMP-NPs delayed the development of an adoptively transferred lymphoma better than free GCs in our disease model, suggesting that BMP-NPs reduce aGvHD in mice and partially retain the GvL effect. Collectively, this work provides new insights into how treatment of aGvHD, in particular with GCs, could be improved in the future.

List of Figures

Figure 1. Pathophysiology of aGvHD	17
Figure 2. Location and genomic structure of the human GR.....	22
Figure 3. Mechanisms of GC action.....	24
Figure 4. Experimental schematic of acute GvHD induction in mice.....	49
Figure 5. Cell type-specific knock-out aGvHD mouse models	49
Figure 6. Gating strategy used for the quality control of T cell-depleted bone marrow cells (A) and purified T cells (B) by flow cytometry	51
Figure 7. Experimental schematic of the combined aGvHD/GvL mouse model	53
Figure 8. Scheme of the long-term treatment of the aGvHD/GvL mouse model.....	53
Figure 9. Gating strategy of the flow cytometric analysis of Bcl1 lymphoma cells in the blood	55
Figure 10. Clinical scores of mice suffering from aGvHD after HSCT.....	70
Figure 11. Percentages of CD4⁺, and CD8⁺ T cells as well as Treg cells amongst the GC-resistant and GC-responsive T cells used for transplantation.....	72
Figure 12. Activation state of GC-resistant and GC-responsive T cells	73
Figure 13. Expression levels of adhesion molecules and chemokine receptors on the surface of GC-resistant and GC-responsive T cells	74
Figure 14. Serum protein levels of IFN-γ and IL-6 in the blood of mice suffering from aGvHD.....	75
Figure 15. Gene expression of IFN-γ, Perf-1, GzmB, and IL-17 in spleen, liver and small intestine of mice suffering from aGvHD induced by transfer of GC-resistant T cells.....	76
Figure 16. Gating strategies used to determine the origin of splenocytes as well as myeloid cells in the small intestine of aGvHD mice	83
Figure 17. The origin of splenocytes as well as myeloid cells in the small intestine of aGvHD mice was determined by flow cytometric analysis.....	84
Figure 18. RNA-sequencing analysis of the inflamed small intestine in aGvHD mice transplanted with GC-resistant allogeneic T cells	86

Figure 19. Histological and immunohistochemical analyses of the small intestines in mice suffering from aGvHD 88

Figure 20. Serum protein levels of inflammatory cytokines during the course of aGvHD in mice 90

Figure 21. Cell-type specificity analysis of selected genes identified by RAN-seq. 94

Figure 22. Survival rate and lymphomagenesis of mice treated with different GC formulations 96

Figure 23. Frequency of Bcl₁ cells in the blood of individual mice in a combined aGvHD/GvL mouse model..... 98

Figure 24. Lytic ability of cytotoxic T lymphocytes (CTLs) against Bcl₁ target cells after short-term treatment of aGvHD with BMP-NPs or BMZ 100

List of Tables

Table 1. Instruments	30
Table 2. Consumables	32
Table 3. Reagents and chemicals.....	34
Table 4. Buffers.....	37
Table 5. Primers	38
Table 6. Antibodies.....	44
Table 7. Commercial kits and enzymes	45
Table 8. software.....	46
Table 9. Acute GvHD clinical score system.....	52
Table 10. Preamplification sample Pre-mix.....	57
Table 11. PCR reaction mix.....	62
Table 12. Expression analysis of cytokine and chemokine genes potentially important in the context of murine aGvHD.....	79
Table 13. Expression analysis of genes related to cell surface molecules and intracellular proteins in the context of murine aGvHD	81
Table 14. Expression analysis of genes involved in metabolic changes in the context of murine aGvHD	82
Table 15. Comparison of gene expression levels determined either by Fluidigm® gene chip analysis or RNA-sequencing.....	86
Table 16. Expression analysis of selected genes identified by RNA-seq during an early and late stage of the first phase of aGvHD in mice	92

Abbreviations

aGvHD	acute Graft-versus-Host Disease
APCs	Antigen-Presenting Cells
ATP	Adenosine Triphosphate
BM	Bone Marrow
BMP-NPs	Betamethasone Phosphate Nanoparticles
BMT	Bone Marrow Transplantation
BMZ	Betamethasone
BSA	Bovines Serumalbumin
CBG	Corticosteroid Binding Globulin
CCR	C-C chemokine Receptor
CD	Cluster of Differentiation
cGvHD	chronic Graft-versus-Host Disease
CTLs	Cytotoxic T Lymphocytes
CXCR	C-X-C Chemokine Receptor
DAMPs	Damage-associated Molecular Patterns
DBD	DNA-Binding Domain
DCs	Dendritic Cells
DNA	Deoxyribonucleic Acid
EDTA	Ethylenediaminetetraacetic Acid
ELISA	Enzyme-Linked ImmunoSorbent Assay
EP-NPs	Empty Nanoparticles
FACS	Fluorescence-Activated Cell Sorting

Abbreviations

FoxP3	Forkhead box P3
GCs	Glucocorticoids
GI	Gastrointestinal
GR	Glucocorticoid Receptor
GREs	GC Response Elements
GvHD	Graft-versus-Host Disease
GvL	Graft-versus-Lymphoma
GvT	Graft-versus-Tumor
H&E	Hematoxylin and Eosin
HIF	Hypoxia-Inducible Factor
HLA	Human Leukocyte Antigen
HPA	Hypothalamic-Pituitary-Adrenal
HSCT	Hematopoietic Stem Cell Transplantation
IECs	Intestinal Epithelial Cells
IFC	Integrated Fluidic Circuit
IFN	Interferon
Ig	Immunoglobulin
IL	Interleukine
ILCs	Innate Lymphoid Cells
IOH-NPs	Inorganic-Organic Hybrid Nanoparticles
ISCs	Intestinal Stem Cells
LBD	Ligand-Binding Domain
MHC	Major Histocompatibility Complex
MR	Mineralocorticoid Receptor

Abbreviations

NK	Natural Killer
PAMPs	Pathogen-associated Molecular Patterns
PB	Peripheral Blood
PBS	Phosphate-Buffered Saline
PCA	Principle Component Analysis
PCR	Polymerase Chain Reaction
RIC	Reduced Intensity Conditioning
RNA	Ribonucleic Acid
RNA-seq	RNA-sequencing
RT	Room Temperature
RT-qPCR	Real Time-quantitative PCR
STA	Specific Target Amplification
TBI	Total Body Irradiation
TCD	T-Cells-Depleted
TCR	T-Cell Receptor
TF	Transcription Factor
TGF	Transforming Growth Factor
Th	T helper
TNF	Tumor Necrosis Factor
UCB	Umbilical Cord Blood
UV	Ultraviolet

1. Introduction

1.1 Hematopoietic stem cell transplantation

Hematopoietic stem cell transplantation (HSCT) is one of the most effective therapeutic approaches to treat many blood-related malignancies (Appelbaum F.R., 2001; Copelan, 2006) and as well as to various non-hematological diseases, such as solid tumors (Ljungman et al., 2010) and severe autoimmune disorders (Sykes and Nikolic, 2005). In 1957, more than 60 years ago, Thomas and his co-workers attempted and successfully conducted the intravenous infusion of bone marrow from healthy donors to treat patients with aplastic anemia or hematologic neoplasia after irradiating them (Thomas et al., 1957). Due to his contributions to the clinical use of HSCT, Thomas was awarded the Nobel Prize in Medicine in 1990 (Boieri et al., 2016). Ever since then, HSCT has been widely used in clinical practice. Bone marrow is the richest source of hematopoietic stem cells. Others include peripheral blood (PB) and umbilical cord blood (UCB). HSCT of infused cells from peripheral blood was performed in dogs in 1979 (Korbling et al., 1979) and using UCB as the cellular source in HSCT was first reported in 1995 (Wagner et al., 1995). HSCT can be subdivided into three groups based on the origin of the transplanted cells: 1) *allogeneic HSCT*, transplanted cells are from an unrelated donor, optimally a fully HLA-matched individual; 2) *syngeneic HSCT*, transplanted cells are from a monozygotic twin; and 3) *autologous HSCT*, transplanted cells are obtained from the patients themselves (Saccardi and Gualandi, 2008). Based on data from the *Center for International Blood & Marrow Transplant Research (CIBMTR)*, over 23,000 patients in the US underwent an HSCT in 2018 (8,500 receiving an allogeneic HSCT and 14,500 receiving an autologous HSCT) (D'Souza and Fretham, 2018). Before being treated with a hematopoietic stem cell infusion, patients with a lymphoma or leukemia are commonly given conditioning regimens which aim to decrease tumor burden and to eradicate the host immune system to prevent graft rejection (Gyurkocza and Sandmaier, 2014). High-dose myeloablative condition regimens are administered to patients with hematologic malignancies, such as a high-dose total body irradiation (TBI) or high-dose chemotherapy. Treatment with a TBI is often combined with the administration of immuno-suppressive agents, normally cyclophosphamide, and commonly fractionated. Even though high-dose

conditioning regimens reduce the relapse rate of the patients, they also cause some gastrointestinal, pulmonary and hepatic toxicity and a loss of the patients' hematopoietic system, and are not appropriate to treat elder patients (Jenq and van den Brink, 2010). Therefore, non-myeloablative conditioning or reduced intensity conditioning (RIC) regimens have been developed. Many clinical studies have indicated that the rates of relapse are less in patients undergoing an allogeneic HSCT (allo-HSCT) than those ones transplanted with syngeneic or autologous grafts (Weiden et al., 1979). In the setting of allo-HSCT, it has been shown that allogeneic grafts are capable of eradicating malignant cells of the patients through its graft-versus-tumor (GvT) effect. This discovery has led to the development of non-myeloablative conditioning regimens that are accessible for elder patients who fail not tolerate high-dose TBI or other myeloablative regimens (Gyurkocza and Sandmaier, 2014; Singh and McGuirk, 2016). Diverse non-myeloablative regimens have been developed by many research centers: Fred Hutchinson Cancer Research Center performs a low dose, 2 Gy TBI-based regimen (McSweeney et al., 2001), and the MD Anderson Cancer Center developed a regimen of peritransplant rituximab combined with fludarabine (90 mg/m²) and cyclophosphamide (2250 mg/m²) to treat patients with a relapsed follicular lymphoma (Khouri et al., 2008).

1.2 Graft-versus-Host Disease and Graft-versus-Tumor effects

1.2.1 Graft-versus-Host Disease

Allogeneic HSCT is an effective treatment for the majority of patients suffering from hematological malignancies and is considered to be the only curative approach to treat the patients with aggressive T-cell lymphoma/leukemia (ATL) (Utsunomiya, 2019). However, it is accompanied by the risk of developing Graft-versus-Host Disease (GvHD), which is responsible for the high transplant-related morbidity and mortality of these patients (Holtan et al., 2014). According to the report from CIBMTR, GvHD accounts for 11% and 12% of deaths, respectively, that occurred within 100 days or beyond 100 days after allogeneic HSCT in 2015-2016 (Souza A et al., 2018). The human leukocyte antigen (HLA) system, also known as the major histocompatibility complex (MHC), plays a

crucial role in the development of GvHD. There are more than 200 genes located in this region on human chromosome 6 that span more than 4 megabases. However, in the context of allo-HSCT, the three genes HLA-A, HLA-B, and HLA-C play the most important role, forming the HLA barrier to successful HSCT. It is well-known that acute GvHD is mainly driven by donor T cells contained in the graft (Perkey and Maillard, 2018). Namely, CD4⁺ T cells recognize antigens presented by HLA class II molecules and antigens presented by HLA class I molecules are preferentially recognized by CD8⁺ T cells. Donor T cells recognize host cells as foreigners and attack them, leading to tissue damage which is one of the main features of GvHD. T cell-depleted (TCD) grafts have been infused into the host to avoid the development of GvHD (Collins and Fernández, 1994). Although many clinical studies showed that TCD grafts significantly reduced the occurrence and severity of GvHD, it is associated with severe life-threatening infections and increased tumor relapse rates. Besides, the fatal infections are caused by the lack of T cell-mediated immunity against viral antigens, whereas, the high rates of relapse strengthen the importance of donor T cells in eliminating malignant tumor cells after conditioning.

GvHD comes in two distinct forms: acute GvHD (aGvHD) and chronic GvHD (cGvHD). Historically, aGvHD was defined as clinical symptoms arising within 100 days after HSCT, whereas a disease developing later was referred to as cGvHD. More recently, it was noted that both forms differ in pathogenesis, clinical manifestations and organ involvement, criteria henceforth forming the basis for the classification of both types of GvHD (Boieri et al., 2016). Development of aGvHD is responsible for up to 15% deaths of the patients and more than 50% of allo-HSCT patients develop aGvHD. The organs affected by aGvHD include the skin (81% of patients with aGvHD), liver (50%) and gastrointestinal tract (54%) (Martin et al., 1991). Based on the severity of the damage caused to the involved target organs (skin, liver, and gastrointestinal tract) and clinical performance, aGvHD has been divided into four grades (grade I - IV) based on the criteria established by Glucksberg and the *International Bone Marrow Transplant Registry Systems* (Glucksberg et al., 1974; Rowlings et al., 1997). Grade I aGvHD is mild, grade II moderate, grade III severe and grade IV very severe. Of the patients

undergoing HSCT, 30 - 50% develop aGvHD of grade I/II, and approximately 14% have severe aGvHD of grade III/ IV (Zeiser and Blazar, 2017).

1.2.2 Graft-versus-Tumor Effects

Allogeneic donor T cells are thought to be the main cause of aGvHD after allogeneic HSCT. On the other hand, they contribute to a beneficial impact on eradicating malignant cells in the recipients referred to as Graft versus Tumor effects (GvT) or Graft-versus-Lymphoma (GvL) effect (Negrin, 2015). The GvT effect was first discovered by *Barnes et al.* performing allogeneic HSCT in murine studies in 1956. It showed that the leukemia was eliminated in mice receiving allogeneic HSCT compared to those receiving syngeneic HSCT, and mice transplanted with allogeneic cells developed some syndrome of diarrhea which has been recognized as one of the manifestations of GvHD today (Barnes et al., 1956). Subsequent studies indicated that the disease relapse rate was lower in patients suffering from aGvHD or cGvHD, and that the GvT effect existed in the patients undergoing allo-HSCT without the incidence of GvHD, suggesting that GvHD and GvT effect can occur independently (Ringden et al., 2000). Besides, relapsed leukemia after transplantation was successfully treated by a donor lymphocyte infusion (Kolb et al., 1990). Due to the fact that the GvT effect appears to be closely associated with GvHD, many studies have focused on separating the beneficial GvT effect from GvHD, to prevent and control GvHD with the GvT effects being preserved (Kolb, 2008; Rezvani and Storb, 2008).

The GvT effect is mainly mediated by cytotoxic T lymphocytes (CTLs). In the context of HSCT, two cytolytic pathways, the Fas-FasL and the perforin-granzyme pathway, are thought to be highly relevant for the modulation of GvHD and the GvT effect (Van den Brink and Burakoff, 2002). The Fas-FasL pathway seems to be limited to lymphoid malignancies compared to the perforin-granzyme pathway in cancer surveillance. In addition to effector CD8⁺ T cells, natural killer (NK) cells also play important roles in GvT effects, particularly in the absence of a T-cell mediated setting. Thus, it has been proposed as an effective way to augment the ability of NK cells to kill malignant cells

while suppressing GvHD (Rezvani and Storb, 2008). Besides NK cells, the infusion of regulatory T cells co-cultured with PDL-1 has been found to possess anti-tumor effects while suppressing GvHD in an allogeneic HSCT murine model (Stathopoulou et al., 2018).

In conclusion, successful HSCT has three consequences: the first one is that the host may attack the transplanted cells and induce graft rejection, which is prevented by the conditioning regimen; second, the infused cells recognize host cells and tissues as foreign, leading to severe or fatal GvHD, and this reaction needs to be controlled; third, the GvT effect is closely associated with GvHD; this beneficial effect should be exploited and effective approaches are required for the separation of the GvT effect from GvHD.

1.2.3 Pathogenesis of aGvHD

The occurrence and development of aGvHD is complicated. Many cell types including diverse immune cells and even some non-hematopoietic cells are involved (Perkey and Maillard, 2018). Various cytokines and chemokines also play a crucial role in the pathogenesis of aGvHD (Zeiser et al., 2016). More and more studies have revealed the important interactions of commensal microbiota and metabolites in the gastrointestinal tract with the severity of GvHD, recently (Koyama et al., 2019; Stein-Thoeringer et al., 2019; Swimm et al., 2018).

Based on the substantial knowledge derived from animal models and clinical studies, the pathogenesis of aGvHD consists of several stages (**Figure 1**).

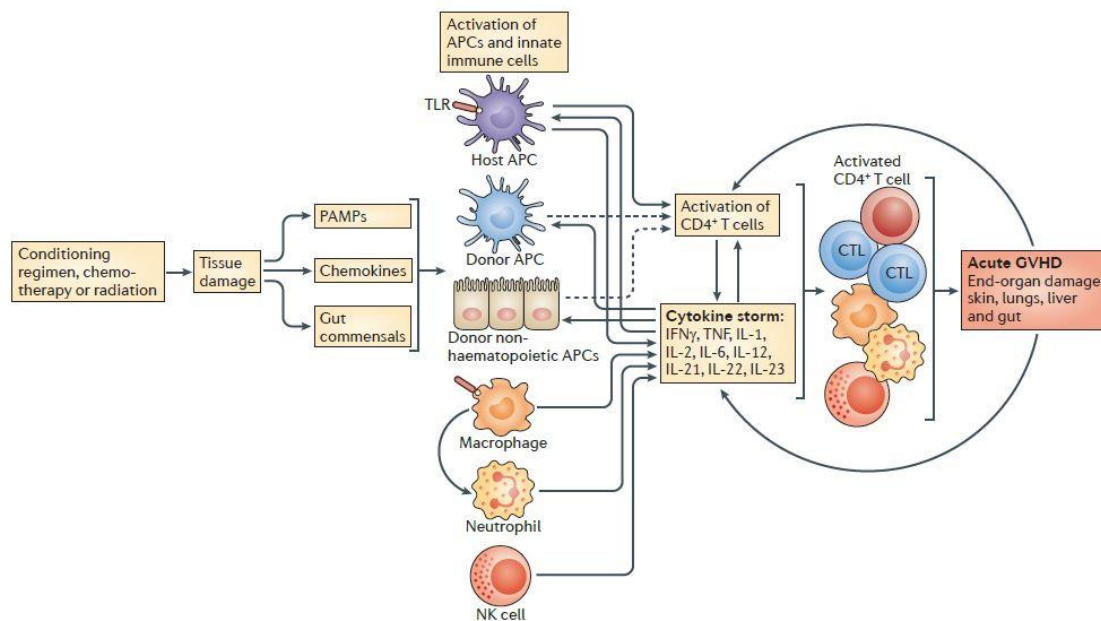


Figure 1. Pathophysiology of aGvHD. The initiation and development of aGvHD have been divided into four phases. In the first phase, tissue damage is triggered by the conditioning regimen, leading to the release of pro-inflammatory cytokines stimulated by PAMPs and interaction with the gut microbiome. In the next phase, donor T cells become activated with the help of host APCs, donor APCs and non-hematopoietic cells, accompanied by the production of cytokines (cytokine storm), forming a positive feedback loop. In the third phase, activated allo-T cells migrate from the secondary lymphoid organs to the target organs. In the end, the effector cells infiltrate the target organs, resulting in end-organ damage, which is the damage to skin, liver and gastrointestinal tract, developing into severe GvHD. The figure is adapted from Blazar et al. (2012).

Patients suffering from hematological malignancies receive conditioning regimens, such as TBI, that trigger the release of pro-inflammatory cytokines, IL-1 β , IL-6 and TNF- α . Some studies have demonstrated that the production of these cytokines remains increased for at least three months after TBI (Dorshkind et al., 2019). High-dose TBI leads to the release of microbial products in gastrointestinal tract, such as lipopolysaccharide (LPS), which stimulates the cytokine cascade through innate immune pathways (Hill et al., 1997). These products derived from the microbiome and intestinal injury are damage-associated molecular patterns (DAMPs) and pathogen-associated molecular patterns (PAMPs) that are recognized by receptors of the innate immune system, resulting in the establishment of a pro-inflammatory microenvironment after the conditioning regimen (Perkey and Maillard, 2018). It has been shown that conditioning intensity impacts the severity and incidence of aGvHD. The increased TBI strength in HSCT gives rise to the

translocation of LPS into the systemic circulation and increased production of TNF- α (Hill et al., 1997). In an aGvHD mouse model, the loss of intestinal stem cells (ISCs) was found in the initial phase of aGvHD, suggesting that conditioning and alloimmunity can target ISCs. During this process, the cytokine IL-22 that is mainly secreted by the innate lymphoid cells (ILCs) is critical to reconstitute the intestinal stem cell niche and contributes to the integrity of the epithelial barrier (Hanash et al., 2012; Lindemans et al., 2015). The conditioning regimens cause neutropenia, and those patients who developed neutropenic fever showed a reduced mortality, and therefore, had to be treated with broad-spectrum antibiotics against Gram-negative bacteria (Hiemenz, 2009). The successful gut decontamination with the antibiotics then reduced the severity of GvHD in both mouse models (Vaishnava et al., 2011) and some clinical studies (Storb et al., 1983). However, it has also suggested that broad-spectrum antibiotics disrupt the homeostasis of the intestinal microbiota and reduce microbiota diversity, resulting in an increased GvHD severity. Thus, it is required to select more specific antibiotics to prevent damage caused by microbiota and to reduce GvHD (Shono et al., 2016).

In the second phase of GvHD, donor T cells are activated by antigen-presenting cells (APCs) and undergo expansion. The conventional dendritic cells (cDCs) are considered to be sufficient to prime donor T cells, and GvHD seemed to be driven by recipient APCs in a CD8⁺ T cell-mediated mouse model (Shlomchik, 1999). It has been demonstrated that donor APCs can amplify the disease later, and moreover, that GvHD can be induced by non-hematopoietic recipient APCs (Koyama et al., 2012). Namely, the expression of MHC class II molecules on epithelial cells was up-regulated in the gastrointestinal tract in an inflammatory microenvironment, especially created by the early phase of GvHD (Koyama et al., 2019). The sites of where allo-T cells get primed remain debatable. The naïve cells classically traffic to the secondary lymphoid organs, such as spleen and lymph nodes, and become activated by diverse APCs. In addition, fibroblasts have been also considered to be capable of driving GvHD in the context of HSCT (Perkey and Maillard, 2018). Differentiation and expansion of allo-T cells require co-stimulatory signaling, such as the crosstalk between CD28 expressed on T cells and CD80 or CD86 expressed on APCs. The upregulation of other co-stimulatory molecules has also been observed in

GvHD, such as Inducible T-cell Costimulator (ICOS) or, 4-1BB (Zeiser et al., 2016). T cells can differentiate into several subsets, such as Th1, Th2, and Th17 cells, that produce lots of cytokines. These cell types and cytokines have been suggested to impact the pathogenesis of GvHD but their contributions are still under investigation (Yi et al., 2009).

The next phase is characterized by the migration of the alloreactive T cells to the target organs, which is mediated by chemokines, chemokine receptors, and integrins. It has been shown that CCR5 is involved in this process and described to recruit effector T cells (Palmer et al., 2010). CCR9 expressed by alloreactive T cells facilitates the T cell recruitment to gut and skin. CCR4 and CCR10 are critical for skin homing, and CXCR3 helps to attract Th1 cells to the sites of cellular injury (Blazar et al., 2012). In addition, L-selectin (CD62L) interacting with integrin $\alpha 4\beta 7$ regulates the homing of T cells to mesenteric lymph nodes and Peyer patches in the context of gut GvHD manifestation (Dutt et al., 2005).

The last stage of GvHD involves tissue damage caused by the alloreactive T cells through cytolytic pathways and further recruitment of other leukocytes. The cytotoxic activity is mainly mediated by two cytolytic pathways: Fas-FasL and perforin-granzyme (Braun, 1996). MHC class I dependent aGvHD is mostly mediated by the perforin-granzyme pathway, while the MHC class II dependent aGvHD is mediated by the Fas-FasL pathway (Graubert et al., 1997).

1.2.4 Prevention and treatment to GvHD

GvHD is the leading cause of transplant-related mortality. Up to 50% of the patients undergoing allo-HSCT are clinically affected by aGvHD (Zeiser and Blazar, 2017). The clinical organ involvement of aGvHD includes skin, liver and gastrointestinal tract (GI). Skin GvHD can be controlled without using systemic immunosuppression and liver GvHD is less relevant. GI manifestation of GvHD, however, is the main contributor to morbidity and mortality in the clinic (Hill and Ferrara, 2000). Treatment with high-dose

systemic glucocorticoids (GCs) is the first-line therapy for grade II-IV aGvHD, though the main mechanisms are still partially unclear (Sung and Chao, 2013). The aGvHD patients are given an initial dose of methylprednisolone or prednisolone at 1-2 mg/kg per day and the dose is increased if there is no significant response to the primary treatment. Despite their wide use, there are many patients who do not respond to systemic GCs in the treatment of aGvHD, which is defined as corticosteroid-refractory or steroid-resistant aGvHD (Garnett et al., 2013). It is noteworthy that patients with steroid-resistant aGvHD only have an overall survival rate of 5 to 30% (Zeiser and Blazar, 2017).

Given the critical role of donor T cells in the pathogenesis of aGvHD, many drugs have been developed that suppress T cell functions such as cytokines and proliferation, and are widely used in clinical setting (Singh and McGuirk, 2016). These include, the calcineurin inhibitors cyclosporine, FK-506 for suppression of IL-2 secretion and methotrexate for suppression of cell proliferation. Another approach is to deplete T cells contained in the graft before transplantation, although this approach compromises GvT effect. To this end, CD34⁺ positive selection *ex vivo* is carried out to discard T cells. To decrease the relapse rate after T cell-depletion, the administration of IL-2 has been performed to boost the function of NK cells (Ho and Soiffer, 2001). Selectively depleting T cells, such as CD8⁺ T cell depletion followed by cyclosporine treatment, has been shown to reduce the occurrence and severity of GvHD while preserving the GvT effect (Champlin et al., 1990). Recently, more and more studies have focused on gut microbiota, and approaches to maintain the homeostasis of the intestinal microbiota appear to be a promising approach to prevent GI GvHD (Shono and van den Brink, 2018), such as probiotic strategies, or restoring the diversity of gut microbiota by fecal matter transplantation (FMT).

1.3 Glucocorticoids

1.3.1 Overview of glucocorticoids

Glucocorticoids (GCs) are a group of steroid hormones with a broad capacity to exert anti-inflammatory effect which has been widely used to treat many autoimmune, inflammatory and allergic diseases, such as rheumatoid arthritis, asthma, and ulcerative colitis (Rhen and Cidlowski, 2005). In contrast, long-term treatment with GCs results in adverse effects, such as hypertension, immunosuppression, increased risk of infections, osteoporosis, depression and impaired wound healing (Cain and Cidlowski, 2017). The discovery of GCs, initially named ‘Compound E’, won Philip S. Hench, Edward Kendall, and Tadeus Reichstein the Noble Prize in Physiology or Medicine in 1950. Endogenous GCs are generated from cholesterol in the mitochondria within the adrenal cortex through a biological process termed as steroidogenesis. The production of GCs is induced by the hypothalamic-pituitary-adrenal axis (HPA axis) upon external stimulation and GCs can suppress the HPA axis reversely, forming a negative feedback loop to regulate the GCs’ production. Stimuli of the HPA axis include mood change, circadian rhythm, pain receptor signaling and pro-inflammatory cytokines, such as IL-1, TNF- α , and IL-6. GCs exert potent anti-inflammatory effects and reduce the production of these cytokines, forming a second negative feedback loop (Dunn, 2000; Rhen and Cidlowski, 2005).

The bio-availability of GCs is controlled by corticosteroid binding globulin (CBG). Once being synthesized in the adrenal cortex, GCs enter the circulation system and bind to CBG in the blood, leaving only 5% of GCs in the free bioactive form (Breuner and Orchinik, 2002). GCs diffuse into cytosol and their biological activation conditions are regulated by two complementary enzymes. Within cells, 11 β -hydroxysteroid dehydrogenase type 1 (11 β HSD1) converts GCs into their active form, e.g. cortisone to cortisol, and type 2 11 β -hydroxysteroid dehydrogenase (11 β HSD2) conversely inactivates GCs by catalyzing the opposite reaction (Yang and Zhang, 2004). Many synthetic GC derivatives have been developed and are widely used in clinic, such as prednisone, beclomethasone, and fluticasone. Compared to endogenous GCs, synthetic drugs are more potent because their activity is, for instance, not affected or inhibited by

CBG binding or the conversion mediated by the two 11β -hydroxysteroid dehydrogenases.

1.3.2 Mechanisms of glucocorticoids

GCs passively diffuse through cell membranes and regulate gene expressions after binding to the GC receptor (GR). The GR exists in almost all nucleated cells. Based on some studies, GCs can regulate more than 20% of the genome (Galon et al., 2002). In humans, the GR is encoded by the gene *NR3C1* (Nuclear receptor subfamily 3, Group C, member 1) (**Figure 2**).

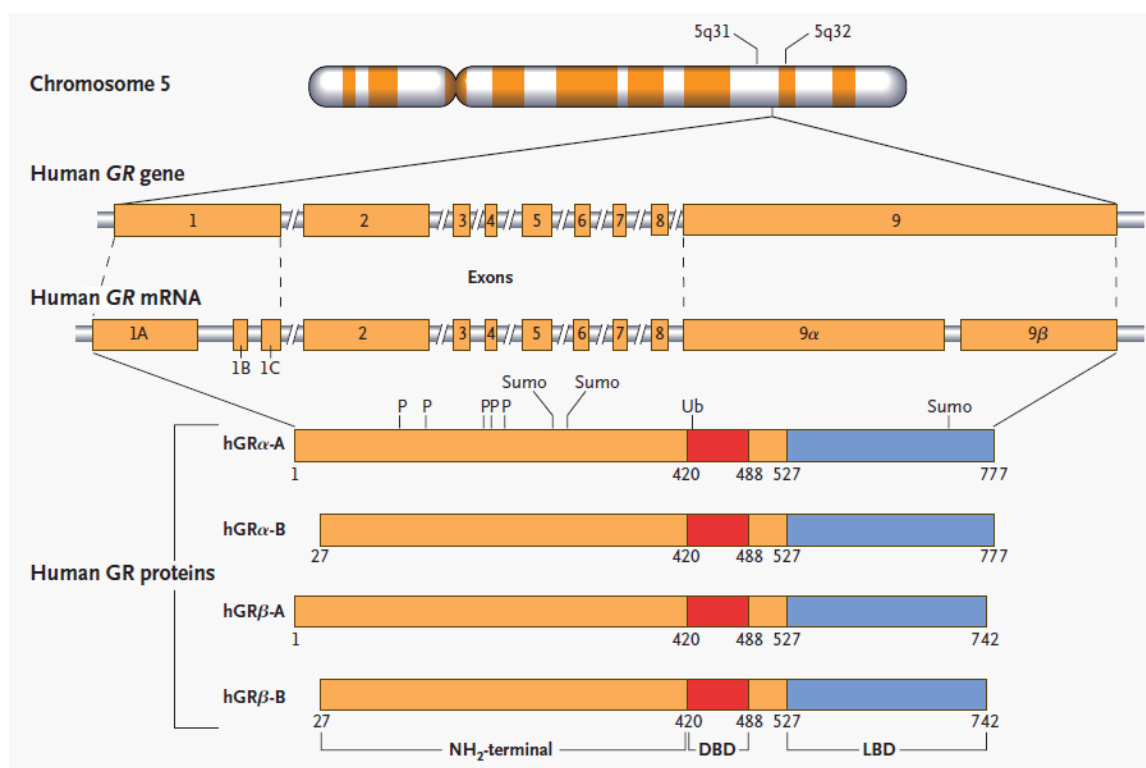


Figure 2. Location and genomic structure of the human GR. The GR consists of nine exons and is located on chromosome 5. The GR has three transcription initiation sites. Alternative splicing at exon 9 α or 9 β produces two isoforms of GR (GR α and GR β). The DBD represents the DNA-binding domain and the LBD represents the ligand-binding domain. The figure is adapted from Rhen and Cidlowski, 2005.

The GR protein is composed of three functional domains: N-terminal domain, DNA-binding domain (DBD), and ligand-binding domain (LBD). Nuclear translocation of the GR depends on a flexible hinge region locating between DBD and LBD (Reichardt et al.,

1998). There are two zinc fingers located at in the DBD, and especially the second zinc finger is important for GR dimerization (Vandevyver et al., 2013). Alternative splicing of exon 9 results in the generation of the two isoforms: GR α and GR β . The GR α variant binds to GCs and specific DNA regions and regulates the expression of target genes, which is the classic subtype. In contrast, GR β exerts negative effects on GR α and does not bind to ligand, thus failing to activate transcription (Rhen and Cidlowski, 2005). It has also been shown that a high level of GR β is associated with GC resistance (Webster et al., 2001). In the cytoplasm, the GR resides in an inactive state without binding to its ligands. The GR remains stable as a multiprotein complex by binding to other proteins, such as heat shock proteins, immunophilins, and other chaperones to prevent degradation (Cain and Cidlowski, 2017; Vandevyver et al., 2013). Besides GR, GCs can also bind to another receptor, the mineralocorticoid receptor (MR, encoded by the *NR3C2* gene), with higher affinity. The expression of the MR is more restricted than that of GR, being expressed only in certain cell types; high expression of MR is observed in the heart, colon, and hippocampus but low expression in leukocytes (Cain and Cidlowski, 2017).

GCs act via two distinct mechanisms: genomic effects and non-genomic effects. The genomic effects of GCs are three-fold: 1) direct binding to target genes, 2) indirect interaction with other transcription factors, and 3) binding to composite response elements (Ramamoorthy and Cidlowski, 2016) (**Figure 3**).

In addition to the regulation of gene expression as homodimers, the GR can function as a monomeric protein by cooperating with other transcription factors, so-called “tethering” mechanisms, without contacting with DNA (Ratman et al., 2013). It is noteworthy that many key transcription factors related to the mediation of inflammation are modulated by the GR based on its “tethering” mechanism, including nuclear factor- κ B (NF- κ B) (Reichardt, 2001), activator protein 1 (AP-1) (Tuckermann et al., 1999), and various members of the signal transducer and activator of transcription (STAT) (Cain and Cidlowski, 2017), leading to transcriptional repression. Another indirect mechanism of the GR is based on “composite” response elements. In this way, the GR binds to DNA elements that contain both a GRE and the response elements of other transcription factors (Diamond et al., 1990).

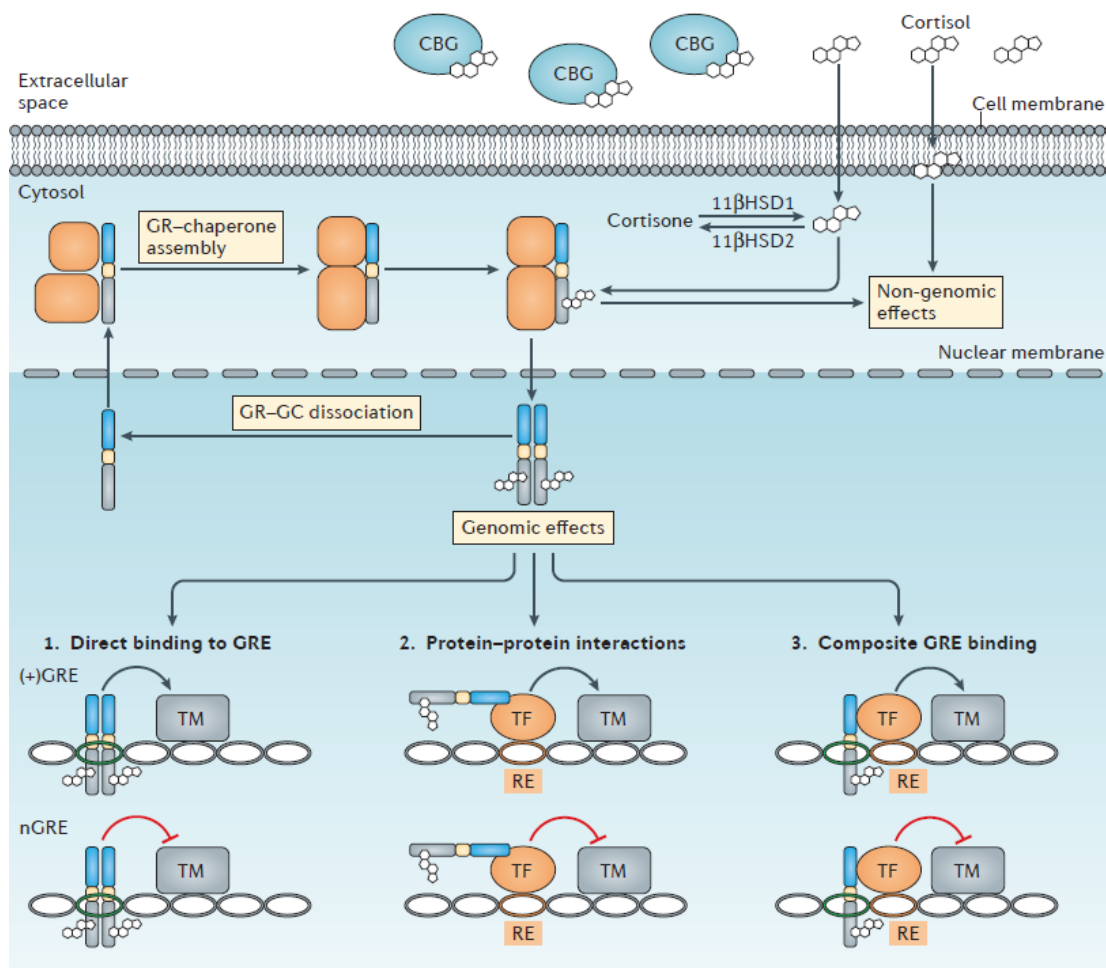


Figure 3. Mechanisms of GC action. GCs can diffuse through cell membranes and bind to the GR located in the cytosol. Upon binding to GCs, the GR translocates into the nucleus and exerts its functions to alter the expression of target genes (activation or suppression) by directly binding to GC response elements (GREs, or negative GREs), by indirectly binding to other transcription factors (TF) through protein-protein interactions, or in a composite fashion. The figure is adapted from Cain and Cidlowski, 2017.

The GR exerts its regulatory functions through non-genomic mechanisms as well, by interacting with cytoplasmic signaling complexes (Revankar, 2005) or unspecific interactions with lipid membranes. GCs achieve their actions mainly through the genomic mechanisms in the context of some inflammatory or autoimmune disorders (Wüst et al., 2008). However, it has also been shown that the ligand-bound GR has an impact on the MAPK pathway and induces apoptosis in mitochondria (Boldizsar et al., 2010; Sionov et al., 2006).

1.3.3 Effects of glucocorticoids on immune cells

Inflammation and diverse immune reactions are mediated by various types of leukocytes. GCs exert their broad anti-inflammatory effects by regulating all the immune cells and by impacting the different phases of inflammation, including the initial alarm phase, the mobilization phase, and the resolution phase (Cain and Cidlowski, 2017).

Dendritic cells (DCs) are considered to be the most proficient APC during infection and inflammation. DCs present peptide antigens to CD4⁺ T cells and CD8⁺ T cells via MHC II and MHC I molecules and activate the adaptive immune system. In general, GCs inhibit the maturation of diverse subtypes of DCs, including migratory DCs, tissue-resident DCs, and plasmacytoid DCs; GCs induce DC apoptosis but they do not affect apoptosis in monocytes (Moser et al., 1995). It has been noted that GCs increase the uptake of antigens by DCs, whereas, they suppress the function of DCs as antigen presenting cell. Moreover, it seems that GCs induce the differentiation of DCs towards the so-called “tolerogenic” type (Chamorro et al., 2009). These tolerogenic DCs inhibit autoimmune diseases and the graft-versus-host response by inducing T-cell anergy, suppressing T cells and promoting the differentiation of regulatory T cells (Rutella et al., 2006).

Macrophages are derived from monocytes and play a critical role in innate immunity. They are characterized by their ability to produce various pro-inflammatory cytokines, which makes macrophages an efficient target of GCs. Based on the studies in GR gene modified mouse models, it has been demonstrated that the majority of cytokines can be suppressed by GCs by dimerization-independent and indirect tethering mechanisms (Reichardt, 2001; Tuckermann et al., 2007). Besides the suppressive effects of GCs on macrophages, GCs can induce the generation of alternatively activated macrophages (M2 subtype). M2 macrophages share the feature of high expression of CD163, CD206, and tyrosine-protein kinase MER, and the production of anti-inflammatory cytokines, such as IL-10 and TGFβ (Martinez, 2008). In the presence of GCs, the gene profile of macrophages alters, facilitating to upregulation of these anti-inflammatory genes and downregulation of CX3CR1, which is the marker of inflammatory monocytes (Varga et

al., 2008).

T cells play a central role in cellular immunity. T cells are generated in the bone marrow and mature in the thymus. During the maturation of T cells in the thymus, T cells undergo a series of changes from the stage of double negative (DN, CD4⁻ CD8⁻), and double positive (DP, CD4⁺ CD8⁺) T cells to the final stage of single positive (SP, CD4⁺ or CD8⁺) T cells. Positive and negative selection occurs at the double-positive stage. The positive selection is mediated by T cell receptor signaling triggered apoptosis, and *in vitro* and *in vivo* studies revealed that thymocytes are sensitive to GC-induced apoptosis (Tuckermann et al., 2005). At the stage of T cell activation and expansion, GCs can mediate expression of several kinases that play important roles in T cell signaling, such as ITK, TXK, and LCK (Petrillo et al., 2014). It was found that the non-genomic mechanism of GCs is also involved in TCR signaling by reducing the activity of LCK and FYN (Löwenberg et al., 2007). Upon encountering antigens, T cells become activated and differentiate into several subsets, including Th1 cells, Th2 cells, Th17 cells and regulatory T cells (T_{reg}). GCs alter the expression of various genes related to these T helper cell subtypes and generally shift Th1 cellular immunity to Th2 humoral immunity (Ramírez et al., 1996). GCs inhibit Th1 response by down-regulating the production of IL-12, suppressing expression of the IL-12 receptor on T cells, reducing the expression of T-bet which is the characteristic transcription factor of Th1 cells, and promoting the production of Th2 cytokines, such as IL-4, IL-10, and IL-13 (Elenkov, 2004; Liberman et al., 2007). It has been demonstrated that Th17 cells play critical roles in many autoimmune diseases, such as multiple sclerosis and rheumatoid arthritis, and the mechanisms of the treatment with GCs in these diseases are linked to targeting Th17 cells; it has been shown that IL-17 deficient mice are resistant to GC treatment (Baschant et al., 2011) and that GC treatment triggers apoptosis of Th17 cells in the context of a mouse model of experimental autoimmune encephalomyelitis (Wüst et al., 2008). Studies in mice and humans revealed that GCs also affect regulatory T cells through enhancing T_{reg} activity and differentiation and resistant to GC-induced apoptosis (Chen et al., 2003). The enhanced activity of T_{reg} cells might be due to the upregulation of FoxP3, the master transcription factor of T_{reg} cells, or related to the increased expression of GILZ

(Bereshchenko et al., 2014).

1.3.4 Targeted delivery of glucocorticoids

GCs are the first-line therapy of choice for many inflammation-related diseases based on their broad immuno-suppressive abilities on various leukocytes as mentioned above. However, high-dose and/or long-term treatment with GCs, as well as steroid-resistance, result in serious adverse effects, which constrains their use and contributes to treatment failure (Kaiser et al., 2020a; Montes-Cobos et al., 2017). Therefore, increasing drug sensitivity and reducing treatment side-effects are in an urgent need. One promising approach or an attempt to achieve this is to innovate and improve drug delivery systems. In recent years, various drug delivery systems have been reported, such as liposomes, nanoparticles, and inorganic scaffolds (Lühder and Reichardt, 2017). Liposomes are biocompatible vesicles that have been modified on their surface to inhibit immediate phagocytosis and increase their bio-stability in the blood circulating system. One example is the modification with polyethylene glycol (PEG). Due to their size, these PEGylated liposomes can passively target tumors and inflammation sites, and further accumulate there based on the so called “enhanced permeability and retention effect” (EPR) (Maeda et al., 2001). However, the disadvantage of this application strategy is that liposomes can also cause the stimulation of the complement system in patients (van den Hoven et al., 2013). Another delivery method of GCs is the use of polymeric micelles. They are spherical, colloidal NPs with a core-shell structure (Jhaveri and Torchilin, 2014), consisting of a hydrophilic corona and a hydrophobic core that is loaded with the drug. Encapsulated drugs in the core of polymeric micelles remain solubilized and are slowly released, thus being protected from degradation. There is another delivery strategy called polymer-drug conjugates, where the active compounds are covalently bound to a macromolecular carrier, leading to conjugates that stabilize the drugs in blood. The most popular example of this category is N-(2-hydroxypropyl) methacrylamide (HPMA) copolymers (Lammers, 2010). In addition to these delivery systems, which are based on organic molecules, compounds can also be encapsulated and delivered by a variety of inorganic material, such as the clay mineral, laponite (LAP) (Ruzicka and Zaccarelli,

2011). However, this delivery system has the limitation of a low drug load (Lühder and Reichardt, 2017).

An alternative to the existing delivery systems is the application of novel inorganic-organic hybrid nanoparticles (IOH-NPs). IOH-NPs possess a general composition of $[M]^{2+} [R_{\text{function}}(\text{O})\text{PO}_3]^{2-}$ ($M = \text{ZrO}, \text{Mg}_2\text{O}$; $R =$ functional organic group), and show multipurpose and multifunctional properties after being loaded with drugs or fluorescent dyes, which gained them a lot of interest in theranostics (Heck et al., 2015). IOH-NPs are insoluble in water due to their inorganic cation, and they allow a load of active drug up to 80%. It has been demonstrated that IOH-NPs are distributed from the peritoneal cavity, accumulate in the abdominal organs, such as liver, small intestine, and stomach, and are finally excreted via the intestinal tract after mice were intraperitoneally injected with them. Moreover, IOH-NPs are selectively taken up by different cell types *in vitro*, preferentially by myeloid cells and fibroblasts, which was shown to predominately occur via the micropinocytosis pathway (Kaiser et al., 2020a). One of the biologically functional forms of IOH-NPs is $[\text{ZrO}]^{2+}-[(\text{BMP})_{0.9}(\text{FMN})_{0.1}]^{2-}$ (BMP = betamethasone phosphate; FMN = flavin mononucleotide, termed BMP-NPs). It has been reported that BMP-NPs were preferentially taken up by macrophages, and that the administration of BMP-NPs shifted the phenotype of macrophages from the classically inflammatory (M1) type to the alternatively activated (M2) type *in vitro* via upregulating RNA levels of *CD163*, and *Ym1*, and reducing the expression of MHC class II, and CD86 on the cell surface. Besides, in a mouse model of multiple sclerosis, the efficacy of BMP-NP therapy was lost in mice with a GR-deficiency in myeloid cells (GR^{lysM}), while being preserved in mice with a GR-deficiency in T cells (GR^{lck}) or brain endothelial cells ($\text{GR}^{\text{sco1c1}}$) (Montes-Cobos et al., 2017).

1.4 Objectives

Allogeneic HSCT is one of the most effective approaches to treat various leukemias and lymphomas, but it is accompanied by the development of life-threatening aGvHD. Much effort has been made to avoid and prevent this fatal disease by targeting the allogenic T cells that play a major role in the pathogenesis of the aGvHD.

Clinically, patients suffering from aGvHD are administered high-dose GCs, a potent anti-inflammatory agent. However, many patients do not respond to the treatment with GCs, and those patients who develop such refractory aGvHD show a low rate of non-relapse survival. Importantly, the mechanisms of GC-resistance remain poorly understood and better insights would allow to improve the available therapy. In addition, biomarkers for refractory aGvHD that may serve to predict long-term outcome are urgently needed, and also the discovery of new potential target genes for the prevention or treatment of aGvHD is highly required. Hence, GC-resistant aGvHD mouse models were used to identify new genes that are linked to a successful treatment of the disease.

Allogeneic T cells are the main driver of aGvHD but they are also responsible for the beneficial GvT effect. We have successfully used GC-loaded IOH-NPs in our group to treat aGvHD in a mouse model and found that they show an increased cell-type specificity, since they are preferentially taken up by macrophages but hardly at all by T cells. Therefore, we tested whether GC treatment using IOH-NPs has the potential to ameliorate aGvHD while preserving the GvT effect of the graft.

This thesis had two main aims:

- To identify new target genes in the context of GC-resistant aGvHD in mice, that can be used as predictive biomarkers or potential therapeutic targets.
- To assess the GvT effect after GC treatment of aGvHD in mice with IOH-NPs, and to test the cytotoxic ability of the CD8⁺ T cells in this model.

2. Material and Methods

2.1 Material

2.1.1 Instruments

If not specifically declared, the manufacturers are located in Germany.

Table 1. Instruments

Equipment	Supplier
Akku-jet [®] pro pipette controller	Brand GmbH, Wertheim
Axio Scope A1	Zeiss, Jena
Axio Scope Aplus	Zeiss, Jena
BD FACS Canto II	BD Biosciences, Heidelberg
BioTek [®] Power Wave 340 Plate Reader	BioTek Instruments, Wetzlar
Cell Incubator, HERACell 240	Heraeus, Hanau
Centrifuge 2-5	Sigma Laborzentrifugen, Osterode
Centrifuge 5417R	Eppendorf, Hamburg
Centrifuge 5804R	Eppendorf, Hamburg
EasyPet 3	Eppendorf, Hamburg
EasySep [™] Magnet	STEMCELL Technologies, SARL, Cologne
Electrophoresis power supply 301	Amersham Biosciences, Freiburg
Fluidigm BioMark [™]	Life Technologies Corporation, South San Francisco, California, USA
Freezer Hera freeze -80 °C	Heraeus, Hanau
Freezer Liebherr Comfort -20 °C	Liebherr-International Deutschland

	GmbH, Biberach an der Riss
Freezer VIP plus -150 °C	SANYO Electric Co., Ltd, Moriguchi, Osaka, Japan
IFC Controller MX	Life Technologies Corporation, South San Francisco, California, USA
Infrared Lamp Balance 100W	Philips, Amsterdam, the Netherlands
Laminar airflow cabinet, HERASafe	Heraeus, Hanau
Microscope Primo Star	Zeiss, Jena
Microscope Telaval 31	Zeiss, Jena
Microtom SM2000R	Leica Biosystems, Wetzlar
Microwave R-212	Sharp, Osaka, Japan
Multichannel pipette S-12, 20-200 µl	Brandt, Wertheim
Nanodrop 2000	Peqlab Biotechnology, Erlangen
Neubauer improved haemocytometer	Henneberg-Sander GmbH, Giessen-Lützellinden
Nunc™ Immuno Wash 12	Thermo Fisher Scientific, Wilmington, DE, USA
pH-Meter 766 Calimatic	Knick Elektronische Messgeräte GmbH & Co.KG, Berlin
Pipettes Eppendorf Research plus 2.5 µl, 20 µl, 200 µl, 1000 µl	Eppendorf, Hamburg
Real-Time PCR System 7500	Applied Biosystems, Foster City, CA, USA
Rotilabo® mini-centrifuge	Carl Roth GmbH & Co.KG, Karlsruhe
RS 225 X-Ray Research System	Gulmay Medical Systems, Camberley, Surrey, UK

Scale Acculab ALC-3100.2	Sartorius, Göttingen
Scale TE313S	Sartorius, Göttingen
Shaker GFL 3006/3005	Gesellschaft für Labortechnik, Burgwedel
Thermocycler Mastercycler EP Gradient	Eppendorf, Hamburg
Thermomixer Comfort	Eppendorf, Hamburg
Tissue Homogenizer Ultra Turrax T18 Basic	IKA, Staufen
Tissue Processor Excelsior ES	Thermo Fisher Scientific, Wilmington, DE, USA
Tissue Tek Prisma Slide Stainer	Sakura Finetek. Staufen
UV System with camera, Gel Imager (Chemostar)	INTAS, Science Imaging Instruments GmbH, Göttingen
VARIOMAG [®] Power direct magnetic stirrer	Thermo Fisher Scientific, Waltham, USA
Vortex Genie-2	Scientific Industries, Bohemia, New York, USA
Water bath W12	Labortechnik Medingen, Dresden
Water Purification System Arium Pro	Sartorius, Göttingen

2.1.2 Consumables

Table 2. Consumables

Consumable	Supplier
BD Falcon 5 ml Polystyrene tubes with Cell-strainer Cap	BD Biosciences, Heidelberg

BD Micro-Fine + Demi U-100 Insulin Syringes (0.3 ml, 30G)	BD Biosciences, Heidelberg
BD Microlance™ 3 (20G 1.5)	BD Biosciences, Heidelberg
BD Microtainer® SST™ tubes	BD Biosciences, Heidelberg
Cellstar Culture Plates (6-well, 12-well, 24-well)	Greiner bio-one GmbH, Frickenhausen
CELLSTAR PS Cell Culture dishes 10 cm	Greiner bio-one GmbH, Frickenhausen
CELLSTAR serological pipettes (5 ml, 10 ml, 25 ml)	Greiner bio-one GmbH, Frickenhausen
CryoTube™ Vials	Nunc, Roskilde, Denmark
EASYstrainer™ (40 µm, 100 µm)	Greiner bio-one GmbH, Frickenhausen
Falcon 5 ml Polystyrene tubes, non-sterile	Th. Geyer GmbH & Co. KG, Renningen
Falcon tubes (15 ml, 50 ml)	Greiner bio-one GmbH, Frickenhausen
Filter paper 66 × 24 mm	DiaTec, Bamberg
Fluidigm 48.48 Dynamic Array™ IFC	Life Technologies Corporation, South San Francisco, California, USA
Fluidigm Control line fluid	Life Technologies Corporation, South San Francisco, California, USA
Glas pipettes (10 ml, 25 ml)	Brand GmbH, Wertheim
Hypodermic needle Sterican® 26G × 0.5, 24G × 1	B Braun, Melsungen
MacrOflow Tissue cassettes	Th, Geyer GmbH & Co. KG, Renningen
Microscope Cover Slips, 24 × 60 mm	Menzel-Gläser, Braunschweig
Microscope Slides SuperFrost Plus	Menzel-Gläser, Braunschweig

Multiply [®] Pro 8-Strip PCR Microtubes	Sarstedt, Nümbrecht
Nunc-Immuno [™] Microwell [™] 96 well plates	eBioScience, San Diego, USA
Optical Adhesive Covers	Applied Biosystems, Foster city, USA
Parafilm	Bemis, Neeth, WI, USA
Pipette tips (10 µl, 200 µl, 1000 µl)	Greiner bio-one GmbH, Frickenhausen
PP tubes sterile 14 ml	Greiner bio-one GmbH, Frickenhausen
Reaction tubes, PP natural (1.5 ml, 2 ml)	Greiner bio-one GmbH, Frickenhausen
Saphire Microplate, 96 well for qPCR	Greiner bio-one GmbH, Frickenhausen
Syringe BD Discardit [™] II (2 ml, 5 ml)	BD Biosciences, Heidelberg

2.1.3 Reagents and Chemicals

Table 3. Reagents and chemicals

Reagent and chemical	Supplier
3,3', 5,5'-Tetramethylbenzidin	Sigma-Aldrich Chemie GmbH, Taufkirchen
Assay Loading Reagent 2 ×	Life Technologies Corporation, South San Francisco, California, USA
BD FACS Clean solution	BD Biosciences, Heidelberg
BD FACS Flow Sheath fluid	BD Biosciences, Heidelberg
BD FACS Shutdown solution	BD Biosciences, Heidelberg
Betamethasone phosphate nanoparticles (BMP-NPs)	Prof. Dr. Klaus Feldmann, Institute of Inorganic Chemistry KIT, Karlsruhe
Bovine serum albumin	Carl Roth GmbH & Co.KG, Karlsruhe

Chloroform	Sigma-Aldrich Chemie GmbH, Taufkirchen
Citric acid	Carl Roth GmbH & Co.KG, Karlsruhe
Dimethylsulfoxid 99.8%	Carl Roth GmbH & Co.KG, Karlsruhe
Disodium hydrogen phosphate	Carl Roth GmbH & Co.KG, Karlsruhe
Dithiothreitol	Sigma-Aldrich Chemie GmbH, Taufkirchen
DNA Binding Dye 20 ×	Life Technologies Corporation, South San Francisco, California, USA
Empty nanoparticles (EP-NPs)	Prof. Dr. Klaus Feldmann, Institute of Inorganic Chemistry KIT, Karlsruhe
Ethanol 99.8%	Carl Roth GmbH & Co.KG, Karlsruhe, Chemsolute® Th. Geyer GmbH & Co. KG, Renningen
Ethidiumbromide solution	Carl Roth GmbH & Co.KG, Karlsruhe
Ethylendiaminetetraacetic acid	Sigma-Aldrich Chemie GmbH, Taufkirchen
Exonuclease I Reaction Buffer 10 ×	NEW ENGLAND, BioLabs®, UK
F-518 Phusion® HF buffer with 7.5 mM magnesiumchlorid	Thermo Fischer Scientific, Waltham, USA
Fetal calf serum	Abbvie, Ludwigshafen
Gene Ruler 1kb DNA ladder	Thermo Fischer Scientific, Waltham, USA
Gibco® 2-Mercaptoethanol	Thermo Fischer Scientific, Waltham, USA
Gibco® RPMI1640 + GlutaMAX™	Thermo Fischer Scientific, Waltham,

	USA
Glycerol	Carl Roth GmbH & Co.KG, Karlsruhe
Hydrogen Peroxide 30%	Carl Roth GmbH & Co.KG, Karlsruhe
Neomycin trisulfate salt hydrate	Sigma-Aldrich Chemie GmbH, Taufkirchen
Nucleoside triphosphate	Genaxxon bioscience, Ulm
OptiLyse [®] B Lysing solution	Beckman Coulter, Inc., France
Orange G sodium salt	Sigma-Aldrich Chemie GmbH, Taufkirchen
Paraffin wax	Sigma-Aldrich Chemie GmbH, Taufkirchen
Paraformaldehyde, 4%	Carl Roth GmbH & Co.KG, Karlsruhe
PegGOLD Universal Agarose	Peqlab Biotechnology GmbH, Erlangen
Penicillin/Streptomycin (10.000 U/ml)	Invitrogen, Carlsbad, CA, USA
Potassium chloride	Merck KGaA, Darmstadt
Potassium dihydrogen phosphate	Merck KGaA, Darmstadt
Power SYBR [®] Green Master mix	Applied Biosystems, Foster City, USA
QIAzol [™] Lysis buffer	Qiagen, Hilden
Sodium carbonate	Merck KGaA, Darmstadt
Sodium chloride, 99.5%	Carl Roth GmbH & Co.KG, Karlsruhe
Sodium hydrogen carbonate	Merck KGaA, Darmstadt
SsoFast EvaGreen Supermix with low ROX 2 ×	Bio-Rad Laboratories GmbH, Munich
Sulfuric acid, 95-98%	Merck KGaA, Darmstadt

TaqMan [®] PerAmp Master mix 2 ×	Applied Biosystems, Foster City, USA
Tween [®] 20%	Carl Roth GmbH & Co.KG, Karlsruhe

2.1.4 Buffers

Table 4. Buffers

Buffer	Component
DNA Suspension buffer	10 mM Tris 0.1 mM EDTA in ddH ₂ O, pH 8.0
EasySep [™] Recommended medium	2 % FCS 1 mM EDTA in PBS
ELISA Assay diluent	10 % FCS in PBS
ELISA Coating buffer	1000 ml ddH ₂ O 8.4 g NaHCO ₃ 3.56 g Na ₂ CO ₃ , pH 9.5
ELISA Developing solution	ELISA Substrate buffer 1 % TMB in DMSO 0.2 % H ₂ O ₂
ELISA Stop solution	1 M H ₂ SO ₄ in ddH ₂ O
ELISA Substrate buffer	0.1 M Citric acid 0.2 M Na ₂ HPO ₄ in ddH ₂ O
ELISA Washing buffer	0.05 % Tween [®] 20 % in PBS
FACS buffer	0.1 % BSA 0.01 % Sodium azide in PBS, pH 7.2
Orange G Loading dye	100 ml ddH ₂ O 100 mg Orange G sodium salt 30 % Glycerol

Phosphate saline buffer (PBS)	137 mM NaCl 2.7 mM KCl 10 μ M Na ₂ HPO ₄ 2 mM KH ₂ PO ₄ in ddH ₂ O
TAC buffer	20 mM Tris 155 mM NH ₄ Cl in ddH ₂ O
TAE buffer	40 mM Tris 20 mM Acetic acid 1 mM EDTA in ddH ₂ O

2.1.5 Primers

Table 5. Primers

Gene	Sequences (5'—3') Forward / Reverse	Accession number	Product length
<i>Acaca</i>	ATG GGC TGC TTC TGT GAC TC GTT CAT CCC TGG GGA CCT TG	NM_133360.2	97
<i>Acot1</i>	GAC AAG AAG AGC TTC ATT CCC GTG CAT CAG CAT AGA ACT CGC TCT TCC	NM_012006.2	100
<i>Aldh1b1</i>	ACC GCA GGT CCT CAG GAT G TTT GGG ATT GGG TTC GGG AG	NM_028270.4	114
<i>Aldoa</i>	CAG ATG GGT CCA GCT TCA AC TGC TTT CCT TTC CTA ACT CTG TC	NM_001177307.1	132
<i>Aoc1</i>	GTC ACT TGG GCC AGG TAT CC CCT CAA AAA CCA CAG GGG GA	NM_001161621.1	112
<i>Arg1</i>	AGC CCG AGC ACA TGC AGC AG ACC CCT CCT CGA GGC TGT CCT	NM_007482.3	118
<i>Arg2</i>	TCC TTG CGT CCT GAC GAG ATC CG	NM_009705.3	150

	AGG TGG CAT CCC AAC CTG GAG AG		
<i>Ccl2</i>	CAC TCA CCT GCT GCT ACT CA GCT TGG TGA CAA AAA CTA CAG C	NM_011333.3	117
<i>Ccl3</i>	ATA TGG AGC TGA CAC CCC GA TCA GGA AAA TGA CAC CTG GCT G	NM_011337.2	122
<i>Ccl5</i>	CTC ACC ATA TGG CTC GGA CA CGA CTG CAA GAT TGG AGC AC	NM_013653.3	119
<i>Ccl7</i>	CCC TGG GAA GCT GTT ATC TTC AA CTC GAC CCA CTT CTG ATG GG	NM_013654.3	75
<i>Ccr2</i>	AGG AGC CAT ACC TGT AAA TGC C TGT CTT CCA TTT CCT TTG ATT TGT	NM_009915.2	132
<i>Cd14</i>	CAG AGA ACA CCA CCG CTG TA CAC GCT CCA TGG TCG GTA GA	NM_009841.4	97
<i>Cd274</i>	CGC CTG CAG ATA GTT CCC AA AGC CGT GAT AGT AAA CGC CC	NM_021893.3	92
<i>Cd28</i>	GGC TCT TTG TGT TAT CTG GAC AAA TAA GGC TTT CGA GTG AGC CC	NM_007642.4	102
<i>Chil3</i>	ACT TTG ATG GCC TCA ACC TG AAT GAT TCC TGC TCC TGT GG	NM_009892.3	173
<i>Cldn4</i>	CCA CTC TGT CCA CAT TGC CT CTT TGC ACA GTC CGG GTT TG	NM_009903.2	141
<i>Cpt1a</i>	TGA CTA TGT GTC CTG TGG CG CGG TGT GAG TCT GTC TCA GG	NM_013495.2	138
<i>Csf1</i>	AGT GCT CTA GCC GAG ATG TG CTG CTA GGG GTG GCT TTA GG	NM_007778.4	70
<i>Csf2</i>	CAG GGT CTA CGG GGC AAT TT ACA GTC CGT TTC CGG AGT TG	NM_009969.4	99

<i>Ctla4</i>	ACG CAG ATT TAT GTC ATT GAT CCA G AAC CCC AAG CTA ACT GCG AC	NM_009843.4	83
<i>Cxcl1</i>	AGA CCA TGG CTG GGA TTC AC AGT GTG GCT ATG ACT TCG GT	NM_008176.3	94
<i>Cxcl10</i>	CCA CGT GTT GAG ATC ATT GCC TCA CTC CAG TTA AGG AGC CC	NM_021274.2	135
<i>Cxcl11</i>	CAG CTG CTC AAG GCT TCC TTA CTT TGT CGC AGC CGT TAC TC	NM_019494.1	129
<i>Cxcl13</i>	GCC TCT CTC CGA GCC ACG GTA AGC CAT TCC CAG GGG GCG TA	NM_018866.2	132
<i>Cxcl2</i>	TGA ACA AAG GCA AGG CTA ACT G CAG GTA CGA TCC AGG CTT CC	NM_009140.2	118
<i>Cxcl5</i>	CCC TAC GGT GGA AGT CAT AGC GCT TTC TTT TTG TCA CTG CCC A	NM_009141.3	117
<i>Cxcl9</i>	GCC ATG AAG TCC GCT GTT CT TAG GGT TCC TCG AAC TCC ACA	NM_008599.4	72
<i>Cxcr6</i>	ACT GGG CTT CTC TTC TGA TGC CTC GTA GTG CCC ATC GTA CA	NM_030712.4	70
<i>Cybb</i>	GGG AAC TGG GCT GTG AAT GA CAG TGC TGA CCC AAG GAG TT	NM_007807.5	147
<i>Dusp1</i>	CTC CAA GGA GGA TAT GAA GCG ACT AGT ACT CAG GGG GAG GC	NM_013642.3	96
<i>Esrra</i>	CTC TGG CTA CCA CTA CGG TG TAT ACT CGA TGA TCC CCT GG	NM_007953.2	83
<i>Fasl</i>	CTG GGT TGT ACT TCG TGT ATT CC TGT CCA GTA GTG CAG TAG TTC AA	NM_010177.4	154
<i>Gilz</i>	GGA GGT CCT AAA GGA GCA GAT TC	NM_001077364.1	80

	GCG TCT TCA GGA GGG TGT TC		
<i>Gzmb</i>	TGT GGG CCC CCA AAG TGA CAT AAA GGC AGG GGA GAT CAT CGG G	NM_013542.3	185
<i>H2-Aa</i>	TGA TTC TGG GGG TCC TCG CCC ACG TGG TCG GCC TCA ATG TCG	NM_010378.3	76
<i>Hif1a</i>	CAC AGA AAT GGC CCA GTG AGA GAA TAT GGC CCG TGC AGT GA	NM_001313919.1	148
<i>Hk2</i>	GCC TCG GTT TCT CTA TTT GGC ATA CTG GTC AAC CTT CTG CAC T	NM_013820.3	115
<i>Hmgcr</i>	ACG TGG TGT GTC TAT TCG CC CAA GCT CCC ATC ACC AAG GA	NM_008255.2	111
<i>Hmox1</i>	AGG CTT TAA GCT GGT GAT GGC TGG GGC ATA GAC TGG GTT CT	NM_010442.2	94
<i>Hprt</i>	GTC CTG TGG CCA TCT GCC TA GGG ACG CAG CAA CTG ACA TT	NM_013556.2	91
<i>Ifng</i>	ACT GGC AAA AGG ATG GTG AC TGA GCT CAT TGA ATG CTT GG	NM_008337.4	237
<i>Il10</i>	AGG CAG AGA AGC ATG GCC CA CGG GAG AAA TCG ATG ACA GCG CC	NM_010548.2	104
<i>Il12</i>	GCT CAG CTC CTG TCA CAT CA CAG TTC CCC AAT CGC CTT GA	NM_016971.2	118
<i>Il17a</i>	TCC AGA AGG CCC TCA GAC TA AGC ATC TTC TCG ACC CTG AA	NM_010552.3	239
<i>Il18r1</i>	AAC CAC CCA CAA CGA TCC TG CGG TGA ATA CAA CTT TTT GAG GC	NM_008365.2	130
<i>Il1b</i>	CTC ATC TGG GAT CCT CTC CA AAG CAG CCC TTC ATC TTT TG	NM_008361.4	158

<i>Il1r1</i>	CAG CCA GTG TTT ATT TGC TCA G GCA CTT TCA TAT TCT CCA TTT GTG T	NM_008362.2	115
<i>Il2</i>	ACT TGC CCA AGC AGA CCA CA CCA GAA CAT GCC GCA GAG GTC C	NM_008366.3	78
<i>Il33</i>	TTC CTG TCT GTA TTG AGA AAC CT TTT GCC GGG GAA ATC TTG GA	NM_001164724.2	75
<i>Il6</i>	AGT TGC CTT CTT CGG ACT GA CAG AAT TGC CAT TGC ACA AC	NM_031168.2	191
<i>Itgal</i>	CTT CCA CTT CCC GAT CTG CAT AAG GTC TCA GGA TAG GCT GC	NM_001253872.1	134
<i>Itgam</i>	CAT CCC CCT GCA AGT ACC TC GGG GGA CAG TAG AAA CAG CC	NM_001082960.1	74
<i>Itgb2</i>	CCC AGG AAT GCA CCA AGT ACA AGT GAA GTT CAG CTT CTG GCA C	NM_008404.5	92
<i>Itk</i>	AAA CAA ATG ACA GCC CCA AGC GTC GAG TGA CCA AAC CTC CT	NM_010583.3	111
<i>Klrk1</i>	GCT GGT TAA GTC CTA TCA CTG G TTG AGC CAT AGA CAG CAC AG	NM_033078.4	143
<i>Ldhd</i>	GCA AAC TTA ACT GCC CCG TG TGA GTG ATT GCC TCT GTG CG	NM_027570.4	100
<i>Mapk1</i>	AAT TGG TCA GGA CAA GGG CT GAG TGG GTA AGC TGA GAC GG	NM_011949.3	105
<i>Mt2a</i>	TCG ACC CAA TAC TCT CCG CT GAT CCA TCG GAG GCA CAG GA	NM_008630.2	149
<i>Mtor</i>	CAG CTA CCC CAG CTC ACA TC ACA GCC AAC TCA AGG TCT CG	NM_020009.2	80
<i>Myc</i>	TTG GAA ACC CCG CAG ACA G	NM_010849.4	88

	GCT GTA CGG AGT CGT AGT CG		
<i>Nos2</i>	GGT GAA GGG ACT GAG CTG TT ACG TTC TCC GTT CTC TTG CAG	NM_010927.4	103
<i>Orm2</i>	ATT GGT GCG GCT GTC CTA AA ACA CAG TGG TCA TCT ATG GTG T	NM_011016.2	137
<i>Otc</i>	TGC TGC AAA ATT CGG GAT GC AGC CAC TTT GGC AGT CTT CA	NM_008769.4	262
<i>Pdha1</i>	AGA TGA TTG CCG CTG TAT CC GCC GAT GAA GGT CAC ATT TCT TAA T	NM_008810.3	129
<i>Pfkfb3</i>	GTC GCC GAA TAC AGC TAC GA CCC ACA GGA TCT GGG CAA C	NM_133232.3	106
<i>pfkl</i>	CTA CGT GAA GGA TCT GGT GGT CTC CTC GCT GTA CAT GAC CC	NM_008826.5	77
<i>Ppargc1a</i>	AGT CCC ATA CAC AAC CGC AG ACC CTT GGG GTC ATT TGG TG	NM_008904.2	95
<i>Prfl</i>	TGT TAA AGT TGC GGG GGA GGG C GTG GCT GGC TCC CAC TCC AA	NM_011073.3	178
<i>Prkaal</i>	CAG GAA GAT TGT ACG CAG GC GGA GGG TTC CAC ACA GCA AA	NM_001013367.3	81
<i>Ptges</i>	GAA GAA GGC TTT TGC CAA CCC TCC ACA TCT GGG TCA CTC CT	NM_022415.3	78
<i>Ptgs2</i>	CAG ACA ACA TAA ACT GCG CCT T GAT ACA CCT CTC CAC CAA TGA CC	NM_011198.4	71
<i>Rgs1</i>	CTT GCC AAC CAG ACA GGT CA GTC CTC ACA AGC CAA CCA GA	NM_015811.2	93
<i>Slpr1</i>	CTT GAG CGA GGC TGC TGT TT GGT CAG CGA GCA ATC CAA TG	NM_007901.5	86

<i>Slc1a5</i>	CGC TAT CGT CTT TGG TGT GG GGG TGC GTA CCA CAT AAT CC	NM_009201.2	124
<i>Slc2a1</i>	AGC ATC TTC GAG AAG GCA GG ACA ACA AAC AGC GAC ACC AC	NM_011400.3	98
<i>Slc2a3</i>	CTC TTC AGG TCA CCC AAC TAC GT CCG CGT CCT TGA AGA TTC C	NM_011401.4	121
<i>Slc7a5</i>	GGG GAA GGA CAT GGG ACA AG ATA GTT CCA TCC TCC GTA GGC G	NM_011404.3	133
<i>Sphk1</i>	ACA GTG GGC ACC TTC TTT C CTT CTG CAC CAG TGT AGA GGC	NM_011451.3	114
<i>Tlr4</i>	TGG TTG CAG AAA ATG CCA GG TAG GAA CTA CCT CTA TGC AGG G	NM_021297.3	120
<i>Tnf</i>	ATG GCC TCC CTC TCA TCA GT CTT GGT GGT TTG CTA CGA CG	NM_013693.3	105
<i>Tnfrsf9</i>	CAG CAC AGA GAG CTG ACA GG ATG CAC AGG ACA CCA AAG GT	NM_011612.2	87

2.1.6 Fluorochrome-conjugated monoclonal antibodies

Table 6. Antibodies

Antibody	Clone name	Supplier
APC anti-mouse CD8 α	53-6.7	BioLegend, San Diego, USA
APC anti-mouse CXCR3	CXCR3-173	BioLegend
APC anti-mouse EpCam	G8.8	BioLegend
APC anti-mouse Foxp3	FJK-16s	eBioscience, San Diego, USA
APC-Cy7 anti-mouse CD25	PC61	BioLegend

APC-Cy7 anti-mouse CD62L	MEL-14	BioLegend
APC-Cy7 anti-mouse Gr-1	RB6-8C5	BioLegend
FITC anti-mouse CD49d	R1-2	BD Biosciences, Franklin Lakes, USA
FITC anti-mouse TCR- β	H57-597	BD Biosciences
PE anti-mouse CD44	IM7	BD Biosciences
PE anti-mouse CD45.1	A20	BD Biosciences
PE anti-mouse CD45R/B220	RA3-6B2	BD Biosciences
PE anti-mouse Ig λ	RML-42	BioLegend
PE-Cy7 anti-mouse CD11a	2D7	BD Biosciences
PE-Cy7 anti-mouse CD11b	M1/70	BioLegend
PerCP anti-mouse CD4	RM4-5	BioLegend
PerCP-Cy5.5 anti-mouse CD45.2	104	BD Biosciences

2.1.7 Commercial kits and Enzymes

Table 7. Commercial kits and enzymes

Commercial kit				Manufacture
EasySep™	Mouse	APC	positive	STEMCELL™ Technologies SARL, Cologne
EasySep™	Mouse	CD8+	T cell isolation kit	STEMCELL™ Technologies SARL, Cologne
EasySep™	Mouse	CD90.2	positive	STEMCELL™ Technologies SARL, Cologne
EasySep™	Mouse	T cell isolation kit		STEMCELL™ Technologies SARL,

Cologne

ELISA MAX™ Standard set mouse IFN γ	BioLegend, San Diego, USA
ELISA MAX™ Standard set mouse IL6	BioLegend, San Diego, USA
ELISA MAX™ Standard set mouse TNF α	BioLegend, San Diego, USA
Foxp3 Staining Buffer set	eBioscience®, San Diego, USA
iScript™ cDNA Synthesis kit	Bio-Rad Laboratories GmbH, Munich
Qiagen RNeasy Plus Universal Mini kit	Qiagen, Hilden
Quick-RNA™ MiniPrep	Zymo Research Epigenetics, Irvine, USA

2.1.8 Software

Table 8. software

Software	Company
7500 System SDS software version 1.4.0.25	Applied Biosystems, Foster City, CA, USA
BD FACS Diva™ software version 6.1.2	BD Biosciences, Heidelberg
BioMark™ Data collection software	Life Technologies Corporation, South San Francisco, California, USA
BioMark™ Real-Time PCR analysis software	Life Technologies Corporation, South San Francisco, California, USA
BioTek® Gen 5 version 1.09.8	BioTek Instruments, Bad Friedrichshall
FlowJo version 10 and 7.6.5	Tree Star, Inc., Ashland, USA

GraphPad Prism 5	GraphPad Software, La Jolla, CA, USA
Nanodrop 2000	Thermo Scientific, Wilmington, WA, USA

2.2 Methods

2.2.1 Mice and housing conditions

C57BL/6 and BALB/c wild type mice used for the experiments were purchased from Janvier Labs (St. Berthevin, France). B6.SJL-PtprcaPepcb/BoyJ (CD45.1-congenic C57BL/6) mice were originally obtained from Charles River (Sulzfeld, Germany) and kindly provided by Dr. Fred Lühder (Institute of Neuroimmunology).

All genetically modified mice used in the experiments are listed in the following: Nr3c1^{tm2Gsc} mice on the genetic background of C57BL/6 or BALB/c strains (designated as GR^{flox}), Nr3c1^{tm2Gsc}Tg^{(Lck-cre)1Cwi} mice on the C57BL/6 genetic background (designated as GR^{lck}) and Nr3c1^{tm2Gsc}Lyz2^{tm1(cre)lfo/J} mice on the BALB/c genetic background (designated as GR^{lysM}). GR^{lck} mice are characterized by a lack of the GR in the entire T cell lines (Theiss-Suennemann et al., 2015) and GR^{lysM} mice are characterized by the absence of the GR in the majority of myeloid cells (Baake et al., 2018). GR^{flox} litter mates from each strain were used as a control for their knock-out counterparts.

All mice were bred and kept in the animal facility of the University Medical Center Göttingen, and housed in individually ventilated cages under specific-pathogen-free conditions (SPF) in a 12-hour light/dark cycle. Food and water were supplied *ad libitum*. Mice were used at the age of 8-12 weeks. All animal experiments were performed according to national and international guidelines and approved by the responsible authority of Lower Saxony (*Niedersächsisches Landesamt für Verbraucherschutz und Lebensmittelsicherheit*).

2.2.2 The acute GvHD mouse model

This mouse model is based on a complete mismatch of MHC molecules between donor and recipient. To induce aGvHD, bone marrow cells and splenic T cells are isolated from C57BL/6 mice (H-2^b), which are used as donors, and injected into BALB/c mice(H-2^d), which are used as recipients, via the tail vein.

2.2.2.1 Induction of aGvHD

2.2.2.1.1 Experimental set-up

Female wild type, GR^{flox} or GR^{lysM} BALB/c mice were used as recipients and given neomycin (25 µg/ml) via the drinking water starting two days (-2 day) before bone marrow transplantation (BMT). The drinking water containing neomycin was refilled every two days during the entire aGvHD experiment. One day before BMT (-1 day), the recipient mice underwent total body irradiation at a dose of 8.5 Gy using an X-Ray source at 200 kV, 15 mA and 0.5-mm Cu filtration. On day 0, cell transplantation was performed, 1×10^7 T-cell-depleted (TCD) bone marrow cells and 2×10^6 splenic T cells isolated from wild type, donor GR^{lck} or GR^{flox} C57BL/6 donor mice, and injected into recipient BALB/c mice intravenously. The mice only transferred with TCD-bone marrow served as controls. The induction of aGvHD using GR^{lysM} recipient mice was performed by my colleague Tina Kaiser.

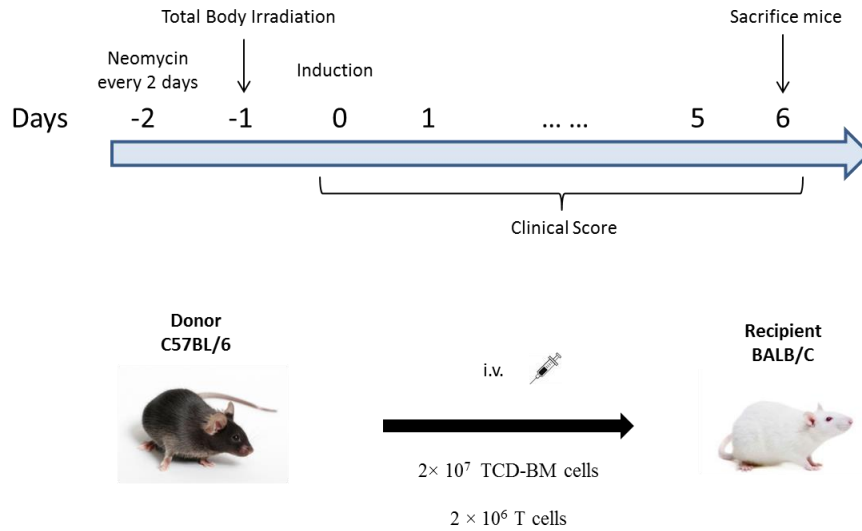


Figure 4. Experimental schematic of acute GvHD induction in mice.

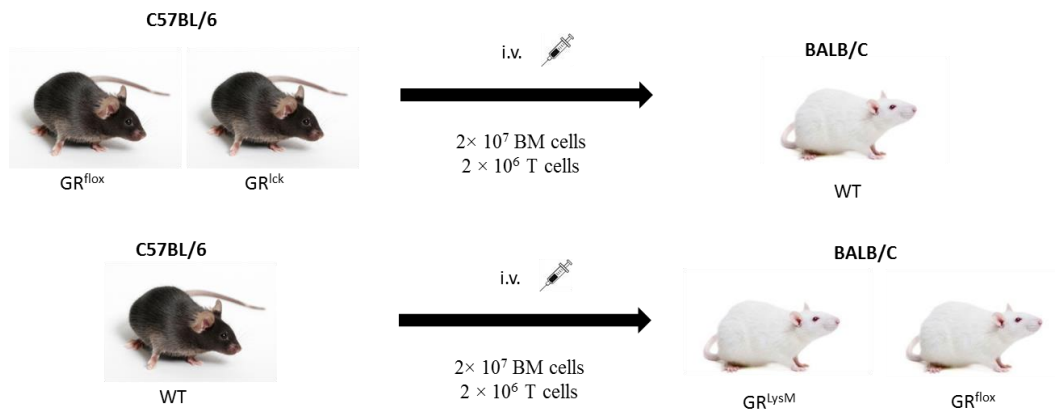


Figure 5. Cell type-specific knock-out aGvHD mouse models.

2.2.2.1.2 T cell depletion of bone marrow cells

The donor mice were euthanized with CO₂, and tibia, femura and humeri were collected. Bone marrow cells were flushed out of the bones using a 5 ml syringe with a 24 G needle filled with PBS + 0.1% BSA. The bone marrow cells were passed through a 40 µm cell strainer into a 50 ml Falcon tube and centrifuged at 300 × g for 7 min at 4 °C, the pellets were resuspended in the recommended medium (PBS + 2% FCS and 1mM EDTA) and adjusted to a concentration of 1 × 10⁸ cells/ml. T cells were depleted from bone marrow

cells with the EasySep™ positive selection Mouse CD90.2 Kit II according to the manufacturer's instructions. Briefly, a cocktail containing component A (25 µl/ml) and B (25 µl/ml) was prepared and incubated at room temperature (RT) for 5 min, subsequently added to the sample in a FACS tube (50 µl/ml) for incubation of 3 min. RapidSpheres™ was added and left for 3 min at RT, the recommended medium was added to top up the sample to 2.5 ml and mixed by gently pipetting up and down 2-3 times. Then the FACS tube was placed into the EasySep™ magnet and incubated for 3 min at RT and CD90.2⁺ cells were poured to another 50 ml Falcon tube. The cells were centrifuged ($300 \times g$ for 7 min at 4 °C), resuspended in an appropriate volume, counted and adjusted to 1×10^8 cells/ml with PBS for injection. The recipient mice were injected with 100 µl of the final cell suspension along with the purified T cells or PBS.

2.2.2.1.3 Splenic T cell purification

Spleens were removed from the donor mice after the collection of the bones. Splenic cell suspensions were prepared using a 40 µm cell strainer under sterile conditions, and centrifuged at $300 \times g$ for 7 min at 4 °C, and subsequently the pellets were resuspended in the recommended medium. T cells were then purified with the EasySep™ negative selection Mouse T cell Isolation Kit according to the manufacturer's protocol. In brief, the cells were counted and adjusted to a concentration of 1×10^8 cells/ml. The samples were placed in FACS tubes; Normal Rat Serum (50 µl/ml) and Mouse T cell Isolation Cocktail (50 µl/ml) were added, and incubated at RT for 10 min. Then the RapidSpheres™ (75 µl/ml) was added to the samples, and left at RT for 2.5 min. The samples were filled up to 2.5 ml using the recommended medium and placed in the magnet for 3 min. The desired fraction was poured into a new 50 ml Falcon tube, centrifuged ($300 \times g$ for 7 min at 4 °C), resuspended in an appropriate volume, counted and adjusted to a concentration of 2×10^7 cells/ml with PBS. Each recipient mouse received 100 µl of the final cell suspension. For the mice receiving BM only, PBS was added up to 200 µl instead.

2.2.2.1.4 Quality control of TCD-bone marrow cells and splenic T cells

The purity of the isolated TCD-bone marrow cells and splenic T cells was determined by flow cytometry. The gating strategy is shown in the Figure below.

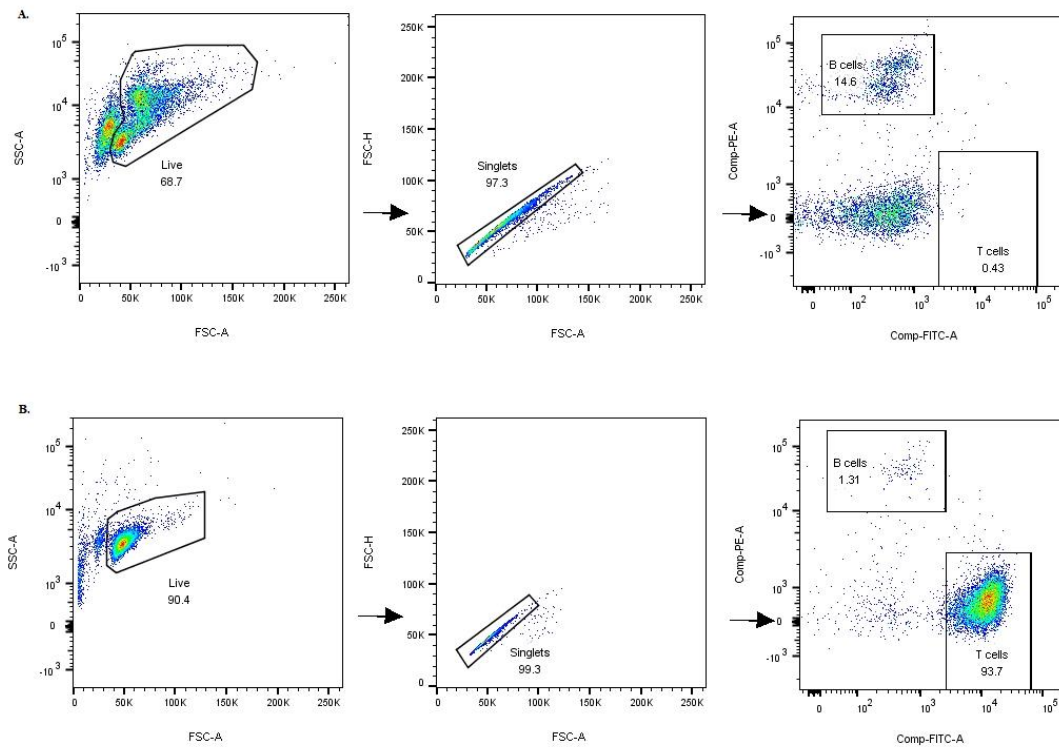


Figure 6. Gating strategy used for the quality control of T cell-depleted bone marrow cells (A) and purified T cells (B) by flow cytometry. Isolated bone marrow cells and T cells were stained with specific fluorochrome-conjugated antibodies: anti-B220 (for B cells) and anti-TCR β (for T cells), and used for flow cytometric analysis.

2.2.2.1.5 Assessment of the severity of aGvHD

The severity and progress of aGvHD were assessed starting on day 2 after bone marrow transplantation based on an established clinical scoring system (Theiss-Suennemann et al., 2015). Five parameters were involved in the scoring system: 1) posture, 2) activity, 3) fur texture, 4) diarrhea and 5) weight loss. Each parameter was assigned a grade between 0 (no symptoms) to 2 (severe symptoms), resulting in a total score of 0 to 10. For ethical reasons, mice with a clinical score of at least 7 or a weight loss of more than 20% were sacrificed.

Table 9. Acute GvHD clinical score system

Parameter	0	1	2
Posture	Normal	Hunching	Impaired movement
Activity	Normal	Less active	Stationary
Fur texture	Normal	Ruffling	Absent grooming
Diarrhea	None	Mild	Severe
Weight loss	0 % - 10 %	10 % - 20 %	More than 20 %

2.2.3 Combined aGvHD/GvL mouse model

2.2.3.1 Experimental set-up

2.2.3.1.1 Acute GvHD induction

Wild type BALB/c recipient mice were given neomycin and subjected to a total body irradiation as described before (2.2.2.1.1). TCD-bone marrow cells (2.2.2.1.2) and splenic T cells (2.2.2.1.3) were purified from wild type C57BL/6 donor mice and transferred into the recipient mice to induce aGvHD (2.2.2.1.1).

2.2.3.1.2 Adoptive B cell lymphoma transfer

Bcl₁ cells (Warnke et al., 1979) were freshly thawed on day 0, corresponding to the time point of aGvHD induction. Bcl₁ cells were rapidly thawed in a water bath at 37 °C, centrifuged at 300 × g, 5 min at 4 °C, and the pellet washed with 3 ml PBS. The samples were then centrifuged again, resuspended, counted, and adjusted to a final concentration of 3 × 10⁴ cells/ml. 3 × 10³ Bcl₁ cells (100 µl) were injected into the recipient mice via the tail vein 4 hours before the transfer of TCD bone marrow cells and splenic T cells for aGvHD induction (Figure 7).

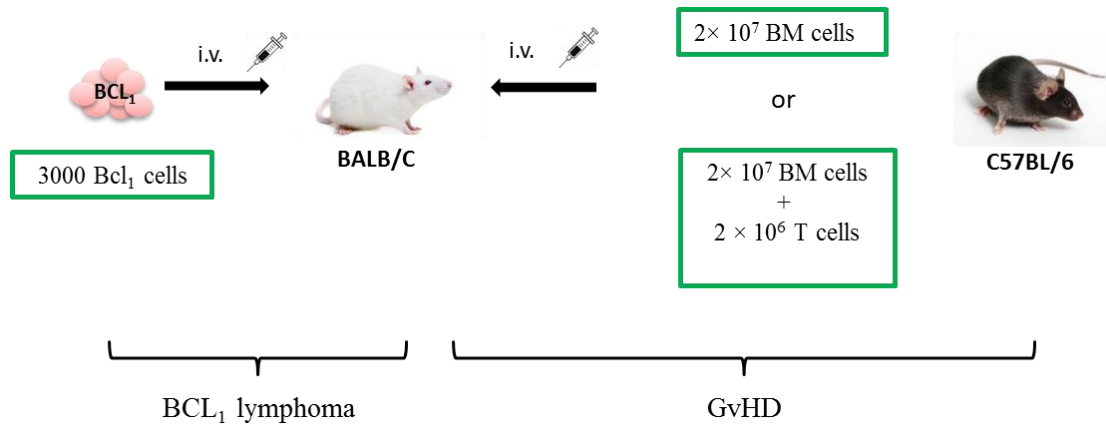


Figure 7. Experimental schematic of the combined aGvHD/GvL mouse model

2.2.3.1.3 Long-term treatment

After the induction of the combined aGvHD/GvL mouse model (day 0), the recipient mice were treated intraperitoneally (i.p.) at day 3, 4, 5, 7, 9, and 12 with either free betamethasone (10 mg/kg, BMZ) or BMP-NPs (10 mg/kg, IOH-NPs, containing betamethasone phosphate) at equivalent dose of the drug. Mice treated with the same volume of PBS or the same volume of EP-NPs (empty IOH-NPs without the drug) served as a control to BMZ or BMP-NPs, respectively (**Figure 8**).

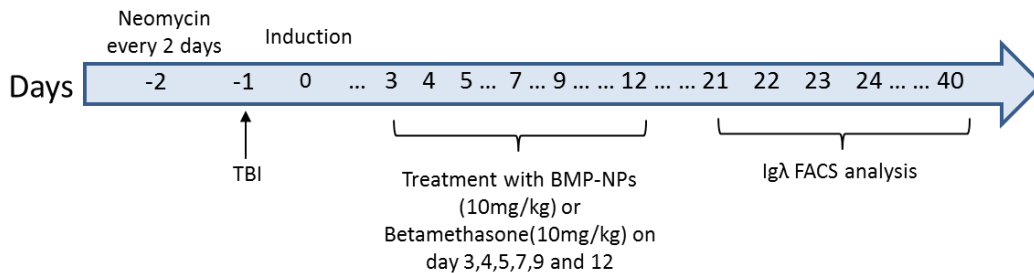


Figure 8. Scheme of the long-term treatment of the aGvHD/GvL mouse model

2.2.3.2 Assessment of disease progression in the aGvHD/GvL mouse model

2.2.3.2.1 Assessment of the severity of aGvHD

The BALB/c recipient mice were scored for the disease from day 2 to 40 (**Figure 8**) based on the aGvHD clinical scoring system and sacrificed for ethical reasons as

described before (2.2.2.2). Mice were euthanized at day 40 if no severe aGvHD symptoms or no Bcl₁ lymphoma features were observed.

2.2.3.2.2 Assessment of Bcl₁ lymphoma progression

The development of the adoptively transferred Bcl₁ lymphoma in the recipient mice was determined by daily flow cytometric analysis of the percentage of Igλ⁺ cells in peripheral blood starting at day 15. Mice were sacrificed if the percentage of Bcl₁ cells exceeded 50 % of all lymphocytes in the peripheral blood. Mice were euthanized at day 40 if no severe aGvHD symptoms or no Bcl₁ lymphoma features were observed.

2.2.3.3 Flow cytometric analysis of Bcl₁ lymphoma cells

Peripheral blood of the mice was collected from the tail tip (5-6 drops/mouse) starting 15 days after the induction of the combined aGvHD/GvL mouse model. FACS tubes were filled with Alsevers solution for the preservation of blood samples. The samples were centrifuged at 350 × g, 5 min at RT, the supernatant was discarded, and next washed with 4 ml FACS buffer. The samples were centrifuged again and the supernatant was removed. The cells were stained with the monoclonal fluorochrome-conjugated antibody: anti-Igλ light chain (1:50,000 dilution) at 4 °C in the dark for 20 min. Then the cells were washed with FACS buffer and the supernatant was removed completely; 100 μl OptiLyse B lysis buffer was added to each sample, and incubated for 12 min at RT in dark. Then 1ml H₂O_{dest} was added to the samples, and incubated for 1 - 2 hours at RT in dark. The cells were washed with 3 ml FACS buffer, centrifuged, the supernatant removed, and used for flow cytometric analysis. The gating strategy is depicted below.

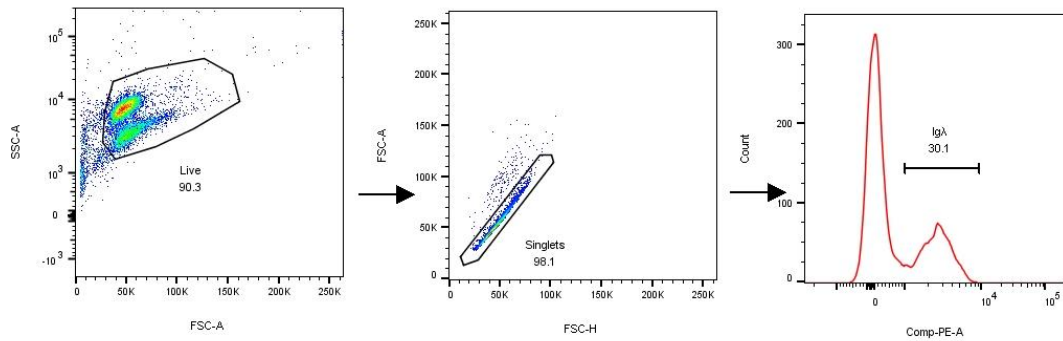


Figure 9. Gating strategy of the flow cytometric analysis of Bcl1 lymphoma cells in the blood. Bcl₁ lymphoma cells in peripheral blood were stained with a PE-conjugated anti-Igλ antibody and their percentage was analyzed by FACS.

2.2.4 Phenotypic analysis of donor T cells

2.2.4.1 Purification of donor T cells

T cells were magnetically purified from individual GR^{flox} and GR^{lck} mice according to the protocol described before (2.2.2.1.3).

2.2.4.2 FACS staining of T cells

1×10^6 purified T cells from each mouse were stained with monoclonal antibodies conjugated with different fluorochromes, used for flow cytometry analysis and the data were analyzed with FlowJo software.

2.2.4.2.1 Extracellular staining

The cells were stained in FACS tubes with pre-diluted antibodies: anti-CD4, anti-CD8, anti-CD25, anti-CD44, anti-CD62L, anti-CD49d, anti-CD11a and anti-CXCR3 for 20 min at 4 °C in dark. Next, the cells were washed with 3 ml FACS Buffer, centrifuged for 5 min at $300 \times g$. The supernatant was discarded; the pellet was resuspended, and used for FACS analysis.

2.2.4.2.2 FoxP3 intracellular staining

The purified T cells were first stained extracellularly with anti-CD4 and anti-CD25 antibodies. Then, a FoxP3 intracellular staining was conducted using the FoxP3 Staining Buffer Set following the manufacturer's protocol. In brief, the Fix/Perm Buffer was prepared by diluting the Fix/Perm Concentrate with the Fix/Perm Diluent at a ratio of 1:4, and the Perm-Buffer was prepared by diluting the 10 × Perm Buffer with H₂O_{dest} (1:10 dilution). 300 µl of Fix/Perm Buffer were added to each sample. The cells were incubated for 30 min at RT in dark, centrifuged, washed with 2 ml PBS, and followed by washing with 1 ml Perm-Buffer. Next, 200 µl Perm-Buffer and 20 µl anti-FoxP3 were added to each sample, vortexed and incubated for 30 min at 4 °C. Thereafter, the cells were washed with 1 ml Perm-Buffer, centrifuged, and washed with 3 ml FACS Buffer. Finally, the supernatant was discarded and used for FACS analysis.

2.2.5 Fluidigm[®] gene chip analysis

2.2.5.1 Preamplification of cDNA using TaqMan PreAmp Master Mix

The cDNA was synthesized from 1 µg total RNA isolated from tissues described above. The cDNA samples were then diluted with DNA Suspension Buffer (10 mM Tris, pH 8.0, 0.1 mM EDTA) at a concentration corresponding to 8 ng/µl of total RNA transcribed into cDNA.

The pooled STA (Specific Target Amplification) master mix was prepared by adding 1 µl of 100 µM of each primer pair (up to a total of 96 primer pairs) to DNA Suspension Buffer to reach a final volume of 200 µl.

Subsequently, the Pre-mix was prepared (**Table 10**) and 3.75 µl were added to each tube (8-well strip Micro PCR tube). Then, 1.25 µl pre-diluted cDNA were added, resulting in a total volume of 5 µl. The tubes were vortexed and centrifuged.

Table 10. Preamplification sample Pre-mix

Component	Volume/ Reaction (μ l)	Volume for 48 Reactions w/Overage (μ l)	Volume for 96 Reactions w/Overage (μ l)
Pre-mix	TaqMan PreAmp	2.5	132
	Master Mix		264
	Pooled STA	0.5	26.4
	Master Mix		52.8
	DNA Suspension	0.75	39.6
	Buffer		79.2
cDNA (μ l)		1.25	
Total volume (μ l)		5	

The tubes were placed in the ThermoCycler using the following PCR program.

Step	Temperature ($^{\circ}$ C)	Time	Cycles
Hold	95	10 min	1
Denaturation	95	15 sec	14
Annealing/elongation	60	4 min	
Hold	4		∞

After the preamplification, unincorporated primers were removed by performing the following Exonuclease I step.

Component	Per 5- μ l Sample (μ l)	48 Samples w/Overage (μ l)	96 Samples w/Overage (μ l)
DNase-free water	1.4	84	168
Exonuclease I Reaction Buffer	0.2	12	24
Exonuclease I (20 U/ μ l)	0.4	24	48
Total (μ l)	2	120	240

2 μ l of the above Master mix was added to each tube, then the tubes were vortexed, centrifuged and placed in the ThermoCycler, using the PCR program listed below.

Cycles	Temperature ($^{\circ}$ C)	Time
Digestion	37	30 min
Inactivation	80	15 min
Hold	4	∞

The products were diluted 5-fold by adding 18 μ l DNA Suspension Buffer to the final volume of 25 μ l. The diluted reactions were stored at -20° C for further use.

2.2.5.2 Preparing Sample Pre-Mix and samples

The Sample Pre-Mix was prepared and 3.3 μ l of it was added to each well of a 96-well plate. Next, 2.7 μ l of preamplified and Exonuclease I-treated samples were added to the individual wells. The plate was vortexed thoroughly and centrifuged. The component of the Sample Mix is depicted below:

Component		Volume per inlet (μl)	Volume per inlet with overage (μl)	Volume for 48.48 IFC overage (μl ; 60 samples)
Sample Pre-Mix	2 \times SsoFast EvaGreen Supermix with low ROX	2.5	3	180
	20 \times DNA Binding Dye	0.25	0.3	18
PreAmp and Exo I-treated sample		2.25	2.7	-
Total Volume (μl)		5	6	-

2.2.5.3 Preparing the Assay Mix

The individual specific forward (100 μM) and reverse (100 μM) primers were combined and 0.6 μl of the combined primers were added to each well of a 96-well plate. 5.4 μl of the Assay Mix were added to each well and the plate was vortexed, centrifuged before pipetting the assays into the Integrated Fluidic Circuit (IFC) inlets. The component of the Assay Mix is shown below:

Component		Volume per inlet (μl)	Volume per inlet with overage (μl)
Assay mix	2 \times Assay Loading Reagent	2.5	3
	1 \times DNA Suspension Buffer	2	2.4
Combined forward and reverse primers (50 μM)		0.5	0.6
Total (μl)*		5	6

* The final concentration of each primer is 5 μM in the inlet and 500 nM in the final reaction

2.2.5.4 Priming and loading the Dynamic Array IFC

To prime the 48.48 IFC, the control line fluid was injected into each accumulator on the IFC. The film on the bottom of the IFC was removed subsequently. Next, the IFC was placed in an integrated fluidic circuit Controller MX (for 48.48 Dynamic Array), and the program: Prime (113×) was used. After the priming step, 5 µl of each assay and 5 µl of each sample were loaded in the respective inlets. Then, the IFC was returned to the IFC Controller MX for loading the chip and the load script: Load Mix (113×) was run. Any dust particles or debris were removed from the IFC surface using a Scotch Tape. The chip was run with the Biomark Gene expression Data Collection software. Parameters required by the set-up of the Biomark were selected and double-checked, and the “thermal protocol: GE 48 × 48 PCR + Melt v2.pcl” was used. The Table Results and Heat Map were imported; the data were analyzed using the $\Delta\Delta C_t$ method, and normalized to the house-keeping gene (*Hprt*).

2.2.6 Real-time quantitative PCR

2.2.6.1 Total RNA isolation

Mice were sacrificed by CO₂ inhalation; the organ biopsies were collected, frozen in dry ice and stored at -80 °C for further analysis.

RNA extraction was performed using the Qiagen RNeasy[®] Plus Universal Kit according to the manufacturer’s protocol. The samples were added to 900 µl of QIAzol™ in 14 ml RNase-free tubes, and homogenized with the Tissue Homogenizer Ultra Turrax T18 Basic. Then 100 µl of gDNA eliminator were added to each sample, and vigorously vortex for 15 s. 180 µl of chloroform were added to the samples, vortexed for 15 s and incubated at RT for 2-3 min. After incubation, the samples were centrifuged at 14,000 rpm for 15 min at 4 °C. The aqueous phase (roughly 600 µl) was transferred to new tubes, and the same volume of 70 % ethanol was added, mixed and subsequently transferred to RNeasy-Mini columns. In the next step, the columns were centrifuged at 14,000 rpm for 20 s at RT. The supernatant was discarded and 700 µl RWT buffer were added to the

columns, centrifuged at 10,000 rpm for 20 s at RT. The flow-through was discarded and 500 µl of RPE buffer were added to the columns, centrifuged at 10,000 rpm for 2 min at RT. The columns were subsequently placed in new collection tubes, centrifuged at 10,000 rpm for 1 min at RT for complete removal of residual liquid. Then the columns were washed twice with 35 µl RNase-free water by centrifugation of 10,000 rpm for 1 min. The desired RNA was contained in the eluate. The RNA samples were stored at -80 °C and the concentration was measured using a Nanodrop device. Protein contamination was measured by its absorbance at 260 nm, and organic contamination was measured at a wavelength of 230 nm. The integrity of RNA was detected using a 1 % agarose gel electrophoresis containing ethidium bromide. RNA was considered intact if two bands of 28 S and 18 S were visible under UV light.

2.2.6.2 Complementary DNA (cDNA) reverse transcription

An amount of 1 µg total RNA was transcribed into double-stranded cDNA using the iScript™ cDNA Synthesis Kit according to the manufacturer's protocol. Briefly, 4 µl of 5 × iScript Reaction Mix and 0.25 µl of iScript Reverse Transcriptase were added to each RNA sample, adjusted to a final volume of 20 µl with Nuclease-free water. The reverse transcription reaction was performed in a thermocycler: Priming for 5 min at 25 °C; Reverse Transcription for 30 min at 42 °C; Inactivation for 5 min at 85 °C.

2.2.6.3 Conventional polymerase chain reaction

The integrity of transcribed cDNA was confirmed by conventional PCR via amplification of house-keeping gene hypoxanthine guanine phosphoribosyl transferase (*Hprt*) and subsequent agarose gel electrophoresis. The PCR reaction mix for each sample is listed in the following:

Table 11. PCR reaction mix

Reagent	Volume (μl)
dd H ₂ O	12.7
Phusion Reaction buffer HF	4
Combined forward/reverse <i>Hprt</i> Primer (10 μM)	1
dNTPs (5 mM)	1
cDNA template	1
PhuS (DNA polymerase)	0.3

The PCR reaction was performed with a Thermocycler Mastercycler EP Gradient using the following reaction program:

Step	Temperature ($^{\circ}\text{C}$)	Time	Cycles
Initialization	98.5	2 min	1
Denaturation	98.5	20 s	
Annealing	64	15 s	30
Elongation	72	20 s	
Final elongation	72	2 min	1

5 μl of Orange G (loading buffer) were added to the PCR products and loaded on a 1 % agarose gel.

2.2.6.4 Real-time quantitative PCR (RT-qPCR)

A RT-qPCT was performed to analyze the relative expression of the target genes using the Applied Biosystems 7500 Real-Time PCR System. For each well, the reaction mix contained 12.5 μl SYBR green, 11 μl ddH₂O, 0.5 μl primer mix and 1 μl of cDNA, loaded into a 96-well Optical Reaction Plate, and the plate was sealed with Bemis[®] Parafilm. The results were analyzed with the $\Delta\Delta\text{Ct}$ method and normalized to the house-keeping gene (*Hprt*).

2.2.7 Enzyme-linked Immunosorbent Assay

Mice were sacrificed on day 4, 5 and 6, blood samples were harvested by heart puncture with a 24G needle, left in BD Microtainer SST tubes for coagulation for at least 30 min at RT, and centrifuged at $14000 \times g$ for 2 min. The serum supernatant was collected after centrifugation and stored at $-20\text{ }^{\circ}\text{C}$ for further analysis.

The protein level of $\text{IFN}\gamma$, IL6 and $\text{TNF}\alpha$ were analyzed using commercial Enzyme Linked Immunosorbent Assay Kits based on the manufacturer's protocol. In brief, Nunc-Immuno™ MicroWell™ 96-well plates were coated with 100 μl coating buffer, sealed with Bemis® Parafilm and incubated overnight in dark at $4\text{ }^{\circ}\text{C}$. On the second day, the plates were washed 4 times with PBST, blocked with 200 μl Assay Diluent and incubated for 1 hour on a shaker at RT. Then the plates were washed 4 times. The serum samples and standards were diluted with Assay Diluent, and added to the appropriate wells. The plates were sealed and incubated at RT for 2 hours with shaking. After washing 4 times, 100 μl Detection Antibody solution was added to each well, the plates were incubated on the shaker for 1 hour at RT. The plates were washed and 100 μl diluted Avidin-HRP solution were added to each well, and incubated for 30 min on a shaker. Afterward, the plates were washed 5 times, soaking for 30 seconds to 1 minute per wash. 100 μl of TMB Substrate Solution were added to each well, incubate in the dark for 15-30 min. In the end, 100 μl Stop Solution were added to each well and the plates were read at 450 nm and 570 nm within 15 min.

2.2.8 Histology and Immunohistochemistry

2.2.8.1 Preparation of biopsies

The biopsies were harvested from mice on day 4, 5 and 6 after the induction of aGvHD. All biopsies of the small intestine were harvested from the central region of the jejunum. The undesired content of the jejunum was flushed out with 4 % PFA using a 24 G needle. Next, the biopsies were fixed with 4 % PFA for 48 hours at RT. After the fixation step, they were cut into three 1 cm pieces, wrapped in filter paper and transferred in histology

cassettes. The samples were dehydrated and embedded in paraffin using the Tissue Processor Excelsior ES at the Institute of Pathology of the University Medical Center Göttingen (Dr. med. Hanibal Bohnenberger). The paraffin-embedded biopsies were sectioned at a thickness of 2 μm using a microtome. Then, hematoxylin and eosin (H&E) and CD3 stainings were performed according to the standard protocols at the Institute of Pathology of the UMG by Jennifer Appelhans from the group of Dr. Bohnenberger using the automatic system Tissue Tek Prisma Slide Stainer.

2.2.8.2 Assessment of histological staining

Histopathological scoring was performed based on H&E staining. Four parameters were assessed in ten fields per slide: 1) Villous blunting (0 = none, 1 = yes; 20 \times magnification), 2) Number of apoptotic cells (40 \times magnification), 3) Inflammation (0 = none, 1 = mild, 2 = moderate without abscess, 3 = presence of abscess, erosion or ulcer; 20 \times magnification), 4) Edema (0 = none, 1 = yes, 20 \times magnification). The sum of all four parameters was used as the final histological score.

The number of CD3⁺ T cells infiltrating to the small intestine was determined based on the immunohistochemical staining. It was counted with photomicrographs using a Zeiss Axio Scope A1 microscope at 20 \times magnification. For each slide, 10 fields were captured, the number of stained T cells was counted, and the average was calculated. All scoring was performed blindly.

2.2.9 RNA sequencing analysis

Total RNA was isolated from the inflamed small intestines and used for RNAseq analysis. Poly(A) RNA was isolated with oligo d(T) beads, transcribed into cDNA, and sequencing libraries were prepared with the TruSeq RNA library Kit. Paired end 50 bp reads from Illumina sequencing were mapped against the mouse mm 9 reference genome with the *Spliced Transcripts Alignment to a Reference* (STAR) software. One outlier sample was removed based on principle component analysis (PCA). Counts were normalized for read depth and only genes with an average read above 100 were used for further analysis using

the BioJupies package with default parameters. The RNAseq was performed and analyzed by Marina Borshiwier under the supervision of Dr. Sebastiaan Meijsing at the Max Planck Institute for Molecular Genetics in Berlin.

2.2.10 Analysis of myeloid cell origin after HSCT in mice

T-cell-depleted bone marrow cells and T cells were isolated from the CD45.1-congenic C57BL/6 mice and transplanted into CD45.2 BALB/c mice to induce aGvHD. On day 6 after disease induction, the mice were sacrificed and spleen and small intestine were harvested.

2.2.10.1 Preparation of splenocytes

The spleens were processed into single cell suspensions by passing through a 40 μ m cell strainer. Next, cells were washed with 40 ml PBS, centrifuged at $300 \times g$ for 7 min at 4 °C, the supernatant was discarded and 4 ml of TAC Lysis Buffer were added to each sample. After incubation at RT for 12 min, the cells were washed with 20 ml PBS, centrifuged and the supernatant discarded. Finally, the splenocytes were resuspended in 1 ml PBS and used for FACS staining.

2.2.10.2 Isolation of lamina propria cells

The small intestine was washed with cold PBS and the Peyer patches were removed, then, the small intestine was cut open longitudinally and placed in a 6-well plate filled with PBS + 60 mM EDTA + 3 mM DTT for 45 min on ice. Next, the samples were transferred to 50 ml tubes filled with 20 ml PBS and shaken vigorously for 1 min to remove the epithelial cells, the process was repeated twice and 10 ml of PBS was used for the last time. 5 ml RPMI++ media were added to the samples to eliminate EDTA, then the samples were cut into small pieces and digested with 4 mg collagenase type II, 4 mg collagenase type 1-A and recombinant 500 U DNase I. The digestion was performed at 37 °C for 30 min, and the samples were vortexed every 10 min during the digestion. In the end, the samples were passed through a 40 μ m cell strainer, centrifuged at $300 \times g$ for

10 min and resuspended with 400 μ l PBS to obtain single cell suspensions. The cells were used for FACS analysis.

2.2.10.3 Flow cytometry analysis

The splenocytes were stained with fluorochrome-conjugated antibodies: anti-CD45.1 and anti-CD45.2, and the lamina propria cells were incubated with anti-mouse CD16/32 for 20 min at 4 °C in dark, and then stained with anti-CD45.1, anti-CD45.2, and anti-CD11b monoclonal antibodies according to our standard protocol. The composition of donor-derived or recipient-derived lymphocytes in spleen and the origin of myeloid cells in lamina propria were analyzed using FACS analysis. The gating strategy is depicted in **Figure 16**.

2.2.11 Preparation of individual cell population from mice

2.2.11.1 Preparation of T cells

T cells were isolated from the spleens of C57BL/6 mice using the EasySep™ Negative Selection Mouse T Cell Isolation Kit as described above (**2.2.2.1.3**).

2.2.11.2 Enrichment of peritoneal macrophages

1 ml of thioglycolate was injected intraperitoneally into BALB/c mice to attract macrophages to the peritoneum. Four days post injection, the mice were sacrificed and a peritoneal lavage was performed. The peritoneal membrane was carefully cut open, and 2 ml of PBS/BSA was injected into the peritoneum, then, it was washed by performing a gentle abdomen massage. The liquid in the peritoneum was collected, and the step was repeated twice. The cells were washed with PBS/BSA, centrifuged 350 \times g, at 4 °C for 5 min and the supernatant was discarded.

2.2.11.3 Preparation of intestinal epithelial cells

The small intestines were harvested from BALB/c mice, and they were processed with the same protocol as for the isolation of lamina propria cells (2.2.10.2), but this time epithelial cells were retained for further analysis after vigorous shaking. The supernatant after each shaking was passed through a 100 μm cell strainer to collect the epithelial cells. The samples were centrifuged at $300 \times g$ for 10 min, and the supernatant was discarded. Next, the pellets were resuspended in 300 μl of EasySep™ Recommended Medium. The cell concentration was adjusted to 1×10^8 cells/ml and used for purification with the EasySep™ Mouse APC Positive Selection Kit based on the manufacturer's protocol. The samples were placed in 5 ml FACS tubes, FcR blocker (10 $\mu\text{l/ml}$) and APC-conjugated CD326 antibody (1 $\mu\text{g/ml}$) were added to each sample, which was then incubated for 15 min at RT. The samples were washed with a 10-fold of excess Recommended Medium, centrifuged and the supernatant was carefully removed with a pipette. The samples were then resuspended in the same initial volume. The Selection Cocktail (100 $\mu\text{l/ml}$) was added to the samples, incubated for 15 min at RT. After the incubation, RapidSpheres™ (50 $\mu\text{l/ml}$) was added and incubated at RT for 10 min. The Recommended Medium was added up to 2.5 ml per sample, mixed and the tubes were placed into the magnet and incubated at RT for 5 min. The supernatant was poured out and the isolated epithelial cells remained in the tubes. This step was repeated two more times and the desired cells were finally harvested from the tubes.

Total RNA was extracted from T cells, peritoneal macrophages and intestinal epithelial cells, reverse transcribed into cDNA, and used for RT-qPCR analysis (2.2.6).

2.2.12 ⁵¹Chromium release assay

2.2.12.1 Preparation of CD8⁺ T cells

On day 6 after the aGvHD induction, CD8⁺ T cells were isolated from the spleens of recipient mice using the EasySep™ Mouse CD8⁺ T Cell Isolation Kit according to the manufacturer's protocol. The single cell suspensions were obtained by passing the spleen

through a 40 μm cell strainer. The cells were adjusted to a concentration of 1×10^8 cells/ml, Rat Serum (50 $\mu\text{l/ml}$) and Isolation Cocktail (50 $\mu\text{l/ml}$) were added to the samples in FACS tubes, and incubated at RT for 10 min. Next, RapidSpheres™ (125 $\mu\text{l/ml}$) was vortexed, added to the samples, and incubated at RT for 5 min. Recommended Medium was then added to each sample up to 2.5 ml. The tubes were placed in the magnet, incubated at RT for 2.5 min, and the enriched CD8⁺ T cells were poured into Falcon tubes for further use.

2.2.12.2 Cytotoxicity assay

Bcl₁ cells were freshly thawed and cultured in a 10 cm cell dish one day before the assay. Bcl₁ cells were harvested and incubated with ⁵¹Chromium at 37 °C for 1 hour. The labeled Bcl₁ cells were subsequently transferred into a 96-well plate, and incubated in the presence of purified CD8⁺ T cells from aGvHD mice at 37 °C for 4 hour. Next, 5 μl of 10% Triton was added to the cells to lyse the cells and release all the chromium. The supernatant from each well was transferred to an absorbent plate. The plate was sealed and the radioactivity was measured using a specific formula. This part of the experiment was performed by Leslie Elsner from the group of Prof. Dr. Ralf Dressel.

2.2.13 Statistical analysis

Statistical analysis was done with GraphPad Prism 5 software. The results of gene expression were analyzed by two-tailed unpaired Student's t-test. A one-way ANOVA followed by a Newman-Keuls multiple comparison test was used for clinical score analysis. The plots of qPCR and histological score were analyzed using Student's t-test. A Log-rank Mantel-Cox test was performed to analyze the survival curve of aGvHD/GvL mouse model and a Kruskal-Wallis test followed by Dunn's Multiple Comparison test was used for the analysis of lymphomagenesis. Data are presented as mean + standard error and considered significant if p-value was ≤ 0.05 , the significance was depicted as: n.s., $p > 0.05$; *, $p < 0.05$; **, $p < 0.01$; ***, $p < 0.001$.

3. Results

3.1 Transplantation of GC-resistant allogeneic T cells as well as GC-resistant myeloid cells into recipients both aggravate aGvHD in mice

Allogeneic T cells are thought to be the main cause of aGvHD (Perkey and Maillard, 2018). In addition, targeting recipient APCs that are largely composed of myeloid cells was also found to be a promising therapeutic intervention to aGvHD (Shlomchik, 1999). Besides, macrophages in the host are the cell population that is most resistant against irradiation during HSCT (Haniffa et al., 2009). Previously, it was shown in our group that GR-deficient allogeneic T cells transferred into recipient mice resulted in a more aggressive aGvHD in comparison to the transfer of wild type allogeneic T cells, which highlighted the importance of endogenous GCs in the modulation of aGvHD (Theiss-Suennemann et al., 2015). More specifically, suppression of the function of CD8⁺ T cells was necessary to control aGvHD by endogenous GCs in this model. To confirm the contribution of GC-resistant (GR^{lck}) allogeneic T cells to aGvHD, we transferred 2×10^6 T cells from GR^{lck} mice or GR^{fllox} mice as a control in combination with 1×10^7 T cell-depleted (TCD) bone marrow cells purified from C57BL/6 mice into lethally irradiated BALB/c mice via tail vein injection to induce murine aGvHD as outlined in **Figure 5**. During the development of aGvHD, we scored the mice from day 2 to 6 based on five clinical parameters. We found that mice transferred with GC-resistant (GR^{lck}) or GC-responsive (GR^{fllox}) T cells both developed aGvHD while those mice only receiving bone marrow cells did not (**Figure 10A**). The disease especially exaggerated between day 5 and 6. Moreover, mice transplanted with GR^{lck} T cells suffered from a more severe aGvHD on day 6 after disease induction than mice receiving GR^{fllox} T cells (**Figure 10B**). To additionally assess the impact of endogenous GCs on recipient myeloid cells, we induced aGvHD by transplanting wild type allogeneic T cells isolated from C57BL/6 mice into GR^{lysM} mice or as a control into GR^{fllox} BALB/c mice (**Figure 5**). It is noteworthy that myeloid cells in GR^{lysM} mice are GC-resistant. On day 6 after transplantation, GR^{lysM} and GR^{fllox} mice both developed aGvHD, and the disease was more severe in GR^{lysM} mice than in GR^{fllox} mice (**Figure 10C**). The murine aGvHD model

involving GC-resistant myeloid cells and its scoring were carried out by my colleague Tina Kaiser.

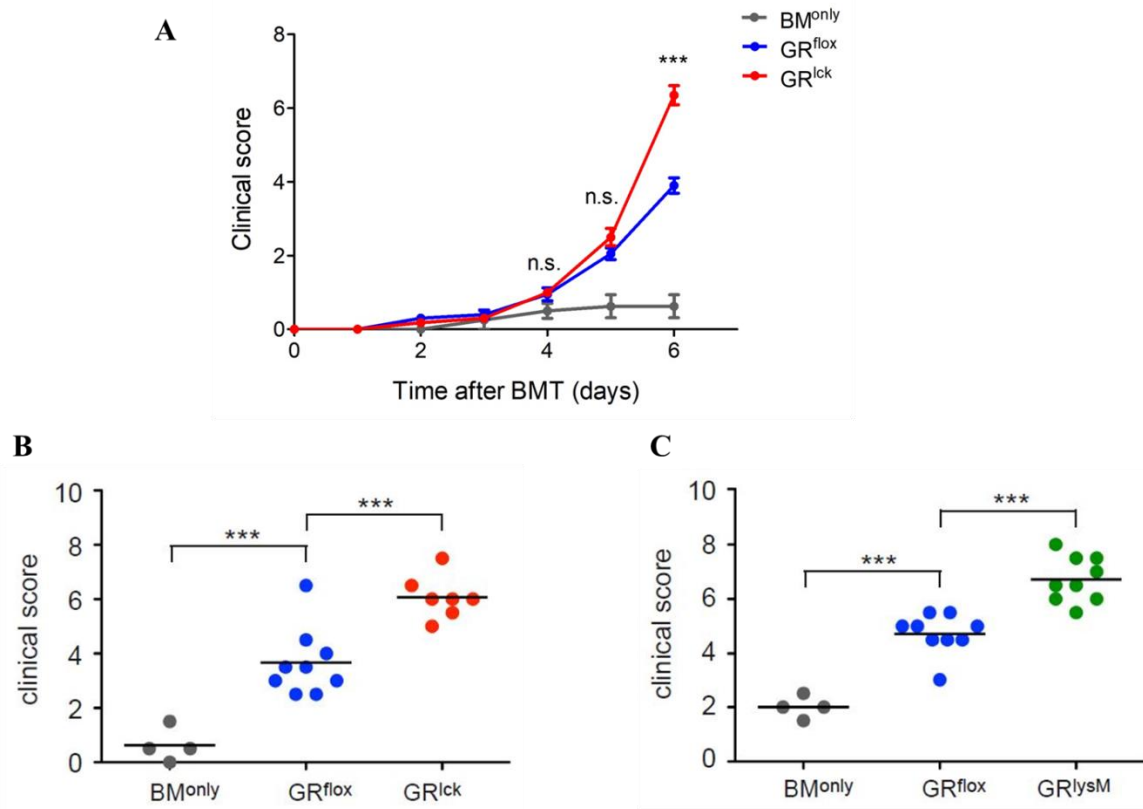


Figure 10. Clinical scores of mice suffering from aGvHD after HSCT. Allogeneic T cells were magnetically purified from C57BL/6 mice and injected into the tail vein of BALB/c mice in combination with TCD bone marrow cells to induce aGvHD, and the transfer of only bone marrow cells (BM^{only}) served as a control. (A) Recipient mice were transferred with either GC-resistant (GR^{lck}) or GC-responsive (GR^{flox}) T cells and were scored from day 2 to 6 based on five parameters: activity, posture, fur texture, diarrhea, and weight loss. N=4/9/7 (BM^{only}/ GR^{flox}/ GR^{lck}). (B) Clinical score on day 6 of individual mice injected with GC-resistant (GR^{lck}) or GC-responsive (GR^{flox}) T cells. Data refer to the same experiment as in panel A. (C) Wild type allogeneic T cells were transferred into recipient mice with GC-resistant (GR^{lysM}) or GC-responsive (GR^{flox}) myeloid cells to induce aGvHD and the clinical score was determined on day 6. N=4/9/9 (BM^{only}/ GR^{flox}/ GR^{lysM}). Statistical analysis was performed using One-way ANOVA followed by a Newman-Keuls Multiple Comparison Test (***) p<0.001; n.s., not significant) (Li et al., 2019).

3.2 GC-resistance does not alter the phenotypes of the transferred allogeneic T cells

To study the impact of endogenous GCs on allogeneic donor T cells in the context of aGvHD in mice, we took advantage of cell type-specific GR-deficient mice, namely GR^{lck} mice in which the GR is deleted in the entire T cell lineage (Theiss-Suennemann et al., 2015). Since aGvHD is mainly driven by allogeneic T cells, and as the difference on the composition of the transplanted T cells might impact the pathogenesis of aGvHD in mice, immunological features including T cell subset frequencies, the activation condition of T cells, and the expression level of adhesion molecules and chemokine receptors on the cell surface were analyzed in both genotypes. To this end, we performed a flow cytometric analysis to compare the phenotype of GC-resistant (GR^{lck}) and GC-responsive (GR^{flox}) T cells.

3.2.1 Lack of the GR in T cells has no impact on cell frequencies

In order to investigate the frequencies of individual subsets amongst the transferred T cells, we purified them from GR^{lck} and GR^{flox} C57BL/6 mice by magnetic negative selection. Then, the cells were stained with specific fluorochrome-labelled monoclonal antibodies. The FACS gating strategies used to determine CD4⁺, CD8⁺ and regulatory (T_{reg}) T cells are depicted in **Figure 11A** and **B**. No significant differences were found in the percentages of these T cell subtypes between GR^{lck} and GR^{flox} mice (**Figure 11C**) and also the ratio of CD4⁺/CD8⁺ T cells was the same (**Figure 11D**).

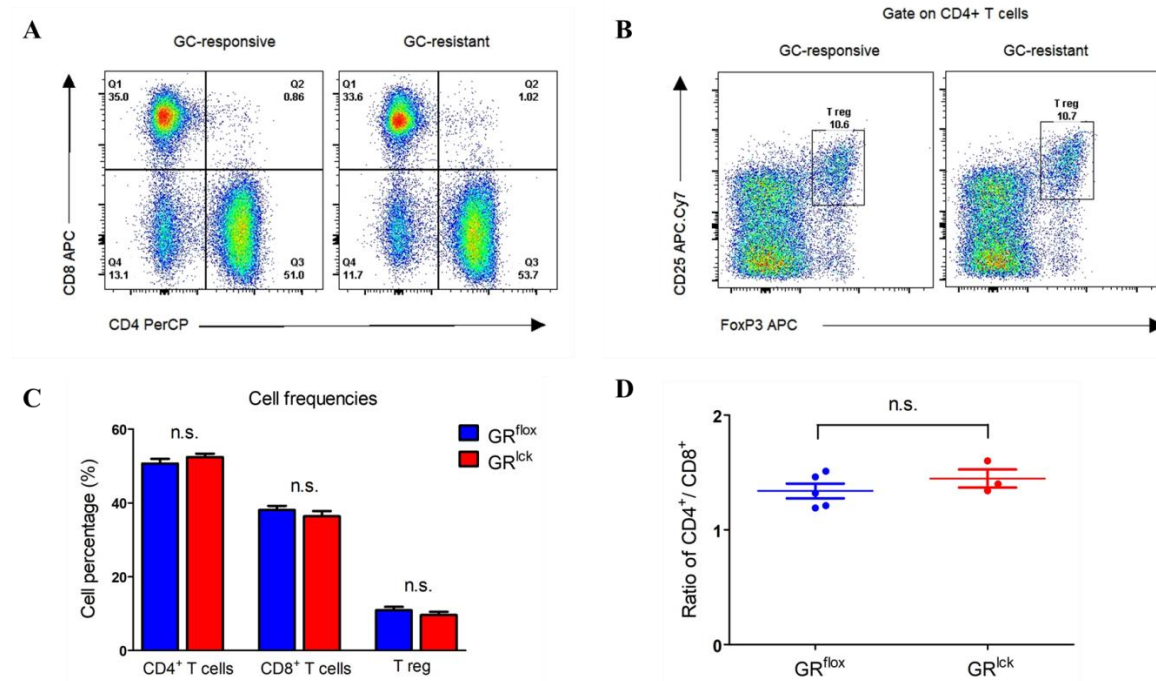


Figure 11. Percentages of CD4⁺, and CD8⁺ T cells as well as Treg cells amongst the GC-resistant and GC-responsive T cells used for transplantation. T cells were magnetically purified from GR^{lck} and GR^{flox} C57BL/6 mice and stained with fluorochrome-conjugated antibodies: CD4⁺ T cells (CD4-PerCP), CD8⁺ T cell (CD8-APC), T_{reg} (CD4-PerCP, CD25-APC-Cy7, and FoxP3-APC). The stained cells were subsequently used for cytometric analysis. (A) Gating strategy for CD4⁺ and CD8⁺ T cells. (B) Gating strategy for T_{reg} cells. (C) Frequencies of T cell subsets amongst GC-resistant and GC-responsive T cells. (D) Ratio of CD4⁺/CD8⁺ T cells amongst GC-resistant and GC-responsive T cells. N= 5/3 (GR^{flox}/GR^{lck}). Statistical analysis was done using unpaired Student's t-test, n.s.: not significant; (Li et al., 2019).

3.2.2 GC-resistant T cells show a comparable activation level as GC-responsive T cells

We additionally stained the isolated T cells from GR^{lck} and GR^{flox} C57BL/6 mice with anti-CD44 and anti-CD62L antibodies to determine their activation state (**Figure 12A**). GC-resistant CD4⁺ T cells showed the same level of activation as GC-responsive CD4⁺ T cells, while CD8⁺ T cells from GR^{lck} mice were slightly more activated in comparison to GR^{flox} CD8⁺ T cells, although the difference was not significant (**Figure 12B**).

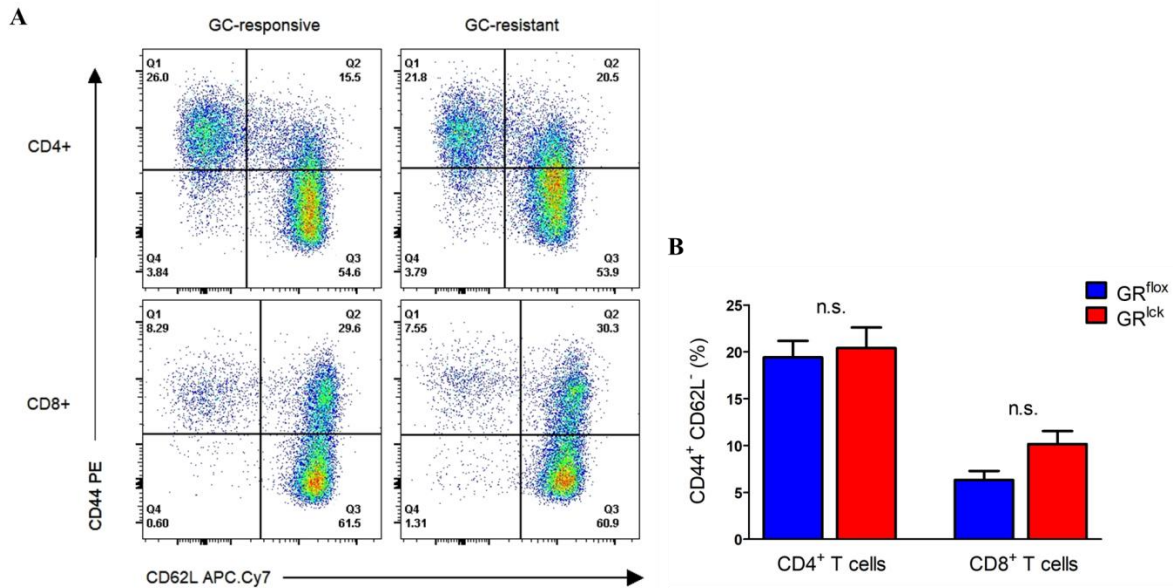


Figure 12. Activation state of GC-resistant and GC-responsive T cells. T cells were magnetically purified from GR^{lck} and GR^{lox} C57BL/6 mice, and stained with fluorochrome-conjugated antibodies: PercP-CD4, APC-CD8, PE-CD44 and APC-Cy7-CD62L. The stained cells were subsequently used for flow cytometric analysis. **(A)** Activated T cells were gated as CD44⁺CD62L⁻ cells in all four experimental groups. **(B)** Percentages of CD44⁺CD62L⁻ cells amongst CD4⁺ T cells and CD8⁺ T cells. N= 5/3 (GR^{lox}/GR^{lck}). Statistical analysis was done using unpaired Student's t-test, n.s.: not significant; (Li et al., 2019).

3.2.3 GC-resistant and GC-responsive T cells show similar levels of adhesion molecules and chemokine receptors on the cell surface

To test the surface expression level of integrins and chemokine receptors on the transplanted T cells, we stained CD4⁺ and CD8⁺ T cells with fluorochrome-conjugated antibodies against CD11a (subunit of LFA-1), CD49d (subunit of VLA-4), and the chemokine receptor CXCR3 (**Figure 13A**). The surface levels of the adhesion molecules CD11a and CD49d as well as the chemokine receptor CXCR3 did not significantly differ between GC-resistant and GC-responsive T cells (**Figure 13B**).

In conclusion, GR-deficiency in T cells neither impacts the phenotypes nor the activation state of the transplanted T cells. Therefore, GC-resistant T cells have similar phenotypic characteristics as GC-responsive T cells.

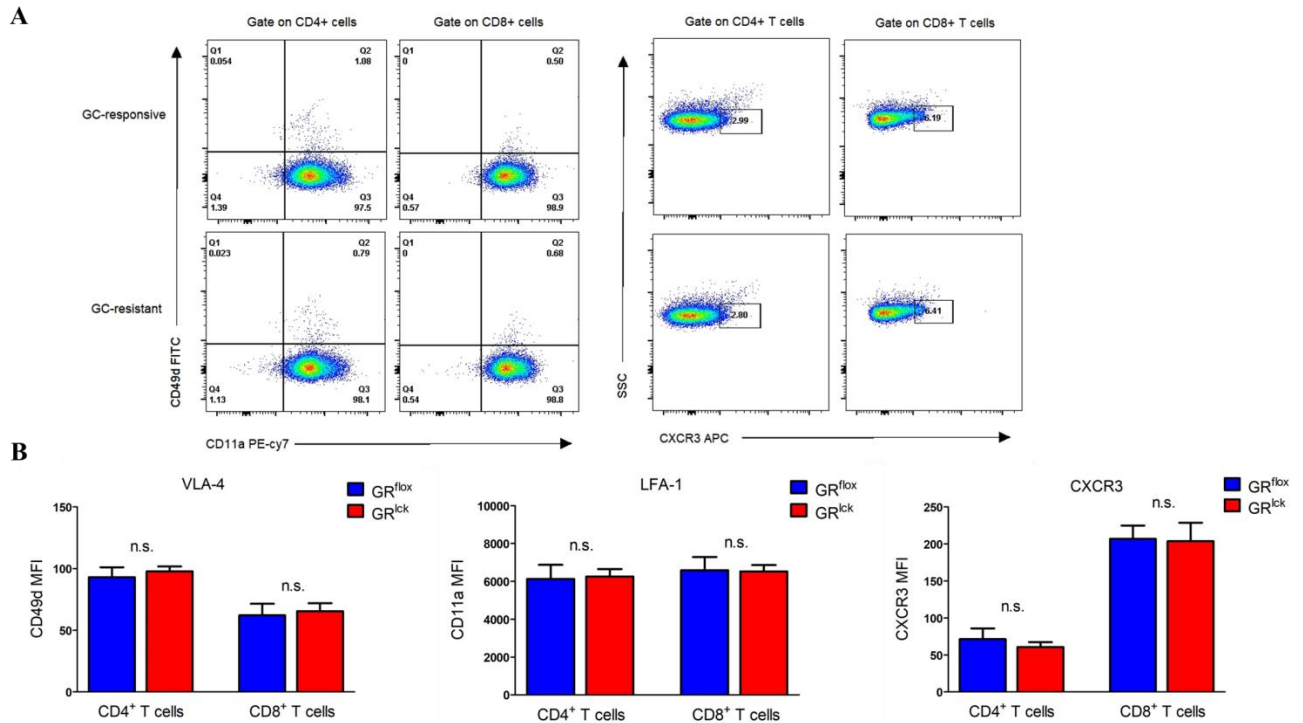


Figure 13. Expression levels of adhesion molecules and chemokine receptors on the surface of GC-resistant and GC-responsive T cells. T cells were magnetically purified from GR^{lck} and GR^{flox} C57BL/6 mice, and stained with fluorochrome-conjugated antibodies: CD4-PerCP, CD8-APC or CD8-PE-Cy7, CD11a-PE-Cy7 and CD49d-FITC or CXCR3-APC. The stained cells were subsequently used for flow cytometric analysis. **(A)** Gating strategies for the analysis of LFA-1, VLA-1, and CXCR3. **(B)** Mean fluorescence intensity of CD11a, CD49d, and CXCR3 on CD4⁺ or CD8⁺ T cells. N= 5/3 (GR^{flox}/GR^{lck}). Statistical analysis was done using unpaired Student's t-test, n.s.: not significant; (Li et al., 2019).

3.3 Transplantation of allogeneic GC-resistant T cells results in increased systemic cytokine level and an up-regulation of disease-associated genes in aGvHD target organs

During the development of aGvHD, pro-inflammatory cytokines such as IFN- γ and IL-6 secreted by T cells, APCs and even non-hematopoietic cells, make an essential contribution (Baake et al., 2018). To test the production of cytokines, we induced aGvHD by infusing GC-resistant (GR^{lck}) and GC-responsive (GR^{flox}) T cells into lethally irradiated mice and sacrificed them on day 6 after disease induction. The blood was collected for the analysis of cytokine production using commercial ELISA kits. Transfer

of allogeneic T cells led to an increased production of IFN- γ and IL-6, compared to the transplantation of only bone marrow cells. Moreover, the serum protein levels of these two cytokines were significantly higher in mice transplanted with GC-resistant T cells compared to those transferred with GC-responsive T cells (**Figure 14**), suggesting that mice receiving GC-resistant T cells experience a more severe aGvHD partially due to the contribution of systemic pro-inflammatory cytokines.

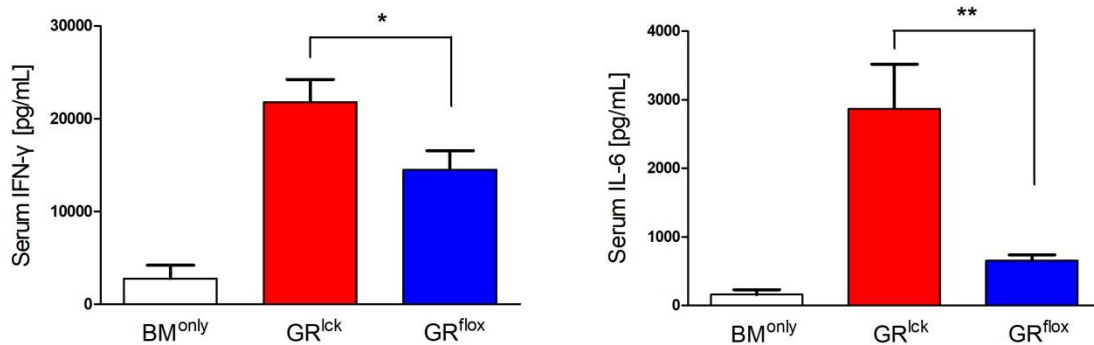


Figure 14. Serum protein levels of IFN- γ and IL-6 in the blood of mice suffering from aGvHD. The lethally irradiated BALB/c mice were transferred with GC-resistant (GR^{lck}) or GC-responsive (GR^{flox}) T cells in combination with TCD bone marrow cells purified from C57BL/6 mice. Mice were sacrificed on day 6 after disease induction and the blood was collected via heart puncture. The protein levels of IFN- γ and IL-6 were measured by ELISA. N=5/9/10 (BM^{only}/GR^{flox}/GR^{lck}). The data were analyzed by unpaired Student's t-test, *, $p < 0.05$; **, $p < 0.01$.

Results

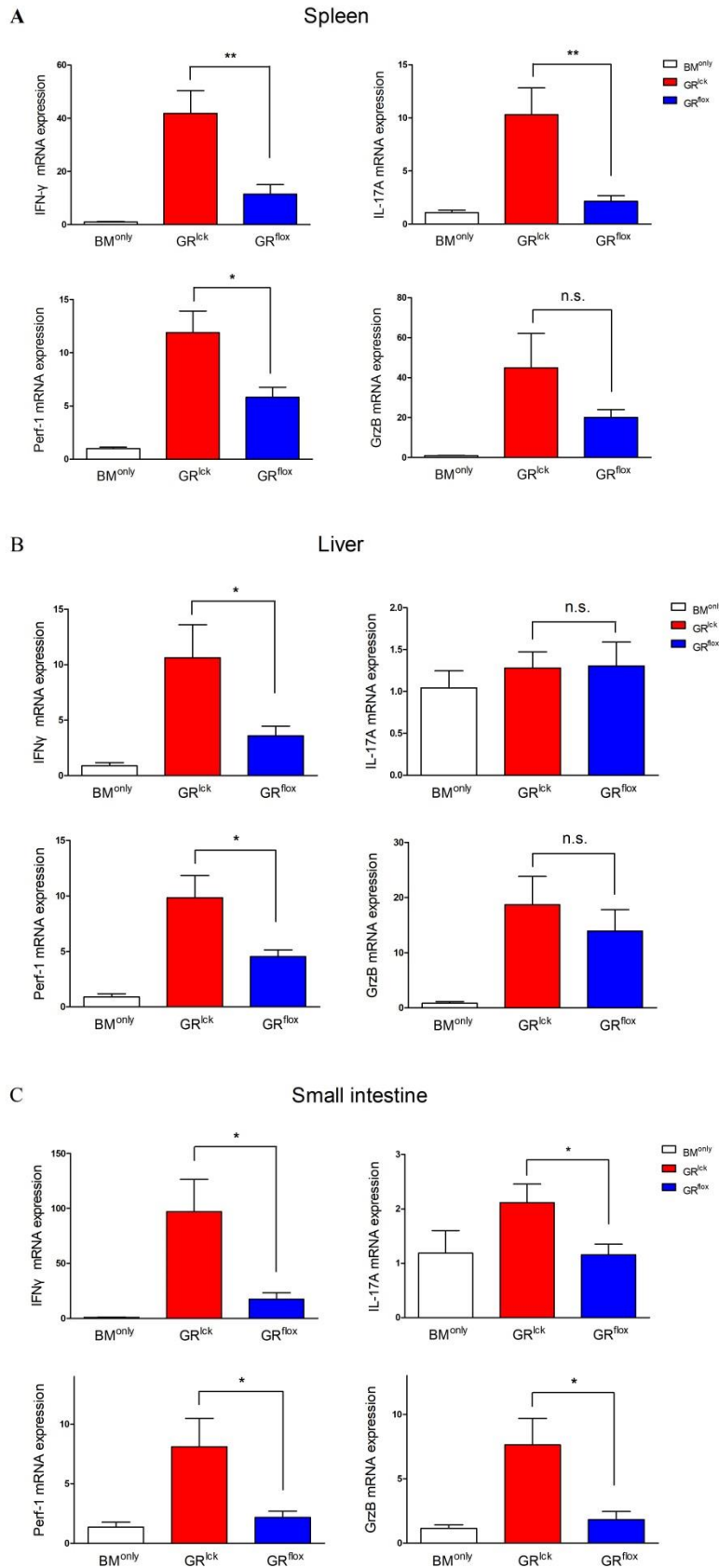


Figure 15. Gene expression of IFN- γ , Perf-1, GzmB, and IL-17 in spleen, liver and small intestine of mice suffering from aGvHD induced by transfer of GC-resistant T cells. Lethally irradiated BALB/c mice were transferred with GC-resistant (GR^{lck}) or GC-responsive (GR^{flx}) T cells in combination with TCD bone marrow cells purified from C57BL/6 mice. Mice were sacrificed on day6 after disease induction. RNA was isolated from the spleen, liver and small intestine, and transcribed into cDNA. The cDNA was used for RT-qPCR analysis. Relative mRNA levels of IFN- γ , Perf-1, GzmB, and IL-17 were analyzed in spleen (A), liver (B), and small intestine (C) after normalization to the house-keeping gene Hprt. N=4/9/8 (BM^{only}/GR^{flx}/GR^{lck}). Statistical analysis was performed by unpaired Student's t-test, *, $p < 0.05$; **, $p < 0.01$; n.s., not significant.

To detect the impact of GR-deficiency in T cells on gene transcription, we isolated RNA from the two aGvHD target organs liver and small intestine and from the secondary lymphoid organ spleen, transcribed it into cDNA and analyzed the relative expression of four genes. In the spleen, *IFN- γ* , *Perf-1*, *Gzmb*, and *IL-17* were up-regulated in aGvHD mice; the expression of *IFN- γ* , *Perf-1*, and *IL-17* were significantly more increased in mice receiving GC-resistant T cells in comparison to those receiving GC-responsive T cells, and *Gzmb* was also further up-regulated in mice transplanted with GR^{lck} T cells but this was not significant (**Figure 15A**). In the liver, only two genes, *IFN- γ* and *Perf-1* were found to be significantly increased in mice transplanted with GC-resistant T cells, compared to those ones transferred with GC-responsive T cells (**Figure 15B**). In contrast, transcriptional levels of all four genes were significantly increased in the small intestine of mice receiving GR^{lck} T cells (**Figure 15C**). Collectively, our data suggest that mice transplanted with GC-resistant T cells suffer from a more severe aGvHD, and show an increased production of pro-inflammatory cytokines at both the protein and mRNA level. Expression analysis of the small intestine indicates that key genes of aGvHD in this target organ are altered in mice, for which reason biopsies of the inflamed small intestine were prepared for further gene expression analysis.

3.4 GC-resistance of allogeneic T cells but not myeloid cells alters the gene expression profile in the inflamed small intestine in mice undergoing aGvHD

The pathogenesis of aGvHD in mice can be subdivided into several phases as outlined earlier: priming of APCs, activation, proliferation and migration of donor allogeneic T cells, and the effector phase of activated donor T cells in the target organs (Ferrara et al., 2009). During the development of aGvHD, various cytokines, chemokines, and chemokine receptors play a critical role, and allogeneic donor T cells are considered as the main contributor to aGvHD. Furthermore, T cells undergo a series of metabolic changes upon being activated, to meet dramatic needs for ATP production and metabolic intermediates required by biomass synthesis and the shift from oxidative phosphorylation at a quiescence state to aerobic glycolysis (Buck et al., 2015; Wahl et al., 2012).

Therefore, metabolism related enzymes, transporters, and regulators of the metabolic switch involved in autoimmune disorders and T-cell metabolism were suggested as targets for therapeutic intervention (MacIver et al., 2013; O'Sullivan and Pearce, 2015). To identify genes that were differentially regulated when allogenic T cells were GC-resistant, we checked the literature and selected 54 genes that we considered to be related to the immunosuppressive functions of GCs in the context of mouse aGvHD. These selected genes were categorized into five groups: category 1 and 2 contained cytokines and chemokines, respectively (**Table 12**); category 3 included cell surface molecules involved in cell adhesion, co-stimulation, apoptosis induction and pathogen-recognition; category 4 encompassed intracellular proteins mostly with enzymatic activity (**Table 13**), and the final category 5 consisted of genes linked to cellular energy metabolism and nutrient transport (**Table 14**).

We induced aGvHD using GC-resistant allogenic T cells (GR^{lck}), recipient mice harboring GC-resistant myeloid cells (GR^{lysM}), or the respective controls, and sacrificed mice on day 6 after disease induction. The inflamed small intestines were collected and used for RNA isolation. The expression levels of the 54 selected genes were determined by Fluidigm[®] gene chip analysis. In the first category related to cytokines, the majority of the selected genes, *Csf2*, *Il4*, *Il2*, *Il1b*, *Il10*, *Il12*, and *Il6*, were significantly up-regulated in mice receiving GC-resistant allogenic T cells (GR^{lck}), relative to mice receiving wild type GC-responsive allogenic T cells (GR^{fllox}). The results are depicted as the fold change between both groups on day 6 after aGvHD induction. In contrast, no differences were found concerning the expression profile of any of the selected genes between GR^{lysM} and wild type GR^{fllox} recipient mice transferred with wild type T cells (**Table 12**).

In the second group, all the selected genes associated with chemokines (*Ccl5*, *Cxcl9*, *Cxcl11*, *Cxcl10*, *Ccl3*, *Ccl7*, *Ccl2*, *Cxcl5*, *Cxcl13*, and *Cxcl1*) were transcriptionally increased in mice transferred with GR^{lck} T cells compared to those ones receiving GR^{fllox} T cells on day 6 after disease induction. Similar to the category 1, the expression profile of these chemokine-related genes was unaltered between mice harboring GR^{lysM} and GR^{fllox} myeloid cells (**Table 12**).

Encoded molecule	Gene symbol	GR ^{lck} vs. GR ^{flox} at day 6		GR ^{lysM} vs. GR ^{flox} at day 6	
		Fold change	Unpaired t-test	Fold change	Unpaired t-test
TNF α	<i>Tnf</i>	1.6	n.s.	0.8	n.s.
M-CSF	<i>Csf1</i>	1.6	n.s.	1.0	n.s.
IL-33	<i>Il33</i>	1.7	n.s.	1.6	n.s.
GM-CSF	<i>Csf2</i>	2.1	*	1.2	n.s.
IL-4	<i>Il4</i>	2.5	**	0.8	n.s.
IL-2	<i>Il2</i>	2.6	***	1.2	n.s.
IL-1 β	<i>Il1b</i>	2.8	*	1.1	n.s.
IL-10	<i>Il10</i>	2.9	*	1.2	n.s.
IL-12	<i>Il12</i>	3.5	***	1.2	n.s.
IL-6	<i>Il6</i>	13.7	*	1.0	n.s.
CCL5	<i>Ccl5</i>	1.7	*	1.1	n.s.
CXCL9	<i>Cxcl9</i>	2.2	*	1.2	n.s.
CXCL11	<i>Cxcl11</i>	2.4	**	1.2	n.s.
CXCL10	<i>Cxcl10</i>	3.1	**	1.2	n.s.
CCL3	<i>Ccl3</i>	3.6	**	1.1	n.s.
CCL7	<i>Ccl7</i>	5.1	**	1.3	n.s.
CCL2	<i>Ccl2</i>	5.3	*	1.0	n.s.
CXCL5	<i>Cxcl5</i>	5.9	**	1.1	n.s.
CXCL13	<i>Cxcl13</i>	6.1	**	1.6	n.s.
CXCL1	<i>Cxcl1</i>	6.4	*	1.2	n.s.

Table 12. Expression analysis of cytokine and chemokine genes potentially important in the context of murine aGvHD. Two mouse aGvHD models were either induced by transferring GC-resistant (GR^{lck}) or GC-responsive (GR^{flox}) T cells isolated from C57BL/6 mice into lethally irradiated wild type BALB/c mice, or by transferring wild type C57BL/6 allogeneic T cells into GR^{lysM} (with GC-resistant myeloid cells) or GR^{flox} BALB/c mice (with GC-responsive myeloid cells). On day 6 after disease induction, RNA was isolated from the inflamed small intestines, transcribed into cDNA, and subsequently used for high-throughput qPCR analysis. The upper part of the table represents the category of cytokines; the lower part represents the category of chemokines. The data are presented as fold-change with a different color code, yellow for no changes, light green for ≤ 3 -fold, and dark green for > 3 -fold changes. N=9/10 (GR^{flox} / GR^{lck}) and N=8/9 (GR^{flox} / GR^{lysM}). Statistical analysis was performed using unpaired Student's t-test, *, $p < 0.05$; **, $p < 0.01$; ***, $P < 0.001$; n.s., not significant; (Li et al., 2019).

In the third group of genes related to cell surface molecules, the transcriptional levels of many of them (*Cd14*, *Klrk1*, *Cd28*, *Itgb2*, *Fasl*, *Chil3*, and *Ctla4*) were increased in mice transplanted with GC-resistant T cells (GR^{lck}), in comparison to those transferred with GC-responsive T cells (GR^{flox}). However, in GR^{lysM} mice receiving wild type allogeneic T cells, only two genes were transcriptionally altered (*Itgam* was down-regulated and *Cd14* was up-regulated), compared to GR^{flox} recipient mice (**Table 13**). In the fourth category, three genes (*Ptgs2*, *Dusp1*, and *Arg1*) were significantly up-regulated in mice transplanted with GC-resistant T cells and only one gene *Ptgs2* was increased on the transcriptional level in recipient mice with GC-resistant myeloid cells (GR^{lysM}), relative to their controls with GC-responsive myeloid cells (GR^{flox}) (**Table 13**).

Encoded molecule	Gene symbol	GR ^{lck} vs. GR ^{flox} at day 6		GR ^{lysM} vs. GR ^{flox} at day 6	
		Fold change	Unpaired t-test	Fold change	Unpaired t-test
MHC II	<i>H2-Aa</i>	1.0	n.s.	0.9	n.s.
CD11a	<i>Itgal</i>	1.5	n.s.	1.7	n.s.
CD11b	<i>Itgam</i>	1.8	n.s.	0.45	*
TLR4	<i>Tlr4</i>	2.1	n.s.	1.6	n.s.
CD14	<i>Cd14</i>	2.2	*	1.8	**
NKG2D	<i>Klrk1</i>	2.2	*	1.2	n.s.
CD28	<i>Cd28</i>	2.6	*	1.1	n.s.
CD18	<i>Itgb2</i>	2.6	**	1.2	n.s.
CD95L	<i>Fasl</i>	3.6	**	1.0	n.s.
YM1	<i>Chil3</i>	5.3	*	0.9	n.s.
CTLA4	<i>Ctla4</i>	5.6	**	1.1	n.s.
ERK2	<i>Mapk1</i>	1.1	n.s.	0.8	n.s.
NOX2	<i>Cybb</i>	1.2	n.s.	1.5	n.s.
GILZ	<i>Tsc22d3</i>	1.3	n.s.	1.0	n.s.
COX2	<i>Ptgs2</i>	1.6	*	1.4	*
iNOS	<i>Nos2</i>	1.8	n.s.	1.3	n.s.
DUSP1	<i>Dusp1</i>	3.9	**	1.3	n.s.
ARG1	<i>Arg1</i>	8.9	*	0.9	n.s.

Table 13. Expression analysis of genes related to cell surface molecules and intracellular proteins in the context of murine aGvHD. Two mouse aGvHD models were either induced by transferring GC-resistant (GR^{lck}) or GC-responsive (GR^{flx}) T cells isolated from C57BL/6 mice into lethally irradiated wild type BALB/c mice, or by transferring wild type C57BL/6 allogeneic T cells into GR^{lysM} (with GC-resistant myeloid cells) or GR^{flx} BALB/c mice (with GC-responsive myeloid cells). On day 6 after disease induction, RNA was isolated from the inflamed small intestines, transcribed into cDNA, and subsequently used for high-throughput qPCR analysis. The upper part of the table represents the category of cell surface molecules; the lower part represents the category of intracellular proteins. The data are presented as fold-change with a different color code, yellow for no changes, light green for ≤ 3 -fold, dark green for > 3 -fold, and light blue ≥ 0.3 -fold changes. N=9/10 (GR^{flx} / GR^{lck}) and N=8/9 (GR^{flx} / GR^{lysM}). Statistical analysis was performed using unpaired Student's t-test, *, $p < 0.05$; **, $p < 0.01$; n.s., not significant; (Li et al., 2019).

In the fifth category, we analyzed the expression of genes relevant for metabolic reprogramming of T cells. Amongst the selected genes, only three (*Hk2*, *Hif1a*, *Slc2a1*) were significantly up-regulated in mice receiving GC-resistant T cells (GR^{lck}), and no genes were found to be altered between GR^{lysM} and GR^{flx} mice transplanted with wild type allogeneic T cells (**Table 14**).

Encoded molecule	Gene symbol	GR ^{lck} vs. GR ^{flx} at day 6		GR ^{lysM} vs. GR ^{flx} at day 6	
		Fold change	Unpaired t-test	Fold change	Unpaired t-test
PGC-1 α	<i>Ppargc1a</i>	0.6	n.s.	0.9	n.s.
Estrogen-related receptor α	<i>Esrra</i>	0.7	n.s.	0.9	n.s.
HMG-CoA reductase	<i>Hmgcr</i>	0.8	n.s.	0.9	n.s.
Carnitine palmitoyltransferase 1A	<i>Cpt1a</i>	0.9	n.s.	1.0	n.s.
Phosphofructokinase, liver type	<i>Pfkl</i>	0.9	n.s.	1.1	n.s.
Slc7a5 / LAT1	<i>Slc7a5</i>	1.0	n.s.	1.0	n.s.
mTOR	<i>Mtor</i>	1.0	n.s.	0.9	n.s.
Pyruvate dehydrogenase E1 α 1	<i>Pdha1</i>	1.1	n.s.	1.1	n.s.
Aldolase A	<i>Aldoa</i>	1.1	n.s.	1.1	n.s.
Acetyl-CoA carboxylase α	<i>Acaca</i>	1.2	n.s.	1.2	n.s.
c-Myc	<i>Myc</i>	1.2	n.s.	1.3	n.s.
Slc1a5 / ASCT2	<i>Slc1a5</i>	1.3	n.s.	1.4	n.s.
AMP-activated protein kinase α 1	<i>Prkaa1</i>	1.3	n.s.	1.1	n.s.
Hexokinase 2	<i>Hk2</i>	2.0	*	1.1	n.s.
Hypoxia-inducible factor 1 α	<i>Hif1a</i>	2.1	*	1.1	n.s.
Slc2a1 / Glut1	<i>Slc2a1</i>	3.4	*	1.0	n.s.

Table 14. Expression analysis of genes involved in metabolic changes in the context of murine aGvHD. Two mouse aGvHD models were either induced by transferring GC-resistant (GR^{lck}) or GC-responsive (GR^{lox}) T cells isolated from C57BL/6 mice into lethally irradiated wild type BALB/c mice, or by transferring wild type C57BL/6 allogeneic T cells into GR^{lysM} (with GC-resistant myeloid cells) or GR^{lox} BALB/c mice (with GC-responsive myeloid cells). On day 6 after disease induction, RNA was isolated from the inflamed small intestines, transcribed into cDNA, and subsequently used for high-throughput qPCR analysis. The data are presented as fold-change with a different color code, yellow for no changes, light green for ≤ 3 -fold, and dark green for > 3 -fold changes. N=9/10 (GR^{lox} / GR^{lck}) and N=8/9 (GR^{lox} / GR^{lysM}). Statistical analysis was performed using unpaired Student's t-test, *, $p < 0.05$; n.s., not significant; (Li et al., 2019).

Taken together, our data on the gene expression profile highlight the importance of T cells as a major target of GC actions in the context of a mouse aGvHD.

3.5 Myeloid cells in the inflamed small intestine are partially reconstituted in recipient mice after aGvHD induction

In our gene expression profiling of 54 selected genes that are involved in potential effects of GCs on aGvHD, we found that the deficiency of the GR in myeloid cells of recipient mice (GR^{lysM}) barely altered the expression levels of the selected genes (**Table 12, 13, and 14**). To explore the possible mechanisms, the origin of myeloid cells in recipient mice was analyzed. We conducted aGvHD induction by purifying allogeneic T cells and TCD-bone marrow cells from wild type C57BL/6 mice on a CD45.1 genetic background, and transferred them into BALB/c mice on a CD45.2 genetic background. Mice were sacrificed on day 6 after disease induction. Single-cell suspensions of splenocytes were obtained by passing them through a cell strainer, and lamina propria cells were isolated by enzymatic digestion as described in the Material and Method section.

The origin of splenocytes as well as of myeloid cells in the inflamed small intestine was analyzed by flow cytometry. On day 6 after aGvHD induction, the majority of splenocytes in recipient mice were donor-derived, approximately 90% of splenocytes expressing the CD45.1 allele (**Figure 17**). However, around 75% of the myeloid cells that reside in the lamina propria of the inflamed small intestine were still derived from the recipient, whereas donor-derived myeloid cells only accounted for a relatively small

proportion of approximately 25% (**Figure 17**). This indicates that myeloid cells in the small intestine are only partially reconstituted in recipient mice after TBI.

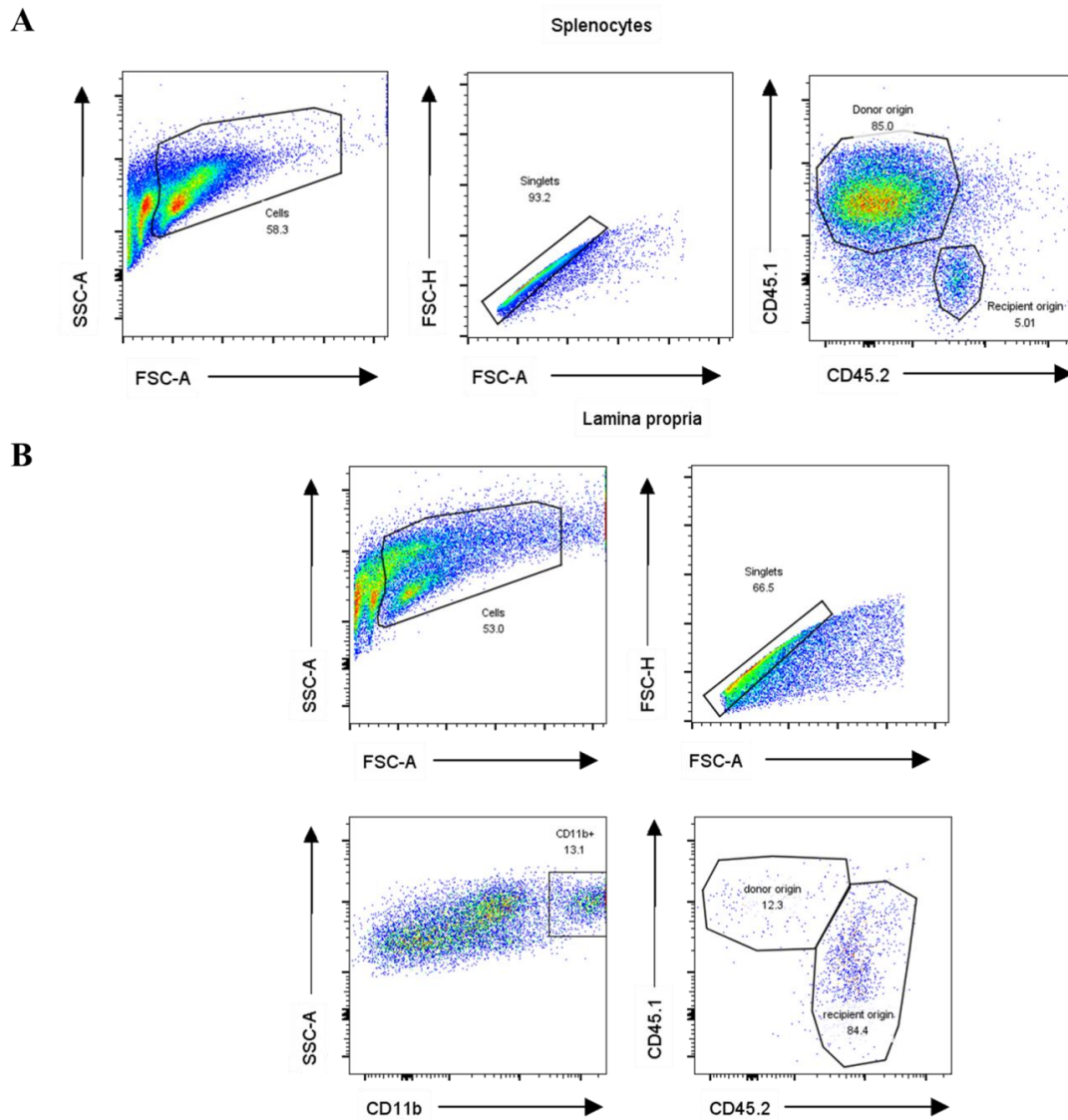


Figure 16. Gating strategies used to determine the origin of splenocytes as well as myeloid cells in the small intestine of aGvHD mice. Murine aGvHD was induced by infusing wild type T cells in a combination with TCD bone marrow cells purified from C57BL/6 mice expressing the CD45.1 allele into lethally irradiated BALB/c mice expressing the CD45.2 allele via the tail vein. On day 6 after disease induction, the spleen and inflamed small intestine were removed from recipient mice. Splenocytes were obtained as single-cell suspensions and lamina propria cells were isolated from the small intestine by enzymatic digestion. (**A**) Splenocytes were stained using anti-CD45.1 and anti-CD45.2 fluorochrome-conjugated antibodies, and live cells were gated based on FSC and SSC. (**B**) Live cells in the lamina propria were identified using FSC and SSC, and an anti-CD11b antibody was used to define myeloid cells. The origin of myeloid cells was determined by anti-CD45.1 and anti-CD45.2 stainings. A representative example for each analysis is shown.

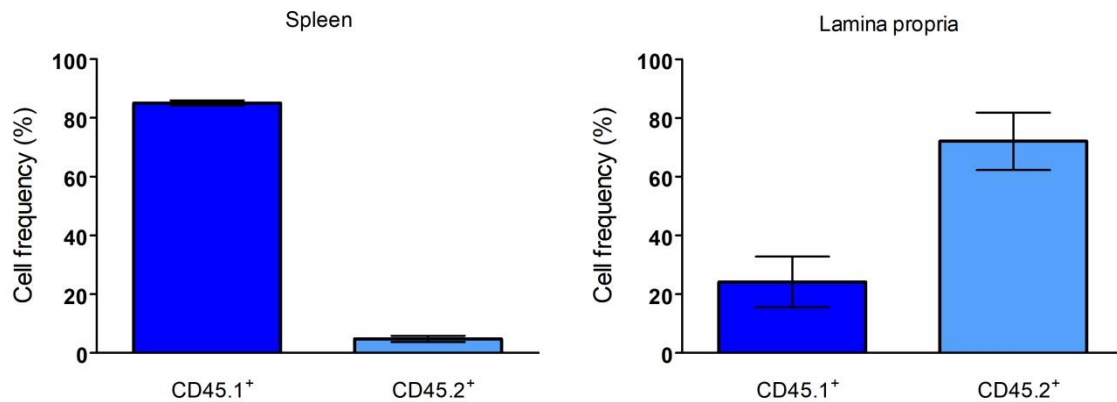


Figure 17. The origin of splenocytes as well as myeloid cells in the small intestine of aGvHD mice was determined by flow cytometric analysis. Murine aGvHD was induced by infusing wild type T cells in a combination with TCD bone marrow cells purified from C57BL/6 mice expressing the CD45.1 allele into lethally irradiated BALB/c mice expressing the CD45.2 allele by tail vein injection. On day 6 after disease induction, the spleen and small intestine were removed from recipient mice. Single-cell suspensions of splenocytes were produced and lamina propria cells were isolated from the small intestine. N=3. (A) Cell frequencies of donor-derived cells (CD45.1⁺) or recipient-derived cells (CD45.2⁺) in the spleen were analyzed by flow cytometry. (B) Percentages of donor-derived myeloid cells (CD11b⁺ CD45.1⁺) and recipient-derived myeloid cells (CD11b⁺ CD45.2⁺) in the lamina propria of the small intestine were analyzed by flow cytometry; (Li et al., 2019).

3.6 Identification of novel candidate genes in murine aGvHD triggered by GC-resistant allogeneic T cells

Our large-scale gene expression analysis showed that amongst the 54 selected genes, many were altered in mice transplanted with GC-resistant T cells, but the analyzed gene profile was limited to the categories that were already known to be regulated by GCs in inflammatory responses. To identify potential new candidate genes involved in the pathogenesis of aGvHD and regulated by GCs, we conducted an RNA-sequencing analysis to compare the transcriptome in the inflamed small intestine of mice transferred with GC-resistant (GR^{lck}) or GC-responsive (GR^{lox}) T cells. Total RNA was isolated from the inflamed small intestines, and used for sequencing analysis. When we carried out principle component analysis (PCA), we found that transplantation of GC-resistant allogeneic T cells profoundly affected the transcriptomic profile of the genes in the inflamed small intestine (**Figure 18 A**). RNA-sequencing data were uploaded to the

ArrayExpress Archive of Functional Genomics Data (<https://www.ebi.ac.uk/arrayexpress/>) with the accession number E-MTAB-7765. Bioinformatic analysis of RNA-sequencing data was performed using the *BioJupies* package with default parameters. An overview of the results can be accessed at the following URL: <https://amp.pharm.mssm.edu/biojupies/notebook/jYXKf7gm0>.

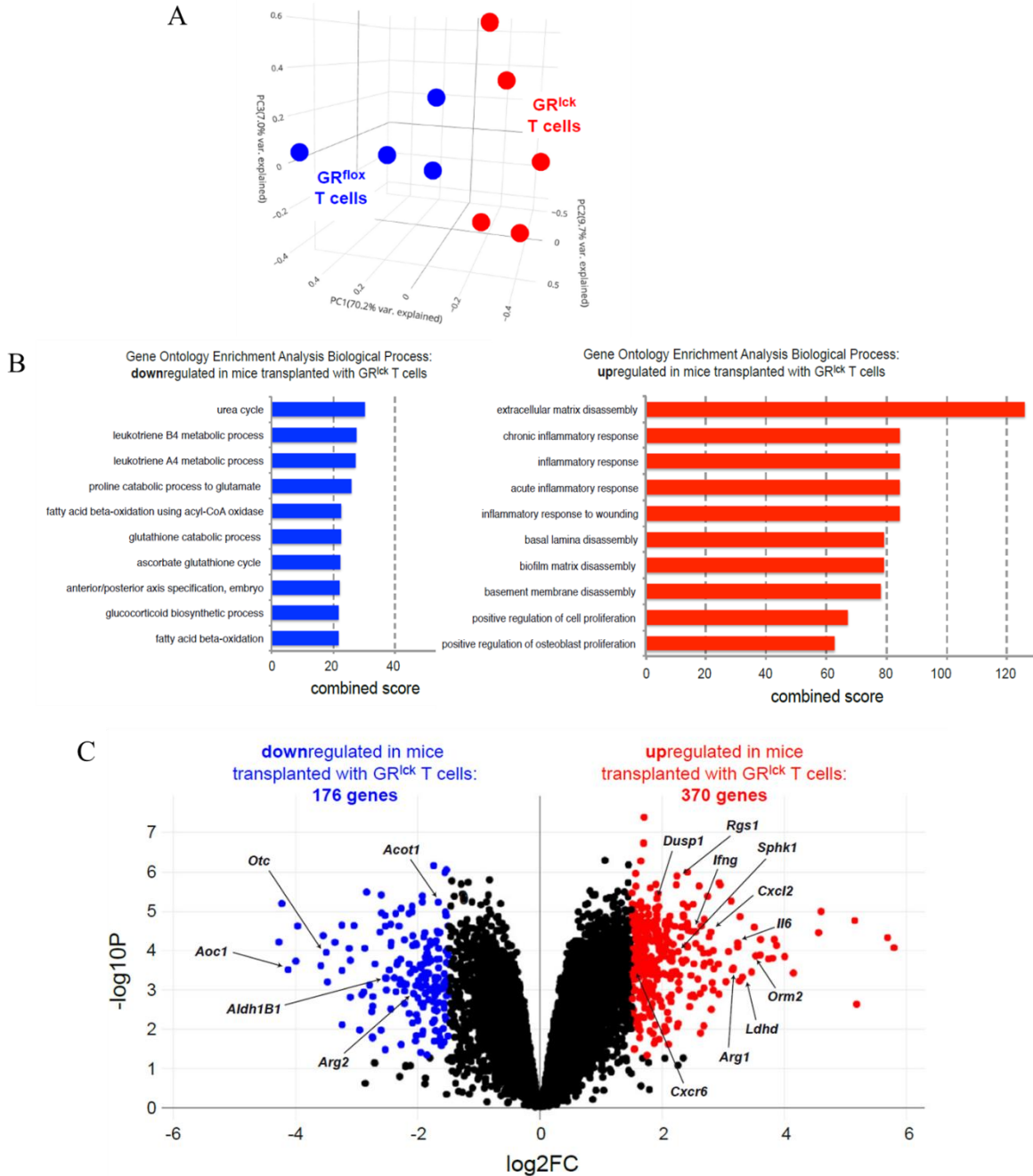


Figure 18. RNA-sequencing analysis of the inflamed small intestine in aGvHD mice transplanted with GC-resistant allogeneic T cells. RNA was extracted from the small intestines of mice receiving either GC-resistant (GR^{lck}) or GC-responsive (GR^{fllox}) T cells on day 6 after disease induction and then used for RNA-sequencing analysis. (A) Three-dimensional principle component analysis (PCA) of 5 GR^{lck} samples and 4 GR^{fllox} samples. (B) Gene ontology enrichment analysis of the up-regulated genes and the down-regulated genes, the top 10 profiles are depicted for each group. (C) Volcano plot of the differentially expressed genes, blue dots represent down-regulated genes, red dots represent up-regulated genes (adjusted p-value: $-\log_{10} P < 0.05$; fold change: $\log_2 FC > 1.5$). Selected genes for further expression analysis are indicated by arrows; (Li et al., 2019).

The gene ontology enrichment analysis indicated that up-regulated and down-regulated genes were significantly enriched in inflammation-related and matrix disassembly profiles or the urea cycle and fatty acid oxidation profile, respectively (**Figure 18B**). Amongst the genes that were differentially expressed, 176 genes were significantly down-regulated and 370 genes were up-regulated in mice transplanted with GC-resistant T cells (**Figure 18C**). RNA-sequencing analysis was performed by Marina Borschiwer in the laboratory of Dr. Sebastiaan Meijnsing.

Encoded molecule	Gene symbol	High-throughput quantitative PCR		RNAseq analysis	
		GR ^{lck} vs. GR ^{fllox} at day 6		GR ^{lck} vs. GR ^{fllox} at day 6	
		Fold change	Unpaired t-test	Fold change	Unpaired t-test
IL-6	<i>Il6</i>	13.7	*	9.4	***
CCL2	<i>Ccl2</i>	5.3	*	3.3	**
CXCL1	<i>Cxcl1</i>	6.4	*	3.5	**
CD95L	<i>Fasl</i>	3.6	**	2.8	**
YM1	<i>Chil3</i>	5.3	*	7.0	*
CTLA4	<i>Ctla4</i>	5.6	**	3.9	**
DUSP1	<i>Dusp1</i>	3.9	**	3.8	**
ARG1	<i>Arg1</i>	8.9	*	8.9	**
Glut1	<i>Slc2a1</i>	3.4	*	3.0	**

Table 15. Comparison of gene expression levels determined either by Fluidigm® gene chip analysis or RNA-sequencing. Murine aGvHD was induced by transplanting allogeneic GC-resistant (GR^{lck}) and GC-responsive (GR^{fllox}) T cells into lethally irradiated wild type BALB/c mice via the tail vein. RNA was isolated from the inflamed small intestines on day 6 after disease induction. Exemplary genes analyzed for the comparison of the two approaches of gene expression analysis, Fluidigm® gene chip analysis and RNA-sequencing, were selected from **Tables 12-14**. The data are presented as fold change in the color of dark green for > 3-fold. Statistical analysis was performed using unpaired Student's t-test, *, $p < 0.05$; **, $p < 0.01$; ***, $P < 0.001$; (Li et al., 2019).

To assess the experimental consistency of the two approaches used for gene expression analysis, namely Fluidigm® gene chip analysis and RNA-sequencing, we compared the expression levels of a few genes selected from **Tables 12-14**. We found comparable results for the fold-change and the statistical significance of the expression levels of these genes, demonstrating similar results for the two distinct approaches (**Table 15**).

3.7 Histological and immunohistochemical analyses indicate tissue damage and lymphocyte infiltration into the inflamed small intestine in aGvHD mice

During the effector phase of aGvHD, infiltration of effector T cells into the small intestine results in massive tissue damage (Holtan et al., 2014). The clinical score curve showed that GR^{lck} mice developed a more severe aGvHD than GR^{fllox} mice did, especially on day 6, the full-blown first phase of the disease (**Figure 10A**). Therefore, we intended to explore the possible mechanisms linked to the effector phase of aGvHD. To this end, we carried out a histological analysis to assess the tissue damage in the small intestine, a major target organ of aGvHD in mice. Furthermore, the infiltration of effector T cells into the small intestine was determined by immunohistochemical staining of CD3. Organ biopsies were harvested from mice receiving either GC-resistant (GR^{lck}) or GC-responsive (GR^{fllox}) T cells on day 4 and 6 after aGvHD induction.

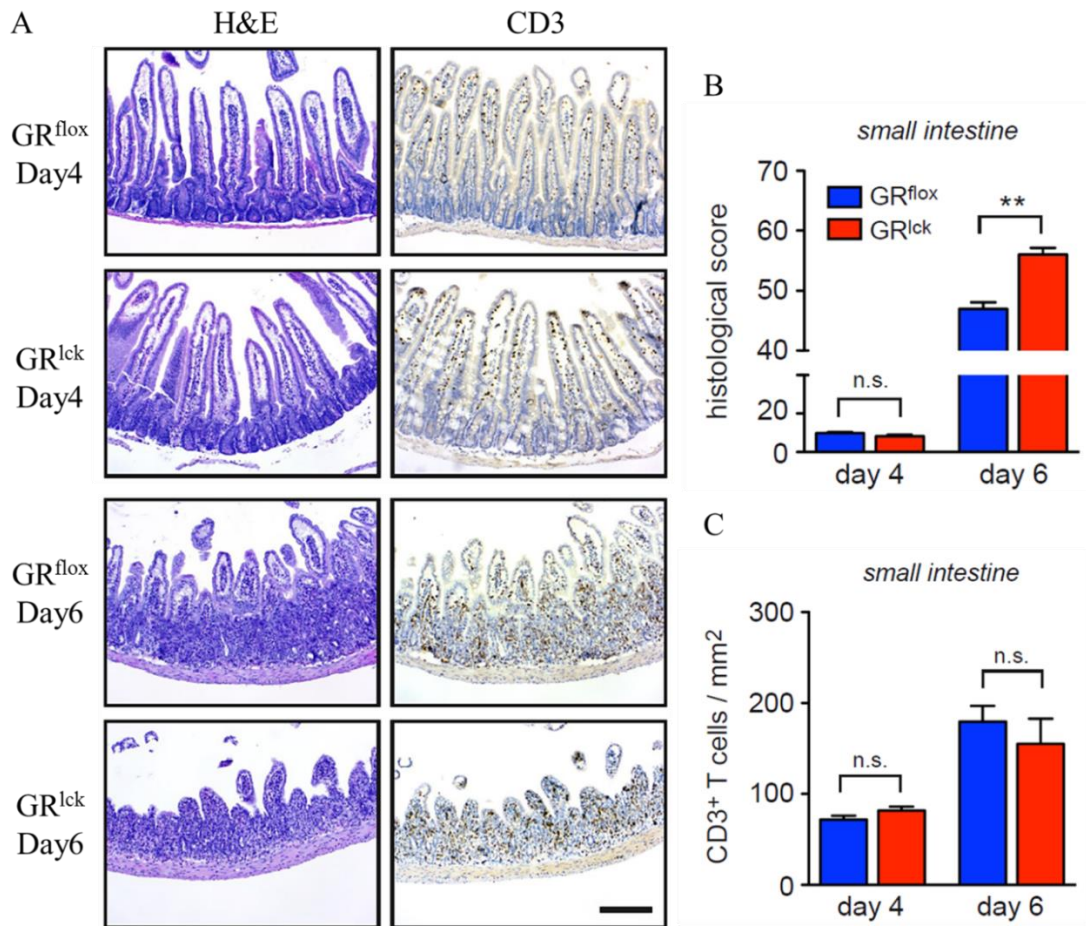


Figure 19. Histological and immunohistochemical analyses of the small intestines in mice suffering from aGvHD. The induction of aGvHD was performed by transferring GC-resistant (GR^{lck}) or GC-responsive (GR^{flox}) allogeneic C57BL/6 T cells into lethally irradiated BALB/c mice. Mice were sacrificed on day 4 or 6 after disease induction, and the small intestines were sectioned, dehydrated, embedded in paraffin, and subsequently processed for hematoxylin and eosin (H&E) staining or anti-CD3 immunohistochemical staining. (A) Microphotographs of stained sections were captured at 20× magnification. Representative examples of histological sections obtained on day 4 and 6 from mice transferred with GR^{flox} and GR^{lck} T cells are shown; scale bar: 200 μm. (B) The histological score was determined in H&E stainings and assessed by an established scoring system as described before. (C) Numbers of infiltrating T cells were determined using anti-CD3 immunohistochemical stainings and counted per mm². N=5 for each group. Statistical analysis was done using unpaired Student's t-test, **, p < 0.01; n.s., not significant; (Li et al., 2019).

On day 4 after aGvHD induction, the villi in mice receiving GR^{flox} and GR^{lck} T cells were morphologically intact (**Figure 19A**); the histological score showed no significant differences between mice receiving GC-resistant T cells and those receiving GC-responsive T cells. Mice transplanted with GR^{lck} T cells developed a more severe aGvHD

compared to those with GR^{fllox} T cells at the full-blown first stage of the disease, which was supported by our histological scoring on day 6 revealing more excessive tissue damage in the former group of mice (**Figure 19B**). The disease was characterized by an increasing infiltration of CD3⁺ T cells from day 4 to 6 into the small intestine. However, GR-deficiency in allogeneic T cells did not impact the number of infiltrating CD3⁺ T cells in the inflamed small intestines; no differences were detected neither on day 4 nor day 6 (**Figure 19C**).

Taken together, these data show that the exaggerated aGvHD is not caused by differential T cell infiltration into the small intestine but must rather be due to differences between instinct effector functions of the allogeneic T cells with GC-resistance and GC-responsiveness.

3.8 Serum protein levels of key inflammatory cytokines are elevated during the course of aGvHD in mice transferred with GC-resistant allogeneic T cells

To investigate whether the tissue damage triggered by the infiltrating T cells in the inflamed small intestines correlated with the systemic levels of inflammatory cytokines, we collected blood from mice suffering from aGvHD via heart puncture on day 4, 5 or 6 after transplantation. The systemic protein levels of IL-6, IFN- γ , and TNF- α were measured by ELISA.

The production of these three cytokines in serum was already significantly increased in the early phase of the disease (day 4) in mice receiving GC-resistant T cells (GR^{lck}) relative to those mice transferred with GC-responsive T cells (GR^{fllox}). This was also the case at the full-blown first stage of the disease (day 6). However, no significant differences in serum protein levels were observed on day 5 between mice receiving GR^{lck} and GR^{fllox} T cells (**Figure 20**). Of note, the level of IFN- γ on day 5 was higher than on day 6 in mice of both experimental groups (**Figure 20B**).

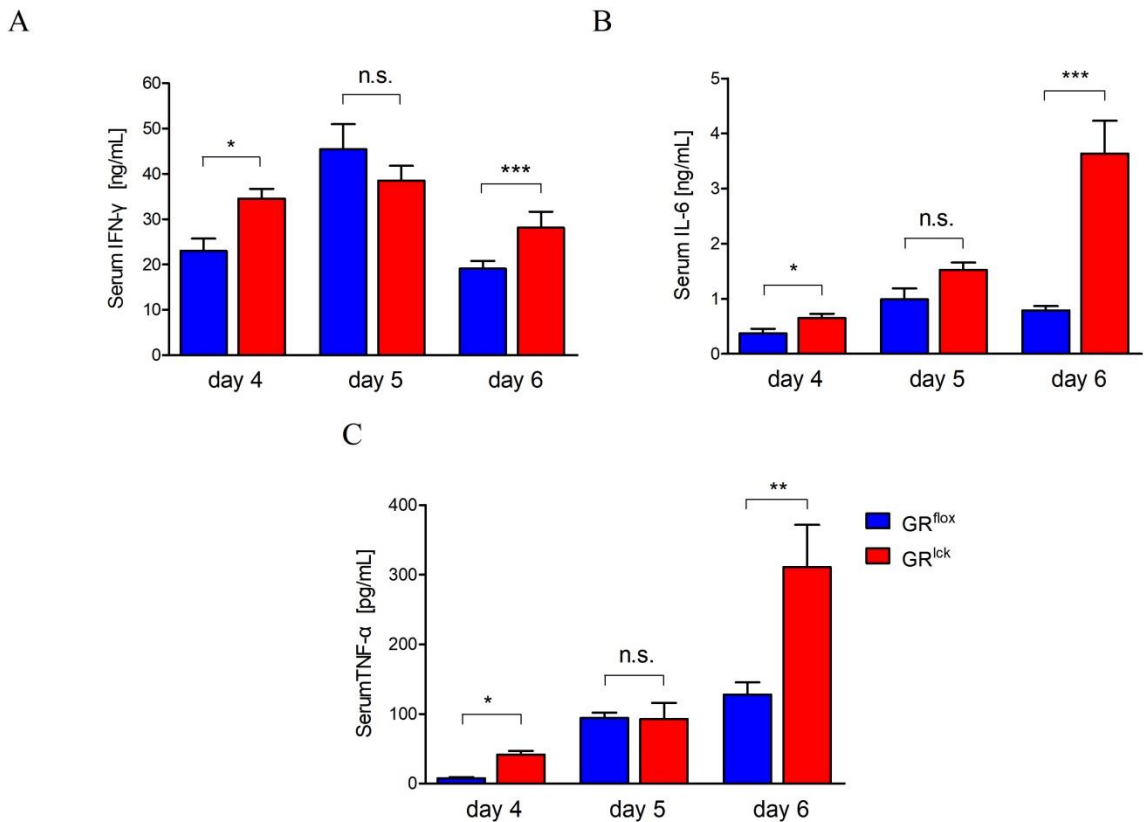


Figure 20. Serum protein levels of inflammatory cytokines during the course of aGvHD in mice. Murine aGvHD was induced by transferring allogeneic GC-resistant (GR^{lck}) or GC-responsive (GR^{lox}) C57BL/6 T cells in combination with TCD bone marrow cells into lethally irradiated BALB/c mice via the tail vein. On day 4, 5, and 6, blood was collected by heart puncture from the recipient mice. Protein levels of IL-6 (A), IFN- γ (B), and TNF- α (C) were determined by ELISA. Sample size: N= 5/5/10 (day 4/5/6). Statistical analysis was performed with unpaired Student's t-test, *, $p < 0.05$; **, $p < 0.01$; ***, $p < 0.001$; n.s., not significant; (Li et al., 2019).

3.9 Expression analysis of the genes previously identified by RNA-sequencing

Our RNA-sequencing data showed that more than 500 genes were differentially regulated in mice receiving GC-resistant T cells on day 6 after aGvHD induction (Figure 18C). Therefore, we selected 26 candidate genes from this list and reanalyzed their expression by high-throughput RT-qPCR. The selection criteria included gene alteration with a high fold change and a p-value, and genes potentially associated with aGvHD pathology, the

gastrointestinal tract, and an involvement in inflammation.

We found that the majority of analyzed genes were significantly altered at the full-blown first stage (day 6) of the disease, but only two genes, *Ifng* and *Cxcl2*, were already up-regulated at the early stage (day 4). The transcriptional levels of genes encoding secreted proteins (*Mt2a*, *Gzmb*, *Ifng*, *Orm2*, and *Cxcl2*), molecules expressed on the cell surface (*Cd274*, *Ccr2*, *Cxcr6*, *Il18r1*, *Tnfrsf9*, *Cldn4*, and *Il1r1*), and intracellular enzymes (*Hmox1*, *Itk*, *Ptges*, and *Rgs1*) were all significantly up-regulated in mice transplanted with GC-resistant allogeneic T cells on day 6. Moreover, the expression level of two genes (*S1pr1* and *Sphk1*) involved in sphingosine signaling was elevated in mice transplanted with GR^{lck} T cells (**Table 16**). We also observed that three genes (*Pfkfb3*, *Ldhd*, and *Slc2a3*) associated with glycolysis were up-regulated in mice receiving GC-resistant T cells. Furthermore, five genes (*Aldh1b1*, *Acot1*, *Arg2*, *Otc*, and *Aoc1*) related to metabolic pathways active in many non-hematopoietic cells, such as the urea cycle, were down-regulated (**Table 16**).

Results

Encoded molecule	Gene symbol	GR ^{lck} vs. GR ^{flox} at day 4		GR ^{lck} vs. GR ^{flox} at day 6	
		Fold change	Unpaired t-test	Fold change	Unpaired t-test
Metallothionein 2a	<i>Mt2a</i>	1.1	n.s.	2.0	*
Granzyme B	<i>Gzmb</i>	1.3	n.s.	2.3	*
IFN γ	<i>Ifng</i>	5.2	*	2.7	**
Orosomucoid 2	<i>Orm2</i>	0.9	n.s.	5.0	**
CXCL2	<i>Cxcl2</i>	2.6	n.s.	6.3	*
PD-L1	<i>Cd274</i>	1.6	n.s.	1.8	*
CCR2	<i>Ccr2</i>	0.6	n.s.	2.2	*
CXCR6	<i>Cxcr6</i>	1.1	n.s.	2.3	*
IL-18R1	<i>Il18r1</i>	1.0	n.s.	2.4	*
4-1BB	<i>Tnfrsf9</i>	1.7	n.s.	2.8	**
Claudin 4	<i>Cldn4</i>	0.9	n.s.	2.8	**
IL-1R1	<i>Il1r1</i>	1.3	n.s.	5.3	***
Heme oxygenase 1	<i>Hmox1</i>	1.3	n.s.	1.9	*
Inducible T-cell kinase	<i>Itk</i>	0.7	n.s.	2.2	*
Prostaglandin E synthase	<i>Ptges</i>	1.3	n.s.	2.5	***
Regulator of gp signaling 1	<i>Rgs1</i>	0.9	n.s.	4.0	**
S1P receptor 1	<i>Slpr1</i>	1.2	n.s.	2.1	*
Sphingosine kinase 1	<i>Sphk1</i>	1.0	n.s.	2.9	**
6-Phosphofructo-2-kinase	<i>Pfkfb3</i>	1.5	n.s.	1.9	**
Lactate dehydrogenase D	<i>Ldhd</i>	0.9	n.s.	2.1	*
Slc2a3 / Glut3	<i>Slc2a3</i>	1.4	n.s.	2.4	**
Aldehyde dehydrogenase 1B1	<i>Aldh1b1</i>	1.1	n.s.	0.50	*
Acyl-CoA thioesterase 1	<i>Acot1</i>	1.3	n.s.	0.42	*
Arginase 2	<i>Arg2</i>	1.0	n.s.	0.26	*
Ornithine transcarbamylase	<i>Otc</i>	0.9	n.s.	0.24	**
Amine oxidase copper 1	<i>Aoc1</i>	1.0	n.s.	0.08	*

Table 16. Expression analysis of selected genes identified by RNA-seq during an early and late stage of the first phase of aGvHD in mice. Murine allogeneic HSCT was conducted by injecting allogeneic GC-resistant (GR^{lck}) or GC-responsive (GR^{flox}) T cells in combination with TCD bone marrow cells isolated from C57BL/6 mice into the tail vein of lethally irradiated BALB/c mice. RNA was isolated from small intestine biopsies on day 4 and 6 after disease induction. Complementary DNA was synthesized and used for Fluidigm[®] gene chip analysis. Expression alterations are depicted as fold-change of GR^{lck} vs. GR^{flox} (yellow for no changes, light green: \leq 3-fold, dark green: $>$ 3-fold, light blue: \geq 0.3-fold, and dark blue: $<$ 0.3-fold). N=4/5 (GR^{flox}/GR^{lck}, day 4), N=10/10 (GR^{flox}/GR^{lck}, day 6). Statistical analysis was done with unpaired Student's t-test, *, $p < 0.05$; **, $p < 0.01$; ***, $p < 0.001$; n.s., not significant; (Li et al., 2019).

3.10 Expression analysis of the genes identified by RNA-seq reveals cell-type specificity

A number of genes identified by RNA-seq had been further confirmed by high throughput gene expression analysis using Fluidigm[®] gene chip technique (**Table 16**). However, there was a limitation. Since we applied total RNA isolated from small intestine biopsies for the gene expression analysis, it could not distinguish between different types of cells that infiltrate or reside in the small intestine in the context of aGvHD, such as T cells, epithelial cells, and macrophages. However, it has been reported that these types of cells contribute differently to the progress of aGvHD (Koyama et al., 2019; Perkey and Maillard, 2018). As a first approach to analyze the cell-type specificity of the identified genes, we purified splenic T cells from C57BL/6 mice, enriched peritoneal macrophages in BALB/c mice, and isolated epithelial cells from the small intestine of BALB/c mice. The specific expression of nine genes in these three cell-types was analyzed by RT-qPCR.

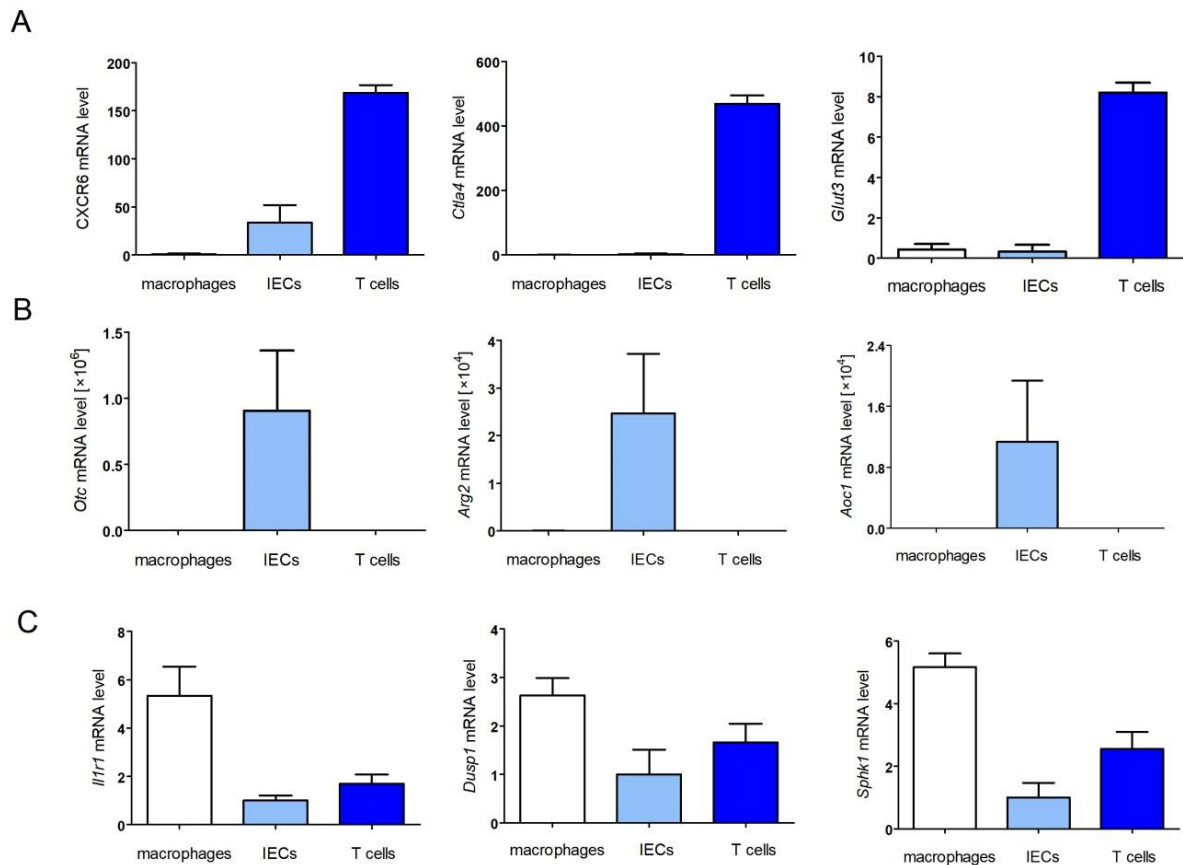


Figure 21. Cell-type specificity analysis of selected genes identified by RAN-seq. Splenic T cells were magnetically purified from C57BL/6 mice. Thioglycolate was intraperitoneally injected into BALB/c mice, and peritoneal macrophages were enriched 4 days later. Intestinal epithelial cells (IECs) were isolated from BALB/c mice. RNA was subsequently isolated from these cell preparations, transcribed into cDNA, and used for RT-qPCR analysis. **(A)** Genes mainly expressed by T cells. **(B)** Genes predominantly expressed by IECs. **(C)** Genes preferentially expressed by macrophages. mRNA expression levels were determined using the $\Delta\Delta C_t$ method and normalized to the house-keeping gene *Hprt*. $N=3/3/5$ (T cells/ IECs/ macrophages); (Li et al., 2019).

Amongst the genes we assessed, three genes, *Cxcr6*, *Cita4*, and *Glut3* were mainly expressed by T cells and barely expressed by macrophages or IECs (**Figure 21A**). *Otc*, *Arg2*, and *Aoc1* that were significantly down-regulated in mice transferred with GC-resistant T cells were dominantly expressed by IECs and their expression in T cells and macrophages was nearly undetectable (**Figure 21B**). We also found that *Il1r1*, *Dusp1*, and *Sphk1* were more strongly expressed by peritoneal macrophages with a relatively low expression in the other two cell-types (**Figure 21C**). Collectively, our data indicate that

genes that are differentially expressed under conditions when allogeneic T cells are GC-resistant, show a highly cell type-specific expression pattern, therefore, highlighting the contributions of this cell-type specificity to mouse aGvHD.

3.11 Administration of BMP-NPs alleviates aGvHD in mice with the beneficial GvL effect retained

BMP-NPs are a type of functional inorganic-organic nanoparticles (IOH-NPs) used for targeted delivery of GCs to endocytic cells. They are composed of $[\text{ZrO}]^{2+}[(\text{BMP})_{0.9}(\text{FMN})_{0.1}]^{2-}$ (BMP: betamethasone phosphate; FMN: flavin mononucleotide). In previous experiments of our group, it was demonstrated that BMP-NPs were preferentially taken up by macrophages but hardly by T cells both *in vitro* and *in vivo* (Kaiser et al., 2020a; Montes-Cobos et al., 2017). Importantly, APCs such as macrophages make an essential contribution to the development of aGvHD in mice (Shlomchik, 1999). Based on the discovery of the cell type-specificity of BMP-NPs, we hypothesized that treatment of aGvHD with BMP-NPs not only reduces the severity of the disease in mice, but may also preserve the beneficial GvL effects compared to free GCs with the GR ubiquitously expressed in all nucleated cells.

To analyze the GvL effect, we induced a combined aGvHD/GvL mouse model. It has been previously reported that the Bcl₁ lymphoma shows massive splenic involvement and expresses a monoclonal λ -type immunoglobulin that could serve as a convenient marker to track down Bcl₁ lymphomagenesis (Warnke et al., 1979). Prior to standard aGvHD induction, 3,000 Bcl₁ cells were injected into recipient BALB/c mice via the tail vein to induce lymphomagenesis. Mice were monitored daily for their aGvHD clinical score and either treated with PBS, free betamethasone (BMZ), EP-NPs ($[\text{ZrO}]^{2+}[(\text{HPO}_4)_{0.9}(\text{FMN})_{0.1}]^{2-}$), or BMP-NPs on day 3, 4, 5, 7, 9, and 12. FACS analysis of the percentage of λ -type immunoglobulin cells in peripheral blood was carried out starting from day 21. Mice were sacrificed for ethical reasons according to the assessment of aGvHD disease symptoms or once the percentage of Bcl₁ cells in the blood exceeded

50%.

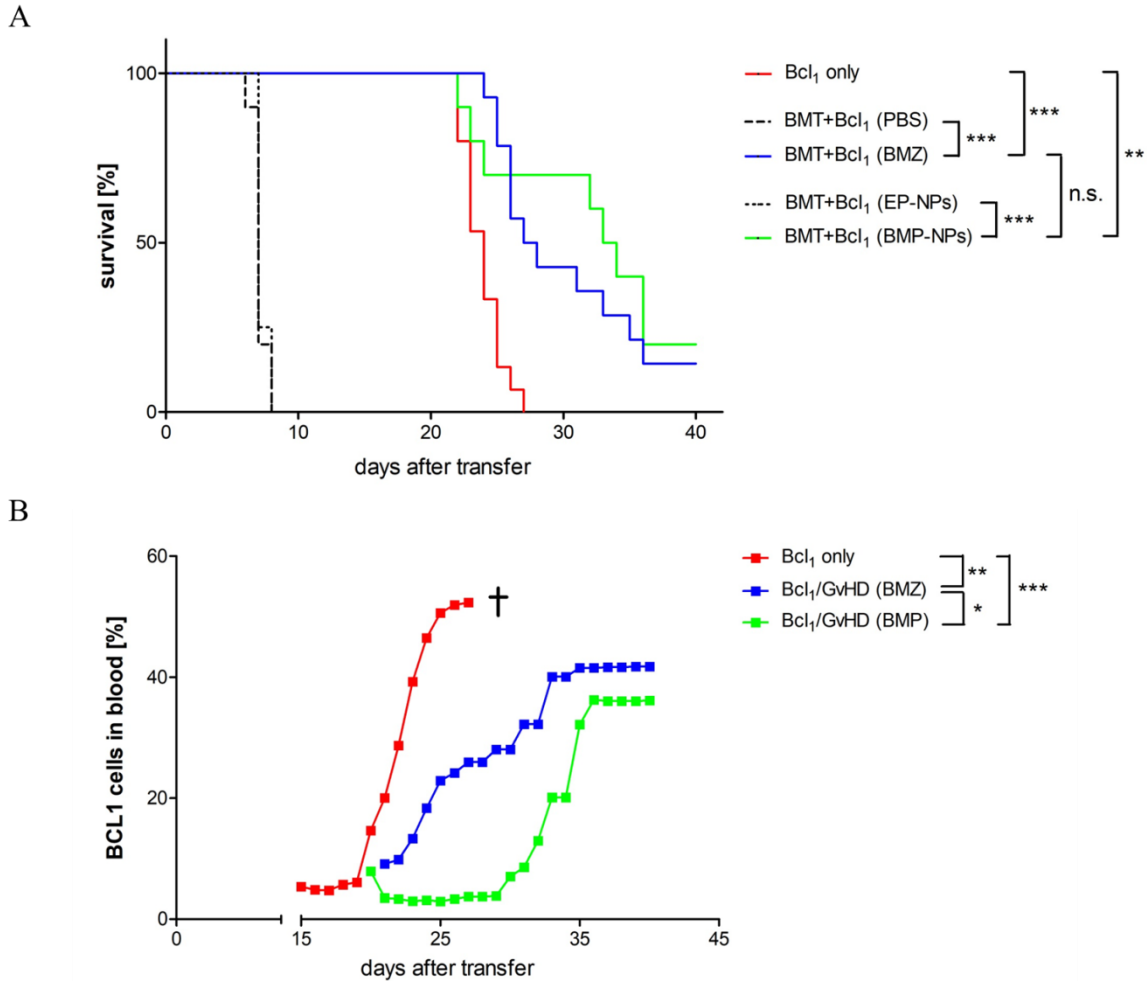


Figure 22. Survival rate and lymphomagenesis of mice treated with different GC formulations. Induction of aGvHD was performed by transferring 1×10^7 T cell-depleted (TCD) bone marrow cells and 2×10^6 splenic T cells isolated from C57BL/c mice into BALB/c mice via the tail vein. Adaptive Bcl₁ lymphoma cell transfer was conducted by injecting 3,000 Bcl₁ cells into the BALB/c mice 4 hours before the induction of aGvHD, and mice receiving Bcl₁ cells only served as a control. Mice were treated with PBS, free betamethasone (BMZ), EP-NPs, or BMP-NPs on day 3, 4, 5, 7, 9, and 12. The severity of aGvHD and GvL was assessed based clinical symptoms and the frequency of Bcl₁ cells in the blood. Mice were sacrificed when severe manifestations of aGvHD were observed or the percentage of Bcl₁ cells in peripheral blood surpassed 50%. Sample size: N=15/10/14/4/10 (Bcl₁ only / PBS / BMZ / EP-NPs / BMP-NPs). **(A)** Survival rate of mice in the combined aGvHD/GvL model (BMT+Bcl₁) treated with PBS, BMZ, EP-NPs, or BMP-NPs, or of mice only receiving Bcl₁ cells. **(B)** Development of a lymphoma in mice based on the average frequency of Bcl₁ cells in the blood is shown for the three experimental groups surviving pass day 10. The data were pooled from five independent experiments. Survival rate was analyzed with Log-rank Mantel-Cox test, and Bcl₁ lymphomagenesis was analyzed using Kruskal-Wallis test followed by Dunn's Multiple Comparison test. *: p<0.05; **: p<0.01; ***: p<0.001; n.s.: non-significant; (Kaiser et al., 2020b).

Mice transferred with BMT and Bcl₁ cells and either treated with PBS or EP-NPs were all sacrificed no later than on day 8 due to the severe aGvHD symptoms. Mice transferred only with Bcl₁ cells were killed starting from day 22 and all sacrificed within the third week after the induction of the combined aGvHD/GvL mouse model. Besides, mice administered with BMZ or BMP-NPs were sacrificed due to aGvHD symptoms or the development of a Bcl₁ lymphoma, and showed a better survival rate than those mice only receiving Bcl₁ cells. Moreover, treatment with BMP-NPs could slightly better prolong the survival of mice compared to BMZ treatment, though not significantly (**Figure 22A**).

In order to investigate the progress of the Bcl₁ lymphoma, we detected the percentage of Bcl₁ cells in the peripheral blood using FACS Igλ staining and analyzed lymphomagenesis in all mice combined as well as in individual animals (**Figure 22B and 23**). Mice transferred with only Bcl₁ cells demonstrated the occurrence of a lymphoma starting from day 21 after transplantation, and the percentage of Bcl₁ cells in the peripheral blood rapidly increased thereafter, reaching the maximal amount of 50 percent. Relative to those mice receiving only Bcl₁ cells, mice with aGvHD and treated with BMZ or BMP-NPs showed a trend to a delayed Bcl₁ lymphoma development. Besides, the progress of the Bcl₁ lymphoma was slower in mice treated with BMP-NPs compared to those administered with BMZ (**Figure 22B**).

All 15 mice receiving only Bcl₁ cells had over 50 percent of lymphoma cells in the blood until day 27. In the BMZ treatment group, 7 mice died of aGvHD, and 7 mice developed a lymphoma or remained healthy until day 40 when the experiment was terminated. Amongst the mice administered with BMP-NPs, 4 died of aGvHD and 6 developed a lymphoma or were healthy until day 40 (**Figure 23**). These data suggest that transfer of allogeneic T cells combined with GC treatment delays Bcl₁ lymphomagenesis in mice significantly better when BMP-NPs are used instead of free BMZ, although in the end, the outcome of both treatments was comparable.

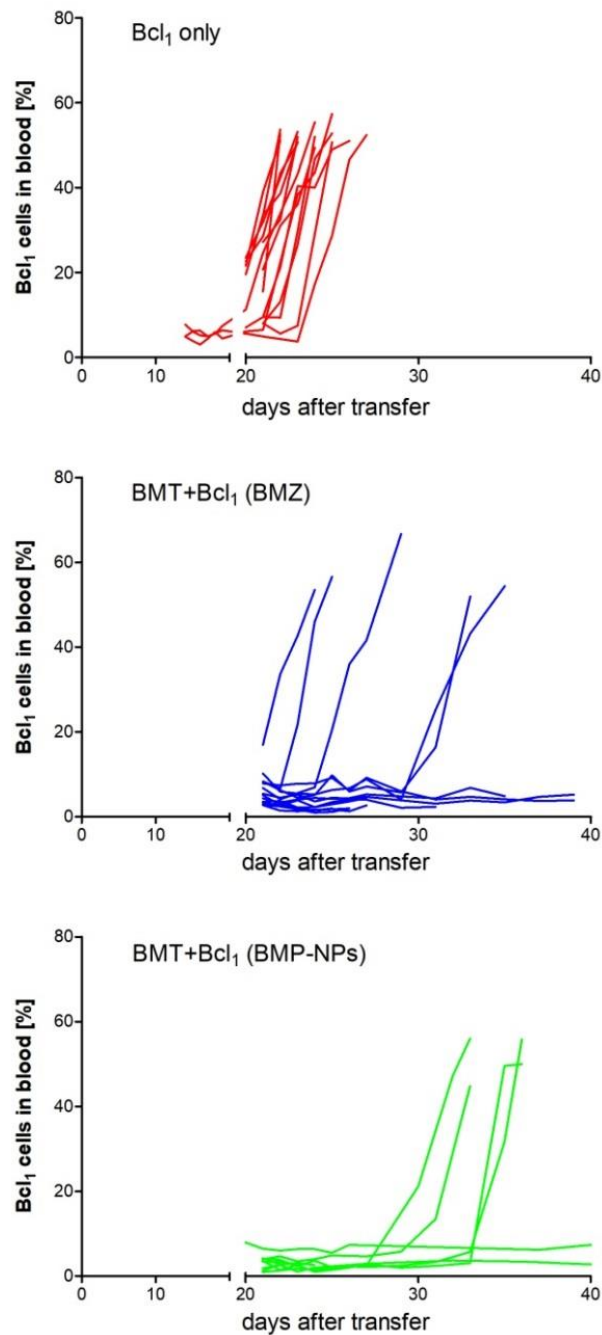


Figure 23. Frequency of Bcl₁ cells in the blood of individual mice in a combined aGvHD/GvL mouse model. Murine aGvHD was induced by transferring 1×10^7 T-cell-depleted (TCD) bone marrow cells and 2×10^6 splenic T cells isolated from C57BL/c mice into BALB/c mice via the tail vein. Mice were treated with BMZ or BMP-NPs on day 3, 4, 5, 7, 9, and 12. Adaptive transfer of a Bcl₁ lymphoma was induced by injecting 3,000 Bcl₁ cells into the BALB/c mice 4 hours before aGvHD induction, and mice receiving only Bcl₁ cells served as a control. The expansion of Bcl₁ cells in the peripheral blood was measured by FACS analysis based on Ig λ staining. Sample size: N=15/14/10 (Bcl₁ only / BMZ / BMP-NPs). The data refer to the same experiments as depicted in Figure 22; (Kaiser et al., 2020b).

3.12 Cytolytic ability of CD8⁺ T cells after short-term treatment with BMP-NPs

We found that the administration with BMP-NPs delayed the development of a Bcl₁ lymphoma in the combined aGvHD/GvL mouse model. Next, we aimed to assess the cytolytic ability of splenic cytotoxic lymphocytes (CTLs) *in vivo* after short-term treatment with BMP-NPs or BMZ. To achieve this goal, we induced aGvHD by transplanting magnetically purified allogeneic T cells in a combination with TCD bone marrow cells into BALB/c mice via the tail vein, and treated the mice with PBS, BMZ or BMP-NPs on day 3, 4, and 5 intraperitoneally. On day 6 after the aGvHD induction, splenic CD8⁺ cells were isolated from the recipient mice and tested for their cytolytic ability on target Bcl₁ cell using a ⁵¹chromium release assay. The lysis assay was carried out by Leslie Elsner in the laboratory of Prof. Dr. Ralf Dressel.

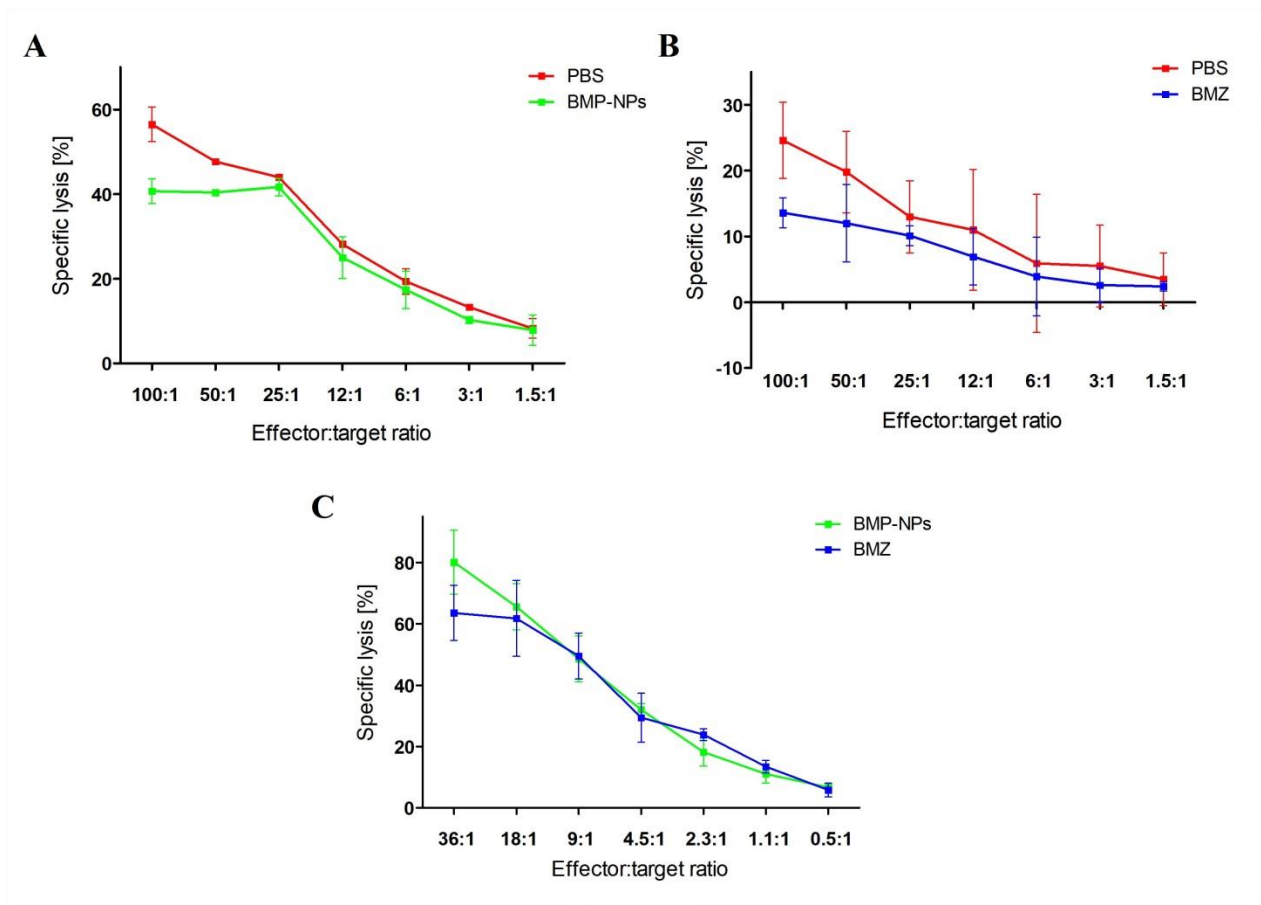


Figure 24. Lytic ability of cytotoxic T lymphocytes (CTLs) against *Bcl1* target cells after short-term treatment of aGvHD with BMP-NPs or BMZ. Splenic CD8⁺ T cells were magnetically isolated from mice suffering from aGvHD on day 6 after disease induction. *Bcl1* cells used as target cells were co-cultured in medium in the presence of effector CTLs, and the specific lysis was measured at different effector: target ratios by ⁵¹chromium release assay. **(A)** Specific lysis compared between mice treated with PBS or BMP-NPs, N=3/4 (PBS / BMP-NPs). **(B)** Specific lysis compared between mice treated with PBS or BMZ, N=3/6 (PBS / BMZ). **(C)** Specific lysis compared between mice treated with BMP-NPs or BMZ, N=6/6 (BMP-NPs / BMZ). Data are shown as mean ± SD.

The cytolytic ability of splenic CTLs isolated from aGvHD mice on day 6 administrated with BMZ or BMP-NPs was decreased in comparison of those CTLs treated with PBS *in vivo* (**Figure 24A** and **B**). Furthermore, when mice were treated with the two different GCs in one trial, CTLs from BMP-NPs treated mice were slightly more efficient in killing target cells than those from mice receiving BMZ (**Figure 24C**).

4. Discussion

4.1 GC-resistance of allogeneic donor T cells causes aggravated aGvHD in mice

HSCT is a potentially curative and effective therapeutic approach to treat various hematological diseases. However, its broader use is limited by the frequent occurrence of GvHD, which is a major complication after allogeneic HSCT and causes high morbidity and mortality (Copelan, 2006; Deeg, 2007). Systemic GCs, such as methylprednisolone, are the most common first-line therapy for the treatment of aGvHD (Sung and Chao, 2013), although a long-term or high-dose treatment with GCs is often accompanied by adverse effects including an increased risk of infection, aseptic necrosis, and osteopenia (Deeg, 2007). Moreover, it may occur that there is no response to GC treatment, which is termed “GC-resistant” or “steroid-refractory”. In the setting of aGvHD, approximately 60% of patients develop steroid-refractory GvHD and do not respond to this first-line therapy (Przepiorka et al., 2020). The mechanisms of steroid-resistance, however, are still poorly understood.

4.1.1 GC-resistant aGvHD in mice

In our experiments, we initially induced murine aGvHD by using GC-resistant (GR^{lck}) allogeneic T cells in which the GR was genetically deleted in the entire T cell lineage. Transplantation of GC-resistant or GC-responsive T cells both resulted in aGvHD in recipient mice, but the disease was exaggerated in the former case. More specifically, mice transferred with GC-resistant allogeneic T cells showed more severe clinical symptoms than those receiving GC-responsive cells. In a previous report, only those mice transplanted with GC-responsive but not GC-resistant allogeneic T cells survived throughout the first phase of aGvHD and then succumbed to death in the second phase of the disease (Theiss-Suennemann et al., 2015). This finding highlights the importance of the effects of endogenous GCs on allogeneic donor T cells in the development and severity of aGvHD in mice. However, not only allogeneic donor T cells but also various types of APCs play an important role in the pathophysiology of aGvHD (Ferrara et al., 2009). Correspondingly, mice with GC-resistant myeloid cells (GR^{lySM}) also developed a

more severe aGvHD relative to mice harboring GC-responsive myeloid cells in the full-blown first phase of the disease, and it was found that the aggravated clinical symptoms observed in GR^{lysM} mice were accompanied by a dramatic drop of body temperature (Baake et al., 2018). Overall, our results as well as earlier ones thus suggest that GC-resistance of donor T cells and recipient myeloid cells both triggers a more severe aGvHD in mice, thus providing ideal models to study GC-resistant aGvHD.

4.1.2 Phenotype of mice transferred with GR^{lck} or GR^{fllox} allogeneic T cells

The different disease course of mice transplanted with GC-resistant or GC-responsive allogeneic T cells could either be caused by intrinsic differences between both cell types or it could be due to their differential responsiveness to GCs. In the pathophysiology of aGvHD, activated donor allogeneic T cells migrate to the target organs after being primed by APCs, and this progress is mediated by various adhesion molecules and chemokine receptors expressed on the surface of T cells (Zeiser et al., 2016). T cell-depletion in the graft is an option to prevent aGvHD after HSCT, however, accompanied by higher rates of infection and relapse. Therefore, specific removal of alloreactive precursors contained in donor T cells would be a potent treatment of aGvHD (Li Pira et al., 2016), which also highlights the importance of the activation condition of donor T cells. Classically, T cells are divided into CD4 and CD8 subsets, which recognize MHC II and MHC I complexes expressed on APCs, respectively. Targeted deletion of CD4⁺ donor T cells is linked to altered production of inflammatory cytokines in mouse aGvHD (Ni et al., 2017), and suppression of CTL activity of CD8⁺ T cells appears crucial for endogenous GCs to control aGvHD (Theiss-Suennemann et al., 2015). Furthermore, FoxP3⁺ T_{reg} cells have the ability to maintain peripheral tolerance in many inflammation-related disorders. For instance, it has been reported that donor-derived T_{reg} cells were capable of suppressing lethal aGvHD after HSCT, and adoptive transfer of T_{reg} cells has therefore emerged as a promising therapeutic approach to prevent or treat GvHD (Cohen et al., 2002; Hoffmann et al., 2002).

Our flow cytometric data suggest that the frequencies of different subsets amongst GC-resistant and GC-responsive T cells were largely similar, and that the expression of

adhesion molecules and chemokine receptors remained at a comparable level, indicating that GC-resistant and GC-responsive T cells possess an equal ability of cell migration. It has to be noted that GC-resistant CD8⁺ T cells were slightly more activated than GC-responsive ones, which could at least to some extent contribute to the aggravation of the disease in this experimental group. Nevertheless, the majority of differences in aGvHD severity are most likely caused by GC-resistance of T cells contained in the transplant rather by their different composition.

4.1.3 Systemic levels of inflammatory cytokines during aGvHD in mice

Acute GvHD is characterized by donor allogeneic T cells attacking vital recipient organs. These target organs of aGvHD include skin, liver and GI tract (Ferrara et al., 2009). Patients with hematological malignancies are often treated with conditioning regimens aiming at the removal of tumor cells and creating suitable conditions for receiving transfused stem cells. However, these regimens, such as high-dose TBI, commonly cause tissue damage and particularly result in the loss of epithelial cell integrity of the GI system, which triggers the release of inflammatory cytokines (IFN- γ , IL-1, and TNF- α) (Perkey and Maillard, 2018). IFN- γ is a hallmark of inflammation and is involved in many autoimmune and metabolic diseases (Ivashkiv, 2018), but the role of IFN- γ in the context of aGvHD is debatable. It was reported that IFN- γ reduced the injury of epithelial GvHD target tissues and increased the desired GvL effect (Wang et al., 2009). TNF- α is highly present in aGvHD patients and specifically plays an important role in the GI manifestations of GvHD (Deeg, 2007). Moreover, the anti-TNF- α monoclonal antibody infliximab has been used to treat aGvHD. Similarly, administration of tocilizumab, a monoclonal antibody targeting IL-6 receptor, attenuated aGvHD in mice (Chen et al., 2009). Also, a murine aGvHD induced in GR^{dim} recipient mice, in which the dimerization of the GR is impaired (Reichardt et al., 1998), showed alleviated disease manifestations after the treatment with an anti-IL-6 monoclonal antibody (Baake et al., 2018).

In this work, we found that systemic serum levels of IFN- γ and IL-6 were increased in mice transferred with GC-resistant T cells during the full-blown phase of mouse aGvHD. Furthermore, the production of IL-6 and TNF- α were consistently elevated during the

development of aGvHD in mice, even at the early stage of the disease, suggesting that the signs of inflammation were caused by the tissue damage in the initial phase after TBI. Besides, higher systemic serum levels of these two cytokines and IFN- γ were detectable in mice receiving GC-resistant T cells compared to ones transplanted with GC-responsive T cells at either the early or late full-blown phase of the disease, highlighting the contribution of endogenous GCs in controlling the initiation and rapid aggravation of mouse aGvHD by donor allogeneic T cells. Interestingly, the production of IFN- γ reached its highest level before the full-blown stage of aGvHD and was then lowered at the full-blown stage. Moreover, IFN- γ serum levels are in agreement with its gene expression pattern in the early and full-blown phases of the disease, characterized by increased mRNA levels in mice receiving GC-resistant T cells compared to those transplanted with GC-responsive T cells. Thus, our data further confirm the contribution of systemic inflammatory cytokines to the development of aGvHD and the GCs' biological functions to suppress them at a systemic level in the context of this disease.

4.1.4 Histological and immunohistochemical analyses of the small intestine of aGvHD mice

In the effector phase of aGvHD, the target organs undergo severe damage, which is highlighted by massive infiltration of effector T cells (Zeiser and Blazar, 2017). In line with our clinical data, histological staining only showed significant difference in the full-blown first phase between the inflamed small intestines of mice receiving GC-resistant and GC-responsive T cells, but not in the initiation phase of the disease. Concerning our gene expression data, which were obtained by analyzing total RNA from an entire section of the inflamed small intestine, it was necessary to test whether the alterations were caused by different numbers of infiltrating effector T cells or by cell-intrinsic differences in mRNA levels. Therefore, we carried out immunohistochemical stainings, which revealed similar numbers of infiltrating CD3⁺ T cells in the small intestine at different time points of the disease, indicating that the altered gene expression profile is a result of the distinct effector functions caused by resistance of T cells to endogenous GCs.

4.2 GC-resistance in allogeneic T cells alters the gene expression profile of mice suffering from aGvHD

Patients who develop aGvHD are treated with systemic GCs, such as methylprednisolone, at a dose of 2 mg/kg, followed by a gradually reduced dose if they respond. For non-responders, a higher dose of GCs is given in combination with immunosuppressants (Deeg, 2007). Those patients who are GC-resistant show poor clinical outcome with a low survival rate. An important question is, when second-line therapy should be initiated. Therefore, there is an urgent need for the development of biomarkers that would allow to predict GC-resistance and thus to timely start a second-line therapy. In a previous study, it has been proposed to use serum levels of suppressor of tumorigenicity-2 (ST2) and regenerating islet-derived protein 3 (REG3) to predict steroid-refractory aGvHD after one week of GC treatment, reflecting a better prognostic outcome than only relying on clinical criteria (Major-Monfried et al., 2018). Similarly, T-cell immunoglobulin mucin-3 (TIM3) has been shown to be closely associated with severe aGvHD in patients and particularly linked to steroid-refractory GvHD (McDonald et al., 2017). In contrast to these serum biomarkers, up to now, there are only a few studies focusing on discovering genes that are correlated to GC-resistance in the treatment of aGvHD. In an experimental aGvHD mouse model, expression of inflammatory cytokines, chemokines, and adhesion molecules, as well as their receptors, was found to be down-regulated after prednisolone treatment (Bouazzaoui et al., 2011). However, the relevance of these results is limited by the small scale of investigated genes. In previous experiments of our group, it was found that the transfer of GC-resistant allogeneic T cells led to an alteration of gene expression in spleen, namely *Ifng* and cytotoxicity-related genes largely secreted by CD8⁺ T cells (Theiss-Suennemann et al., 2015). However, the number of the analyzed genes was also small and gene expression analysis was limited to a secondary lymphoid organ instead of any of the main target organs of aGvHD. It is against this background that we hypothesized that genes could potentially be identified that are suitable for the predication or targeted treatment of aGvHD, by using a high-throughput technique to analyze gene expression in the small intestine, one of the main target organs, in a setting of endogenous GC-resistance.

4.2.1 Gene expression analysis of mice receiving GR^{lck} T cells or harboring GR^{lysM} myeloid cells

We initially conducted a Fluidigm[®] gene chip assay to analyze the expression of genes already known to be involved in the pathophysiology of aGvHD. Based on literature, we categorized these genes into five groups. We found that the expression pattern of these genes was mostly altered due to the transplantation of GC-resistant allogeneic T cells in the full-blown first phase of the disease. Even though the recipient mice with GC-resistant myeloid cells showed severe clinical aGvHD symptoms at this stage of the disease as well, the gene expression profile remained mostly unaffected in the GR^{lysM} aGvHD mouse model. As a matter of fact, it is likely that the aggravated disease symptoms here are predominantly caused by the elevated release of systemic inflammatory cytokines, such as IL-6 and TNF- α (Baake et al., 2018). Resident macrophages in the lamina propria of the intestine are the most radio-resistant part of myeloid cells (Bosurgi et al., 2013) and therefore many GC-resistant myeloid cells still existed in our aGvHD mouse model. However, our data also show that donor-derived myeloid cells contained in graft migrated into the inflamed small intestine and thereby contributed to the composition of myeloid cells in this target organ. Hence, in the case of the GR^{lysM} aGvHD mouse model, it is likely that donor-derived GC-responsive myeloid cells infiltrate into the inflamed small intestine, thereby concealing the effects of GC-resistance of recipient-derived myeloid cells on gene expression.

Our data indicate that genes in the category “cytokines & chemokines” were strongly affected by GC-resistance of allogeneic T cells. It is not surprising that we observed that *Il1b* and *Il6* were up-regulated in mice transplanted with GC-resistant allogeneic T cells due to their inflammatory functions in the disease, as well as that *Il2* and *Il12* were increased due to their critical role in T cell proliferation and differentiation. It has been reported that GM-CSF secreted by Bhlhe40⁺ donor T cells promoted GvHD by recruiting and activating donor dendritic cells in the GI tract (Piper et al., 2020). In agreement, the expression of *Csf2* was increased in mice receiving GC-resistant T cells. Besides, donor T cells become alloactivated in the context of aGvHD; it is thus reasonable that expression levels of *Il4* and *Il10*, two signature cytokines of Th2 cells, increased in mice

developing more severe disease. Furthermore, it is known that GCs inhibit the expression of the majority of cytokines (Cain and Cidlowski, 2017). In addition, various chemokines exert their functions by regulating the migration of effector T cells into target organs of GvHD (Zeiser et al., 2016). For instance, CXCL10 which is induced by IFN- γ becomes strongly expressed after conditioning and is consistently expressed during the development of GvHD (Mapara et al., 2006). In our study, the selected genes encoding chemokines were all up-regulated in mice transferred with GC-resistant allogeneic T cells compared to mice transplanted with GC-responsive allogeneic T cells, reflecting the impact of GCs on modulating chemotaxis of immune cells towards the small intestine, a main target organ of aGvHD.

In our study, genes related to leukocyte surface antigens were also analyzed. Our data reveal that GC-resistance resulted in a changed expression of genes associated with T cells (*Cd28*, *Fasl*), macrophages (*Cd14*, *Chil3*), and NK cells (*Klrk1*), demonstrating that different types of immune cells were affected in the GI tract in GC-resistant aGvHD. In the case of intracellular proteins, myeloid cell-specific genes (*Ptgs2*, *Arg1*) were presumably indirectly affected by GC-resistance in T cells, which is probably due to the severe inflammatory response in mice receiving GC-resistant T cells.

Reprogramming of T-cell metabolism has been widely investigated in recent years. A series of metabolic changes occur during the processes of T-cell activation and differentiation, which are required to meet a rapidly increased need for biosynthesis of many metabolites as well as ATP production (Wahl et al., 2012). It has been reported that alloreactive donor T cells present in GvHD showed increased aerobic glycolysis and oxidative phosphorylation (Gatza et al., 2011). These metabolic changes occurring during GvHD can be fueled by glycolysis and glutamine metabolism. c-Myc is capable of directing the expression of the majority of genes involved in these two metabolic processes (MacIver et al., 2013), and low activity of c-Myc is linked to low aerobic glycolysis in murine GvHD (Kato et al., 2010). However, in our aGvHD mouse model, the expression level of *Myc* was unaffected. The two genes *Glut1* and *Hk2*, which are important in the context of aerobic glycolysis, were significantly up-regulated in the context of GC-resistance in T cells, whereas expression of the glutamine transporters

Slc7a5 and *Slc1a5* was unaltered in our aGvHD mouse model. EER α plays an important role in regulating mitochondrial metabolic pathways and in modulating the expressions of genes associated with mitochondrial energy, such as *Ppargcla* and *Cpt1a* (Giguère, 2008). Nevertheless, the expression of these two genes was unaffected by GC-resistance in T cells. Besides c-Myc, HIF-1 α also boosts glycolysis during activation of immune cells, which can be achieved by activating lactate dehydrogenase (LDH) while inhibiting pyruvate dehydrogenase (PDH) (Kim et al., 2006). Such a metabolic function of HIF-1 α was further confirmed on the gene expression level by our data with *Hif1a* being up-regulated and *Pdhal* being unchanged.

4.2.2 Expression analysis by RNA-sequencing

We additionally performed an unbiased RNA-sequencing analysis and found approximately 500 genes to be differentially expressed in the inflamed small intestine of mice receiving GC-resistant allogeneic T cells in comparison to mice transplanted with GC-responsive allogeneic T cells. Amongst the large number of newly identified genes, we reanalyzed the expression of 26 candidates in either the early or full-blown phase of the disease by high-throughput RT-qPCR. Importantly, our data revealed that the altered gene expression profile was only observed in the full-blown phase of the disease.

Amongst the 26 genes, those related to key effector functions of T cells showed a significantly increased expression due to the GC-resistance of allogeneic T cells, such as *Ifng* and *Gzmb*. Metallothioneins (MTs) are a type of stress-sensors that are linked to immune responses. It has been reported for a DSS-induced colitis mouse model, that MT-deficiency in mice resulted in a decreased severity of colitis, and that administration of an Mt2 monoclonal antibody improved clinical outcome (Devisscher et al., 2014). In our study, *Mt2a* was transcriptionally increased because of the GC-resistance in T cells, suggesting a potential role of this protein in the context of aGvHD as well, thus recommending it as a potential therapeutic target in this disease. The protein encoded by *Orm2* belongs to a family of acute-phase proteins responding to cytokines (Lee et al., 2010), and this gene was also up-regulated in our GC-resistant aGvHD model. Not surprisingly, another chemokine gene, namely *Cxcl2* was found to be transcriptionally

increased in mice transferred with GC-resistant T cells, being in line with the previous observation that a majority of chemokine-related genes showed a similar trend in our gene expression analysis by high-throughput RT-qPCR.

Membrane proteins are a promising drug target due to their accessibility by monoclonal antibodies and small molecular compounds. It has been shown that transplantation of PD-L1-deficient T cells alleviated aGvHD in mice (Saha et al., 2015). In agreement with this finding, we observed an increase of *Cd274* at the transcriptional level in mice receiving GC-resistant allogeneic T cells. Additionally, GC-resistance in transferred T cells also resulted in an upregulation of several genes associated with T cell function (*Il18r1*, *Il1r1*, *Tnfrsf9*) as well as migration (*Cxcr6*). IL-18 belongs to the IL-1 cytokine family and can be produced by non-hematopoietic cells; its receptor IL-18R1 is highly expressed by intestinal CD4⁺ T cells, thus contributing to chronic inflammatory diseases (Harrison et al., 2015). 4-1BB encoded by *Tnfrsf9* can lead to the expansion of CD8⁺ T cells and enhance their cytotoxic ability (Shuford et al., 1997). Moreover, 4-1BB monoclonal antibodies have been developed and tested in a clinical trial (Ascierto et al., 2010). In another study, it was shown that CXCR6 was highly expressed by liver-infiltrating CD8⁺ T cells and was responsible for GvHD-induced liver inflammation because of its recruitment ability (Sato et al., 2005). Besides genes mainly expressed by immune cells, *Cldn4* was up-regulated in mice transplanted with GC-resistant T cells. This gene encodes a protein belonging to the claudin family, which is the main component of the tight junctions. Additionally, claudins are tightly associated with many intestinal disorders that cause weight loss and diarrhea (Barmeyer et al., 2015). Overall, our data indicate that genes expressed by various types of cells can be potentially targeted in aGvHD, used as a biomarker for its treatment, or even assist with the prognosis of GC-resistant disease, suggesting the massive involvement of different cells in the inflamed small intestine.

Our gene expression data also show that intracellular proteins were involved in mouse aGvHD. However, intracellular proteins are not as convenient as cell membrane antigens for therapeutic targeting, since drug delivery would demand translocation into the cytoplasm. Heme oxygenase-1(HO-1) encoded by *Hmox1* was found to be linked to GCs

and hypoxia (Yamamoto et al., 2019), and elevated expression of HO-1 alleviated aGvHD in both humans and mice (Yu et al., 2016). *Itk* plays an essential role in CD8⁺ T cells, and inhibition of ITK was found to have a curative effect on GvHD (Schutt et al., 2015). *Rgs1* encodes the regulator of G protein, which is the only gene without enzymatic activity in the group of intracellular proteins in our analysis. Previously, it was reported that this gene was involved in guiding T cell trafficking into the gut (Gibbons et al., 2011), indicating that the high expression of *Rgs1* in our model might contribute to further intestinal damage by mediating the infiltration of effector T cells into this target organ. *Slpr1* and *Sphk1*, two genes associated with S1P signaling, were upregulated in our aGvHD mouse model. In an earlier study, treatment with a specific agonist of S1P receptors was capable of controlling the development of aGvHD by reducing the number of macrophages in a target organ of the disease (Cheng et al., 2015). Moreover, it has been shown that S1P1 plays an essential role in modulating the egress of matured T cells from the thymus to peripheral tissues (Allende et al., 2004). Thus, our gene expression data combined with these findings could indicate the upregulation of *Slpr1* and *Sphk1* contributes to the enhanced migration of effector T cells into the inflamed small intestine in our GC-resistant aGvHD mouse model.

In our previous gene expression data, we had discovered that the expression level of three genes (*Slc2a1*, *Hif1a*, *Hk2*) involved in T-cell metabolism, especially glycolysis, were significantly increased in mice receiving GC-resistant T cell. Amongst the 26 genes that were identified by RNA-seq analysis, three other genes closely associated with T-cell metabolic reprogramming, namely *Pfkfb3*, *Ldhd* and *Slc2a3*, were also found to be up-regulated due to the GC-resistance of the transplanted T cells. In the context of GvHD, alloreactive T cells undergo various metabolic changes to promote the development of the disease and to contribute to an aggressive immune response (Wahl et al., 2012). Previous findings suggest that increased glycolysis was required for alloactivated T cells to exert their functions in the initiation and development of aGvHD, and that targeting of the key glycolytic enzyme 6-phosphofructo-2-kinase/fructose-2,6-biphosphatase 3 (PFKFB3) attenuated the severity of GvHD in mice (Nguyen et al., 2016). The increased expression of *Ldhd* was correlated with the upregulation of *Hif1a*, which is required for

the activation of Th17 cells (Dang et al., 2011). Furthermore, lactate dehydrogenase D encoded by *Ldhd* metabolizes D-lactate produced by microorganisms in gut (Ewaschuk et al., 2005). Therefore, we suppose that D-lactate could be utilized as a conditional energy supply for effector function and alloactivation of T cells in the inflamed small intestine. In line with the upregulation of *Glut1* in our previous analysis, the expression of another glucose transporter *Glut3* was also increased, which further demonstrates the critical role of glucose as nutrient fueling glycolysis in the development of aGvHD in mice. Finally, our data show that three genes (*Otc*, *Arg2*, *Aoc1*) involved in the urea cycle and fatty acid along with amino acid metabolism were downregulated in mice transferred with GC-resistant T cells. Since these genes are predominately expressed in intestinal epithelial cells, their reduced mRNA levels could reflect the destruction of this cell type during the development of murine aGvHD. Overall, our data show that GC-resistance of allogeneic T cells in mouse aGvHD alters the expression profile of genes related to glycolysis, especially glucose uptake and other energy sources, indicating that T-cell metabolism plays, at least partially, a role in the therapeutic action of GCs.

In conclusion, our data provide a general overview of genes being differentially expressed in the context of endogenous GC-resistance in mouse aGvHD, suggesting that these genes could be considered as potential biomarkers to predict GC-refractory GvHD or even to be targeted as a therapeutic approach to treat aGvHD. However, the technique we used for gene expression analysis has its limitations. Firstly, we only analyzed gene expression in one target organ, namely the small intestine. Damage in this target organ mainly contributes to the high morbidity and mortality of aGvHD, but inflammation or damage in liver is also a major characteristic of this disease. Therefore, further gene analyses of the inflamed liver are required and a combination of gene expression data in both target organs might more precisely provide information about genes that can serve as therapeutic targets or biomarkers for the prediction of aGvHD. Secondly, since many types of cells exist in inflamed small intestine, particularly in the lamina propria, we have not yet confirmed whether the differentially expressed genes are exclusively expressed by T cells or other cell types, such as intestinal epithelial cells or macrophages. Up to now, we only performed a cell type-specific analysis of a small number of genes identified by

RNA-seq. Thirdly, it is uncertain whether the alterations in gene expression directly contribute to the severe phenotype of aGvHD or whether they are indirectly triggered by inflammation caused by aGvHD, thus only being the result of compensatory mechanisms. To solve this issue, monoclonal antibodies or knock-out mice could be used for specific targeting. To eventually assess the cell-type specificity for each of the identified genes, much more laboratory work is surely needed.

4.3 Glucocorticoids encapsulated in IOH-NPs sustains GvL activity

GvHD is a disease that frequently develops after subjecting patients to allo-HSCT. In this setting, donor allogeneic T cells are the main contributors that lead to a high non-relapse fatality rate. To ensure suitable conditions in patients that will receive donor stem cells, they commonly undergo myeloablative conditionings (Singh and McGuirk, 2016). One disadvantage of these regimens is the limitation that they cannot be used in older patients as shown in clinical trials. Therefore, many non-myeloablative approaches have been developed (Gyurkocza and Sandmaier, 2014). Besides the various conditionings for the eradication of malignant cells, also the existence of the beneficial activity of allogeneic T cells, namely the GvL effects, has been noticed, and numerous studies have aimed at exploiting this beneficial effect to augment GvL activity while suppressing GvHD (Rezvani and Storb, 2008).

GCs being the most widely applied first-line therapy to treat GvHD compromise GvL activity. Hence, the improvement of using GCs to treat GvHD with the GvL effect being preserved is an urgent need. Since GCs are capable of passively diffusing through the cell membrane with equal ability, their application results in an unspecific distribution in the human body. One possible approach to solve this problem is to modify drug delivery of GCs in order to change their uptake efficacy in different tissues or cell types. Henceforth, many drug delivery systems have been developed, and GCs delivered with PEGylated liposomes, polymeric micelles, and as polymer-drug conjugates were shown to have massive potential in the treatment of various inflammatory or autoimmune diseases, such

as rheumatoid arthritis and ulcerative colitis (Lühder and Reichardt, 2017). In contrast, little is known about the tailored drug delivery in the context of aGvHD. In our study, we used a nano-formulation of GCs (BMP-NPs), in which they are encapsulated in inorganic-organic nanoparticles. Previous data revealed that this nano-formulation of GCs was preferentially taken up by macrophages and had a beneficial impact in the treatment of a mouse model of multiple sclerosis (Montes-Cobos et al., 2017). Moreover, IP injection of BMP-NPs was found to lead to the accumulation of the drug in abdominal organs including the small intestine (Kaiser et al., 2020a). Besides, due to the ELVIS mechanism, these nanosized drugs should be preferentially enriched in inflamed tissues (Kopeček, 2013). Our group found that treatment with BMP-NPs in a mouse model of aGvHD reduced the severity of this disease, characterized by alleviated clinical symptoms, less immune cell infiltration and reduced levels of inflammation-related genes expressed locally in small intestine compared to the control group. In this respect, they showed similar therapeutic potency as free GCs (Kaiser et al., 2020b). Based on these findings, we further hypothesized that treatment of mouse aGvHD with BMP-NPs could additionally preserve the GvL activity of GCs. To address this issue, we used a combined aGvHD/GvL mouse model with Bcl₁ cells adaptively transferred into recipient mice.

Our data revealed that mice receiving either of the vehicles PBS and EP-NP died from severe aGvHD, which is consistent with our previous clinical score data. Mice transplanted only with Bcl₁ cells developed a lymphoma from day 22 to 27 after induction. In contrast, treatment with the GC formulations BMZ and BMP-NPs both significantly extended survival. Of note, in this combined aGvHD/GvL model, the survival curve was comparable to that observed in our aGvHD mouse model related to the identical treatments (Kaiser et al., 2020b). We monitored the development of the adaptive Bcl₁ lymphoma by tracking the abundance of lymphoma cells in peripheral blood. Our results indicate that treatment with BMP-NPs delayed lymphomagenesis of Bcl₁, thus, at least partially maintaining GvL activity of the allogeneic T cells. However, it is noteworthy that the overall survival rates after administrations of BMZ and BMP-NPs were similar, which might be explained by the presence of severe aGvHD during the development of the lymphoma, contributing to the overall mortality. Our data also show a

relatively more severe aGvHD in our specific mouse model, causing difficulty in separating non-relapse rate from the overall survival rate. Moreover, the occurrence of lymphomagenesis was mainly unchanged, though the GvL activity was partially retained by the BMP-NPs treatment.

Treatment with GCs compromises the cytotoxic ability of T cells that is required to eliminate residual malignant cells. We hypothesized that the nanosized formulation of GCs does not compromise the cytolytic ability of CD8⁺ T cells in the context of mouse aGvHD as it is the case for the free drug. To test this hypothesis, we induced aGvHD in mice and treated them with free GCs or BMP-NPs for a short time. CD8⁺ T cells were purified from mouse spleen at the full-blown first phase of the disease and further used for a ⁵¹chromium release assay. Our data show that the treatment with BMZ or BMP-NPs both reduced the cytolytic ability of CD8⁺ T cells compared to those isolated from mice treated with PBS. Furthermore, at a relatively low ratio of effector to target cells, the two formulations of GCs had a comparable impact on cytolytic ability. In contrast, it is reasonable to reckon that CD8⁺ T cells treated with BMP-NPs have stronger cytotoxicity than the cells treated with free GCs in the setting of a higher ratio of effector to target cells. Unfortunately, analysis at a high ratio was limited by the number of CD8⁺ T cells that could be isolated from spleen in our experiments. Since the cells were purified at the first full-blown phase of the disease, a large number of effector cells migrate from secondary lymphoid organs into the target organs, such as small intestine or liver in the context of aGvHD. Thus, we suppose that fewer CD8⁺ T cells remain in spleen at the full-blown first phase of the disease, which was also in line with our gene expression analysis, showing a majority of chemokines and genes involved in cell migration were up-regulated. Therefore, a further study might focus on investigating the cytolytic ability of cells in the target organs, or testing the cytotoxicity of CD8⁺ T cells after being treated with different formulations of GCs *in vitro*.

5. References

- Allende, M.L., Dreier, J.L., Mandala, S., and Proia, R.L. (2004). Expression of the Sphingosine 1-Phosphate Receptor, S1P 1 , on T-cells Controls Thymic Emigration. *J. Biol. Chem.* 279, 15396–15401.
- Appelbaum F.R. (2001). Haematopoietic cell transplantation as immunotherapy. *Nature* 411, 385–389.
- Ascierto, P.A., Simeone, E., Sznol, M., Fu, Y.-X., and Melero, I. (2010). Clinical Experiences With Anti-CD137 and Anti-PD1 Therapeutic Antibodies. *Semin. Oncol.* 37, 508–516.
- Baake, T., Jörß, K., Suennemann, J., Roßmann, L., Bohnenberger, H., Tuckermann, J.P., Reichardt, H.M., Fischer, H.J., and Reichardt, S.D. (2018). The glucocorticoid receptor in recipient cells keeps cytokine secretion in acute graft-versus-host disease at bay. *Oncotarget* 9, 15437–15450.
- Barmeyer, C., Schulzke, J.D., and Fromm, M. (2015). Claudin-related intestinal diseases. *Semin. Cell Dev. Biol.* 42, 30–38.
- Barnes, D.W.H., Corp, M.J., Loutit, J.F., and Neal, F.E. (1956). Treatment of Murine Leukaemia with X Rays and Homologous Bone Marrow. *BMJ* 2, 626–627.
- Baschant, U., Frappart, L., Rauchhaus, U., Bruns, L., Reichardt, H.M., Kamradt, T., Brauer, R., and Tuckermann, J.P. (2011). Glucocorticoid therapy of antigen-induced arthritis depends on the dimerized glucocorticoid receptor in T cells. *Proc. Natl. Acad. Sci.* 108, 19317–19322.
- Bereshchenko, O., Coppo, M., Bruscoli, S., Biagioli, M., Cimino, M., Frammartino, T., Sorcini, D., Venanzi, A., Di Sante, M., and Riccardi, C. (2014). GILZ Promotes Production of Peripherally Induced Treg Cells and Mediates the Crosstalk between Glucocorticoids and TGF- β Signaling. *Cell Rep.* 7, 464–475.
- Blazar, B.R., Murphy, W.J., and Abedi, M. (2012). Advances in graft-versus-host disease biology and therapy. *Nat. Rev. Immunol.* 12, 443–458.
- Boieri, M., Shah, P., Dressel, R., and Inngjerdingen, M. (2016). The Role of Animal

Models in the Study of Hematopoietic Stem Cell Transplantation and GvHD: A Historical Overview. *Front. Immunol.* 7.

Boldizsar, F., Talaber, G., Szabo, M., Bartis, D., Palinkas, L., Nemeth, P., and Berki, T. (2010). Emerging pathways of non-genomic glucocorticoid (GC) signalling in T cells. *Immunobiology* 215, 521–526.

Bosurgi, L., Bernink, J.H., Delgado Cuevas, V., Gagliani, N., Joannas, L., Schmid, E.T., Booth, C.J., Ghosh, S., and Rothlin, C. V. (2013). Paradoxical role of the proto-oncogene Axl and Mer receptor tyrosine kinases in colon cancer. *Proc. Natl. Acad. Sci.* 110, 13091–13096.

Bouazzaoui, A., Spacenko, E., Mueller, G., Huber, E., Schubert, T., Holler, E., Andreesen, R., and Hildebrandt, G.C. (2011). Steroid treatment alters adhesion molecule and chemokine expression in experimental acute graft-vs.-host disease of the intestinal tract. *Exp. Hematol.* 39, 238-249.e1.

Braun, M.Y. (1996). Cytotoxic T cells deficient in both functional fas ligand and perforin show residual cytolytic activity yet lose their capacity to induce lethal acute graft-versus-host disease. *J. Exp. Med.* 183, 657–661.

Breuner, C., and Orchinik, M. (2002). Plasma binding proteins as mediators of corticosteroid action in vertebrates. *J. Endocrinol.* 175, 99–112.

Van den Brink, M.R.M., and Burakoff, S.J. (2002). Cytolytic pathways in haematopoietic stem-cell transplantation. *Nat. Rev. Immunol.* 2, 273–281.

Buck, M.D., O’Sullivan, D., and Pearce, E.L. (2015). T cell metabolism drives immunity. *J. Exp. Med.* 212, 1345–1360.

Cain, D.W., and Cidlowski, J.A. (2017). Immune regulation by glucocorticoids. *Nat. Rev. Immunol.* 17, 233–247.

Chamorro, S., García-Vallejo, J.J., Unger, W.W.J., Fernandes, R.J., Bruijns, S.C.M., Laban, S., Roep, B.O., ’t Hart, B.A., and van Kooyk, Y. (2009). TLR Triggering on Tolerogenic Dendritic Cells Results in TLR2 Up-Regulation and a Reduced Proinflammatory Immune Program. *J. Immunol.* 183, 2984–2994.

-
- Champlin, R., Ho, W., Gajewski, J., Feig, S., Burnison, M., Holley, G., Greenberg, P., Lee, K., Schmid, I., and Giorgi, J. (1990). Selective depletion of CD8⁺ T lymphocytes for prevention of graft-versus-host disease after allogeneic bone marrow transplantation. *Blood* *76*, 418–423.
- Chen, W., Jin, W., Hardegen, N., Lei, K., Li, L., Marinos, N., McGrady, G., and Wahl, S.M. (2003). Conversion of Peripheral CD4⁺CD25⁻ Naive T Cells to CD4⁺CD25⁺ Regulatory T Cells by TGF- β Induction of Transcription Factor Foxp3. *J. Exp. Med.* *198*, 1875–1886.
- Chen, X., Das, R., Komorowski, R., Beres, A., Hessner, M.J., Mihara, M., and Drobyski, W.R. (2009). Blockade of interleukin-6 signaling augments regulatory T-cell reconstitution and attenuates the severity of graft-versus-host disease. *Blood* *114*, 891–900.
- Cheng, Q., Ma, S., Lin, D., Mei, Y., Gong, H., Lei, L., Chen, Y., Zhao, Y., Hu, B., Wu, Y., et al. (2015). The S1P1 receptor-selective agonist CYM-5442 reduces the severity of acute GVHD by inhibiting macrophage recruitment. *Cell. Mol. Immunol.* *12*, 681–691.
- Cohen, J.L., Trenado, A., Vasey, D., Klatzmann, D., and Salomon, B.L. (2002). CD4⁺CD25⁺ Immunoregulatory T Cells: new therapeutic for graft-versus-host disease. *J. Exp. Med.* *196*, 401–406.
- Collins, N.H., and Fernández, J.M. (1994). T-Cell Depletion and Manipulation in Allogeneic Hematopoietic Cell Transplantation. *Immunomethods* *5*, 189–196.
- Copelan, E.A. (2006). Hematopoietic Stem-Cell Transplantation. *N. Engl. J. Med.* *354*, 1813–1826.
- D’Souza, A., and Fretham, C. (2018). Current Uses and Outcomes of Hematopoietic Cell Transplantation (HCT): CIBMTR Summary Slides. Available at <https://www.cibmtr.org>.
- Dang, E. V., Barbi, J., Yang, H.-Y., Jinasena, D., Yu, H., Zheng, Y., Bordman, Z., Fu, J., Kim, Y., Yen, H.-R., et al. (2011). Control of TH17/Treg Balance by Hypoxia-Inducible Factor 1. *Cell* *146*, 772–784.
- Deeg, H.J. (2007). How I treat refractory acute GVHD. *Blood* *109*, 4119–4126.

- Devisscher, L., Hindryckx, P., Lynes, M.A., Waeytens, A., Cuvelier, C., Vos, F. De, Vanhove, C., Vos, M. De, and Laukens, D. (2014). Role of metallothioneins as danger signals in the pathogenesis of colitis. *J. Pathol.* 233, 89–100.
- Diamond, M., Miner, J., Yoshinaga, S., and Yamamoto, K. (1990). Transcription factor interactions: selectors of positive or negative regulation from a single DNA element. *Science* (80-.). 249, 1266–1272.
- Dorshkind, K., Höfer, T., Montecino-Rodriguez, E., Pioli, P.D., and Rodewald, H.-R. (2019). Do haematopoietic stem cells age? *Nat. Rev. Immunol.*
- Dunn, A.J. (2000). Cytokine activation of the HPA axis. *Ann. N. Y. Acad. Sci.* 917, 608–617.
- Dutt, S., Ermann, J., Tseng, D., Liu, Y.P., George, T.I., Fathman, C.G., and Strober, S. (2005). L-selectin and $\beta 7$ integrin on donor CD4 T cells are required for the early migration to host mesenteric lymph nodes and acute colitis of graft-versus-host disease. *Blood* 106, 4009–4015.
- Elenkov, I.J. (2004). Glucocorticoids and the Th1/Th2 balance. *Ann. N. Y. Acad. Sci.* 1024, 138–146.
- Ewaschuk, J.B., Naylor, J.M., and Zello, G.A. (2005). D-Lactate in Human and Ruminant Metabolism. *J. Nutr.* 135, 1619–1625.
- Ferrara, J.L., Levine, J.E., Reddy, P., and Holler, E. (2009). Graft-versus-host disease. *Lancet* 373, 1550–1561.
- Galon, J., Franchimont, D., Hiroi, N., Frey, G., Boettner, A., Ehrhart-Bornstein, M., O’Shea, J.J., Chrousos, G.P., and Bornstein, S.R. (2002). Gene profiling reveals unknown enhancing and suppressive actions of glucocorticoids on immune cells. *FASEB J.* 16, 61–71.
- Garnett, C., Apperley, J.F., and Pavlů, J. (2013). Treatment and management of graft-versus -host disease: improving response and survival. *Ther. Adv. Hematol.* 4, 366–378.
- Gatza, E., Wahl, D.R., Opipari, A.W., Sundberg, T.B., Reddy, P., Liu, C., Glick, G.D., and Ferrara, J.L.M. (2011). Manipulating the Bioenergetics of Alloreactive T Cells

Causes Their Selective Apoptosis and Arrests Graft-Versus-Host Disease. *Sci. Transl. Med.* 3, 67ra8-67ra8.

Gibbons, D.L., Abeler-Dörner, L., Raine, T., Hwang, I.-Y., Jandke, A., Wencker, M., Deban, L., Rudd, C.E., Irving, P.M., Kehrl, J.H., et al. (2011). Cutting Edge: Regulator of G Protein Signaling-1 Selectively Regulates Gut T Cell Trafficking and Colitic Potential. *J. Immunol.* 187, 2067–2071.

Giguère, V. (2008). Transcriptional Control of Energy Homeostasis by the Estrogen-Related Receptors. *Endocr. Rev.* 29, 677–696.

Glucksberg, H., Storb, R., Fefer, A., Buckner, C.D., Neiman, P.E., Clift, R.A., Lerner, K.G., and Thomas, E.D. (1974). Clinical manifestations of graft-versus-host disease in human recipients of marrow from HL-A-matched sibling donors. *Transplantation* 18, 295–304.

Graubert, T.A., DiPersio, J.F., Russell, J.H., and Ley, T.J. (1997). Perforin/granzyme-dependent and independent mechanisms are both important for the development of graft-versus-host disease after murine bone marrow transplantation. *J. Clin. Invest.*

Gyurkocza, B., and Sandmaier, B.M. (2014). Conditioning regimens for hematopoietic cell transplantation: one size does not fit all. *Blood* 124, 344–353.

Hanash, A.M., Dudakov, J.A., Hua, G., O'Connor, M.H., Young, L.F., Singer, N. V., West, M.L., Jenq, R.R., Holland, A.M., Kappel, L.W., et al. (2012). Interleukin-22 Protects Intestinal Stem Cells from Immune-Mediated Tissue Damage and Regulates Sensitivity to Graft versus Host Disease. *Immunity* 37, 339–350.

Haniffa, M., Ginhoux, F., Wang, X.-N., Bigley, V., Abel, M., Dimmick, I., Bullock, S., Grisotto, M., Booth, T., Taub, P., et al. (2009). Differential rates of replacement of human dermal dendritic cells and macrophages during hematopoietic stem cell transplantation. *J. Exp. Med.* 206, 371–385.

Harrison, O.J., Srinivasan, N., Pott, J., Schiering, C., Krausgruber, T., Ilott, N.E., and Maloy, K.J. (2015). Epithelial-derived IL-18 regulates Th17 cell differentiation and Foxp3⁺ Treg cell function in the intestine. *Mucosal Immunol.* 8, 1226–1236.

Heck, J.G., Napp, J., Simonato, S., Möllmer, J., Lange, M., Reichardt, H.M., Staudt, R.,

-
- Alves, F., and Feldmann, C. (2015). Multifunctional Phosphate-Based Inorganic–Organic Hybrid Nanoparticles. *J. Am. Chem. Soc.* *137*, 7329–7336.
- Hiemenz, J.W. (2009). Management of Infections Complicating Allogeneic Hematopoietic Stem Cell Transplantation. *Semin. Hematol.* *46*, 289–312.
- Hill, G.R., and Ferrara, J.L.M. (2000). The primacy of the gastrointestinal tract as a target organ of acute graft-versus-host disease: rationale for the use of cytokine shields in allogeneic bone marrow transplantation. *Blood* *95*, 2754–2759.
- Hill, G.R., Crawford, J.M., Cooke, K.R., Brinson, Y.S., Pan, L., and Ferrara, J.L.M. (1997). Total body irradiation and acute graft-versus-host disease: The role of gastrointestinal damage and inflammatory cytokines. *Blood* *90*, 3204–3213.
- Ho, V.T., and Soiffer, R.J. (2001). The history and future of T-cell depletion as graft-versus-host disease prophylaxis for allogeneic hematopoietic stem cell transplantation. *Blood* *98*, 3192–3204.
- Hoffmann, P., Ermann, J., Edinger, M., Fathman, C.G., and Strober, S. (2002). Donor-type CD4+CD25+ Regulatory T Cells Suppress Lethal Acute Graft-Versus-Host Disease after Allogeneic Bone Marrow Transplantation. *J. Exp. Med.* *196*, 389–399.
- Holtan, S.G., Pasquini, M., and Weisdorf, D.J. (2014). Acute graft-versus-host disease: a bench-to-bedside update. *Blood* *124*, 363–373.
- van den Hoven, J.M., Nemes, R., Metselaar, J.M., Nuijen, B., Beijnen, J.H., Storm, G., and Szebeni, J. (2013). Complement activation by PEGylated liposomes containing prednisolone. *Eur. J. Pharm. Sci.* *49*, 265–271.
- Ivashkiv, L.B. (2018). IFN γ : signalling, epigenetics and roles in immunity, metabolism, disease and cancer immunotherapy. *Nat. Rev. Immunol.* *18*, 545–558.
- Jenq, R.R., and van den Brink, M.R.M. (2010). Allogeneic haematopoietic stem cell transplantation: individualized stem cell and immune therapy of cancer. *Nat. Rev. Cancer* *10*, 213–221.
- Jhaveri, A.M., and Torchilin, V.P. (2014). Multifunctional polymeric micelles for delivery of drugs and siRNA. *Front. Pharmacol.* *5*.

Kaiser, T.K., Khorenko, M., Moussavi, A., Engelke, M., Boretius, S., Feldmann, C., and Reichardt, H.M. (2020a). Highly selective organ distribution and cellular uptake of inorganic-organic hybrid nanoparticles customized for the targeted delivery of glucocorticoids. *J. Control. Release* 319, 360–370.

Kaiser, T.K., Li, H., Roßmann, L., Reichardt, S.D., Bohnenberger, H., Feldmann, C., and Reichardt, H.M. (2020b). Glucocorticoids delivered by inorganic-organic hybrid nanoparticles mitigate acute graft-versus-host disease and sustain graft-versus-leukemia activity. *Eur. J. Immunol.*, DOI: 10.1002/eji.201948464.

Kato, K., Cui, S., Kuick, R., Mineishi, S., Hexner, E., Ferrara, J.L.M., Emerson, S.G., and Zhang, Y. (2010). Identification of Stem Cell Transcriptional Programs Normally Expressed in Embryonic and Neural Stem Cells in Alloreactive CD8+ T Cells Mediating Graft-versus-Host Disease. *Biol. Blood Marrow Transplant.* 16, 751–771.

Khouri, I.F., McLaughlin, P., Saliba, R.M., Hosing, C., Korbling, M., Lee, M.S., Medeiros, L.J., Fayad, L., Samaniego, F., Alousi, A., et al. (2008). Eight-year experience with allogeneic stem cell transplantation for relapsed follicular lymphoma after nonmyeloablative conditioning with fludarabine, cyclophosphamide, and rituximab. *Blood* 111, 5530–5536.

Kim, J., Tchernyshyov, I., Semenza, G.L., and Dang, C. V. (2006). HIF-1-mediated expression of pyruvate dehydrogenase kinase: A metabolic switch required for cellular adaptation to hypoxia. *Cell Metab.* 3, 177–185.

Kolb, H.-J. (2008). Graft-versus-leukemia effects of transplantation and donor lymphocytes. *Blood* 112, 4371–4383.

Kolb, H., Mittermuller, J., Clemm, C., Holler, E., Ledderose, G., Brehm, G., Heim, M., and Wilmanns, W. (1990). Donor leukocyte transfusions for treatment of recurrent chronic myelogenous leukemia in marrow transplant patients. *Blood* 76, 2462–2465.

Kopeček, J. (2013). Polymer–drug conjugates: Origins, progress to date and future directions. *Adv. Drug Deliv. Rev.* 65, 49–59.

Korbling, M., Fliedner, T.M., Calvo, W., Ross, W.M., Nothdurft, W., and Steinbach, I. (1979). Albumin density gradient purification of canine hemopoietic blood stem cells

- (HBSC): Long-term allogeneic engraftment without GVH-reaction. *Exp. Hematol.*
- Koyama, M., Kuns, R.D., Olver, S.D., Raffelt, N.C., Wilson, Y.A., Don, A.L.J., Lineburg, K.E., Cheong, M., Robb, R.J., Markey, K.A., et al. (2012). Recipient nonhematopoietic antigen-presenting cells are sufficient to induce lethal acute graft-versus-host disease. *Nat. Med.* *18*, 135–142.
- Koyama, M., Mukhopadhyay, P., Schuster, I.S., Henden, A.S., Hülsdünker, J., Varelias, A., Vetizou, M., Kuns, R.D., Robb, R.J., Zhang, P., et al. (2019). MHC Class II Antigen Presentation by the Intestinal Epithelium Initiates Graft-versus-Host Disease and Is Influenced by the Microbiota. *Immunity* 1–14.
- Lammers, T. (2010). Improving the efficacy of combined modality anticancer therapy using HPMA copolymer-based nanomedicine formulations☆. *Adv. Drug Deliv. Rev.* *62*, 203–230.
- Lee, Y.S., Choi, J.W., Hwang, I., Lee, J.W., Lee, J.H., Kim, A.Y., Huh, J.Y., Koh, Y.J., Koh, G.Y., Son, H.J., et al. (2010). Adipocytokine Orosomucoid Integrates Inflammatory and Metabolic Signals to Preserve Energy Homeostasis by Resolving Immoderate Inflammation. *J. Biol. Chem.* *285*, 22174–22185.
- Li, H., Kaiser, T.K., Borschiwer, M., Bohnenberger, H., Reichardt, S.D., Lühder, F., Walter, L., Dressel, R., Meijnsing, S.H., and Reichardt, H.M. (2019). Glucocorticoid resistance of allogeneic T cells alters the gene expression profile in the inflamed small intestine of mice suffering from acute graft-versus-host disease. *J. Steroid Biochem. Mol. Biol.* *195*, 105485.
- Li Pira, G., Di Cecca, S., Montanari, M., Moretta, L., and Manca, F. (2016). Specific removal of alloreactive T-cells to prevent GvHD in hemopoietic stem cell transplantation: rationale, strategies and perspectives. *Blood Rev.* *30*, 297–307.
- Liberman, A.C., Refojo, D., Druker, J., Toscano, M., Rein, T., Holsboer, F., and Arzt, E. (2007). The activated glucocorticoid receptor inhibits the transcription factor T-bet by direct protein-protein interaction. *FASEB J.* *21*, 1177–1188.
- Lindemans, C.A., Calafiore, M., Mertelsmann, A.M., O'Connor, M.H., Dudakov, J.A., Jenq, R.R., Velardi, E., Young, L.F., Smith, O.M., Lawrence, G., et al. (2015).

Interleukin-22 promotes intestinal-stem-cell-mediated epithelial regeneration. *Nature* 528, 560–564.

Ljungman, P., Bregni, M., Brune, M., Cornelissen, J., Witte, T. De, Dini, G., Einsele, H., Gaspar, H.B., Gratwohl, A., Passweg, J., et al. (2010). Allogeneic and autologous transplantation for haematological diseases, solid tumours and immune disorders: current practice in Europe 2009. *Bone Marrow Transplant.* 45, 219–234.

Löwenberg, M., Verhaar, A.P., van den Brink, G.R., and Hommes, D.W. (2007). Glucocorticoid signaling: a nongenomic mechanism for T-cell immunosuppression. *Trends Mol. Med.* 13, 158–163.

Lühder, F., and Reichardt, H. (2017). Novel Drug Delivery Systems Tailored for Improved Administration of Glucocorticoids. *Int. J. Mol. Sci.* 18, 1836.

MacIver, N.J., Michalek, R.D., and Rathmell, J.C. (2013). Metabolic Regulation of T Lymphocytes. *Annu. Rev. Immunol.* 31, 259–283.

Maeda, H., Sawa, T., and Konno, T. (2001). Mechanism of tumor-targeted delivery of macromolecular drugs, including the EPR effect in solid tumor and clinical overview of the prototype polymeric drug SMANCS. *J. Control. Release* 74, 47–61.

Major-Monfried, H., Renteria, A.S., Pawarode, A., Reddy, P., Ayuk, F., Holler, E., Efebera, Y.A., Hogan, W.J., Wöfl, M., Qayed, M., et al. (2018). MAGIC biomarkers predict long-term outcomes for steroid-resistant acute GVHD. *Blood* 131, 2846–2855.

Mapara, M.Y., Leng, C., Kim, Y.-M., Bronson, R., Lokshin, A., Luster, A., and Sykes, M. (2006). Expression of Chemokines in GVHD Target Organs Is Influenced by Conditioning and Genetic Factors and Amplified by GVHR. *Biol. Blood Marrow Transplant.* 12, 623–634.

Martin, P., Schoch, G., Fisher, L., Byers, V., Appelbaum, F., McDonald, G., Storb, R., and Hansen, J. (1991). A retrospective analysis of therapy for acute graft-versus-host disease: secondary treatment. *Blood* 77, 1821–1828.

Martinez, F.O. (2008). Macrophage activation and polarization. *Front. Biosci.* 13, 453.

McDonald, G.B., Tabellini, L., Storer, B.E., Martin, P.J., Lawler, R.L., Rosinski, S.L.,

-
- Schoch, H.G., and Hansen, J.A. (2017). Predictive Value of Clinical Findings and Plasma Biomarkers after Fourteen Days of Prednisone Treatment for Acute Graft-versus-host Disease. *Biol. Blood Marrow Transplant.* 23, 1257–1263.
- McSweeney, P.A., Niederwieser, D., Shizuru, J.A., Sandmaier, B.M., Molina, A.J., Maloney, D.G., Chauncey, T.R., Gooley, T.A., Hegenbart, U., Nash, R.A., et al. (2001). Hematopoietic cell transplantation in older patients with hematologic malignancies: Replacing high-dose cytotoxic therapy with graft-versus-tumor effects. *Blood.*
- Montes-Cobos, E., Ring, S., Fischer, H.J., Heck, J., Strauß, J., Schwaninger, M., Reichardt, S.D., Feldmann, C., Lühder, F., and Reichardt, H.M. (2017). Targeted delivery of glucocorticoids to macrophages in a mouse model of multiple sclerosis using inorganic-organic hybrid nanoparticles. *J. Control. Release* 245, 157–169.
- Moser, M., De Smedt, T., Sornasse, T., Tielemans, F., Chentoufi, A.A., Muraille, E., Van Mechelen, M., Urbain, J., and Leo, O. (1995). Glucocorticoids down-regulate dendritic cell function in vitro and in vivo. *Eur. J. Immunol.* 25, 2818–2824.
- Negrin, R.S. (2015). Graft-versus-host disease versus graft-versus-leukemia. *Hematology* 2015, 225–230.
- Nguyen, H.D., Chatterjee, S., Haarberg, K.M.K., Wu, Y., Bastian, D., Heinrichs, J., Fu, J., Daenthansanmak, A., Schutt, S., Shrestha, S., et al. (2016). Metabolic reprogramming of alloantigen-activated T cells after hematopoietic cell transplantation. *J. Clin. Invest.* 126, 1337–1352.
- Ni, X., Song, Q., Cassady, K., Deng, R., Jin, H., Zhang, M., Dong, H., Forman, S., Martin, P.J., Chen, Y.Z., et al. (2017). PD-L1 interacts with CD80 to regulate graft-versus-leukemia activity of donor CD8 + T cells. *J. Clin. Invest.* 127, 1960–1977.
- O’Sullivan, D., and Pearce, E.L. (2015). Targeting T cell metabolism for therapy. *Trends Immunol.* 36, 71–80.
- Palmer, L.A., Sale, G.E., Balogun, J.I., Li, D., Jones, D., Molldrem, J.J., Storb, R.F., and Ma, Q. (2010). Chemokine Receptor CCR5 Mediates AlloImmune Responses in Graft-versus-Host Disease. *Biol. Blood Marrow Transplant.*
- Perkey, E., and Maillard, I. (2018). New Insights into Graft-Versus-Host Disease and

- Graft Rejection. *Annu. Rev. Pathol. Mech. Dis.* 13, 219–245.
- Petrillo, M.G. razi., Fettucciari, K., Montuschi, P., Ronchetti, S., Cari, L., Migliorati, G., Mazzon, E., Bereshchenko, O., Bruscoli, S., Nocentini, G., et al. (2014). Transcriptional regulation of kinases downstream of the T cell receptor: another immunomodulatory mechanism of glucocorticoids. *BMC Pharmacol. Toxicol.* 15, 35.
- Piper, C., Zhou, V., Komorowski, R., Szabo, A., Vincent, B., Serody, J., Alegre, M.-L., Edelson, B.T., Taneja, R., and Drobyski, W.R. (2020). Pathogenic Bhlhe40+ GM-CSF+ CD4+ T cells promote indirect alloantigen presentation in the GI tract during GVHD. *Blood* 135, 568–581.
- Przepiorka, D., Luo, L., Subramaniam, S., Qiu, J., Gudi, R., Cunningham, L.C., Nie, L., Leong, R., Ma, L., Sheth, C., et al. (2020). FDA Approval Summary: Ruxolitinib for Treatment of Steroid-Refractory Acute Graft-Versus-Host Disease. *Oncologist* 25, theoncologist.2019-0627.
- Ramamoorthy, S., and Cidlowski, J.A. (2016). Corticosteroids. Mechanisms of Action in Health and Disease. *Rheum. Dis. Clin. North Am.*
- Ramírez, F., Fowell, D.J., Puklavec, M., Simmonds, S., and Mason, D. (1996). Glucocorticoids promote a TH2 cytokine response by CD4+ T cells in vitro. *J. Immunol.*
- Ratman, D., Vanden Berghe, W., Dejager, L., Libert, C., Tavernier, J., Beck, I.M., and De Bosscher, K. (2013). How glucocorticoid receptors modulate the activity of other transcription factors: A scope beyond tethering. *Mol. Cell. Endocrinol.* 380, 41–54.
- Reichardt, H.M. (2001). Repression of inflammatory responses in the absence of DNA binding by the glucocorticoid receptor. *EMBO J.* 20, 7168–7173.
- Reichardt, H.M., Kaestner, K.H., Tuckermann, J., Kretz, O., Wessely, O., Bock, R., Gass, P., Schmid, W., Herrlich, P., Angel, P., et al. (1998). DNA Binding of the Glucocorticoid Receptor Is Not Essential for Survival. *Cell* 93, 531–541.
- Revankar, C.M. (2005). A Transmembrane Intracellular Estrogen Receptor Mediates Rapid Cell Signaling. *Science (80-.)*. 307, 1625–1630.
- Rezvani, A.R., and Storb, R.F. (2008). Separation of graft-vs.-tumor effects from graft-

- vs.-host disease in allogeneic hematopoietic cell transplantation. *J. Autoimmun.* *30*, 172–179.
- Rhen, T., and Cidlowski, J.A. (2005). Antiinflammatory Action of Glucocorticoids — New Mechanisms for Old Drugs. *N. Engl. J. Med.* *353*, 1711–1723.
- Ringden, O., Labopin, M., Gorin, N.C., Schmitz, N., Schaefer, U.W., Prentice, H.G., Bergmann, L., Jouet, J.P., Mandelli, F., Blaise, D., et al. (2000). Is there a graft-versus-leukaemia effect in the absence of graft-versus-host disease in patients undergoing bone marrow transplantation for acute leukaemia? *Br. J. Haematol.* *111*, 1130–1137.
- Rowlings, P.A., Przepioraka, D., Klein, J.P., Gale, R.P., Passweg, J.R., Henslee-Downey, P.J., Cahn, J.Y., Calderwood, S., Gratwohl, A., Socié, G., et al. (1997). IBMTR Severity Index for grading acute graft-versus-host disease: retrospective comparison with Glucksberg grade. *Br. J. Haematol.* *97*, 855–864.
- Rutella, S., Danese, S., and Leone, G. (2006). Tolerogenic dendritic cells: cytokine modulation comes of age. *Blood* *108*, 1435–1440.
- Ruzicka, B., and Zaccarelli, E. (2011). A fresh look at the Laponite phase diagram. *Soft Matter* *7*, 1268.
- Saccardi, R., and Gualandi, F. (2008). Hematopoietic stem cell transplantation procedures. *Autoimmunity* *41*, 570–576.
- Saha, A., R.S., O., G., T., S.B., L., D.B., D., C.B., W., B.G., V., K., A., P.A., T., A., P.-M., et al. (2015). Loss of programmed death ligand-1 expression on donor T cells lessens acute graft-versus-host disease lethality. *Blood* *126*, 147.
- Sato, T., Thorlacios, H., Johnston, B., Staton, T.L., Xiang, W., Littman, D.R., and Butcher, E.C. (2005). Role for CXCR6 in Recruitment of Activated CD8 + Lymphocytes to Inflamed Liver. *J. Immunol.* *174*, 277–283.
- Schutt, S.D., Fu, J., Nguyen, H., Bastian, D., Heinrichs, J., Wu, Y., Liu, C., McDonald, D.G., Pidala, J., and Yu, X.-Z. (2015). Inhibition of BTK and ITK with Ibrutinib Is Effective in the Prevention of Chronic Graft-versus-Host Disease in Mice. *PLoS One* *10*, e0137641.

- Shlomchik, W.D. (1999). Prevention of Graft Versus Host Disease by Inactivation of Host Antigen-Presenting Cells. *Science* (80-.). 285, 412–415.
- Shono, Y., and van den Brink, M.R.M. (2018). Gut microbiota injury in allogeneic haematopoietic stem cell transplantation. *Nat. Rev. Cancer* 18, 283–295.
- Shono, Y., Docampo, M.D., Peled, J.U., Perobelli, S.M., Velardi, E., Tsai, J.J., Slingerland, A.E., Smith, O.M., Young, L.F., Gupta, J., et al. (2016). Increased GVHD-related mortality with broad-spectrum antibiotic use after allogeneic hematopoietic stem cell transplantation in human patients and mice. *Sci. Transl. Med.* 8, 339ra71-339ra71.
- Shuford, W.W., Klussman, K., Tritchler, D.D., Loo, D.T., Chalupny, J., Siadak, A.W., Brown, T.J., Emswiler, J., Raecho, H., Larsen, C.P., et al. (1997). 4-1BB costimulatory signals preferentially induce CD8+ T cell proliferation and lead to the amplification in vivo of cytotoxic T cell responses. *J. Exp. Med.* 186, 47–55.
- Singh, A.K., and McGuirk, J.P. (2016). Allogeneic Stem Cell Transplantation: A Historical and Scientific Overview. *Cancer Res.* 76, 6445–6451.
- Sionov, R.V., Cohen, O., Kfir, S., Zilberman, Y., and Yefenof, E. (2006). Role of mitochondrial glucocorticoid receptor in glucocorticoid-induced apoptosis. *J. Exp. Med.* 203, 189–201.
- Stathopoulou, C., Gangaplara, A., Mallett, G., Flomerfelt, F.A., Liniany, L.P., Knight, D., Samsel, L.A., Berlinguer-Palmini, R., Yim, J.J., Felizardo, T.C., et al. (2018). PD-1 Inhibitory Receptor Downregulates Asparaginyl Endopeptidase and Maintains Foxp3 Transcription Factor Stability in Induced Regulatory T Cells. *Immunity* 1–17.
- Stein-Thoeringer, C.K., Nichols, K.B., Lazrak, A., Docampo, M.D., Slingerland, A.E., Slingerland, J.B., Clurman, A.G., Armijo, G., Gomes, A.L.C., Shono, Y., et al. (2019). Lactose drives *Enterococcus* expansion to promote graft-versus-host disease. *Science* (80-.). 366, 1143–1149.
- Storb, R., Prentice, R.L., Buckner, C.D., Clift, R.A., Appelbaum, F., Deeg, J., Doney, K., Hansen, J.A., Mason, M., Sanders, J.E., et al. (1983). Graft-versus-Host Disease and Survival in Patients with Aplastic Anemia Treated by Marrow Grafts from HLA-Identical Siblings: Beneficial Effect of a Protective Environment. *N. Engl. J. Med.*

- Sung, A.D., and Chao, N.J. (2013). Concise Review: Acute Graft-Versus-Host Disease: Immunobiology, Prevention, and Treatment. *Stem Cells Transl. Med.* 2, 25–32.
- Swimm, A., Giver, C.R., DeFilipp, Z., Rangaraju, S., Sharma, A., Ulezko Antonova, A., Sonowal, R., Capaldo, C., Powell, D., Qayed, M., et al. (2018). Indoles derived from intestinal microbiota act via type I interferon signaling to limit graft-versus-host disease. *Blood* 132, 2506–2519.
- Sykes, M., and Nikolic, B. (2005). Treatment of severe autoimmune disease by stem-cell transplantation. *Nature* 435, 620–627.
- Theiss-Suennemann, J., Jörß, K., Messmann, J.J., Reichardt, S.D., Montes-Cobos, E., Lühder, F., Tuckermann, J.P., AWolff, H., Dressel, R., Gröne, H.-J., et al. (2015). Glucocorticoids attenuate acute graft-versus-host disease by suppressing the cytotoxic capacity of CD8 + T cells. *J. Pathol.* 235, 646–655.
- Thomas, E.D., Lochte, H.L., Lu, W.C., and Ferrebee, J.W. (1957). Intravenous Infusion of Bone Marrow in Patients Receiving Radiation and Chemotherapy. *N. Engl. J. Med.* 257, 491–496.
- Tuckermann, J.P., Reichardt, H.M., Arribas, R., Richter, K.H., Schütz, G., and Angel, P. (1999). The DNA Binding-Independent Function of the Glucocorticoid Receptor Mediates Repression of Ap-1–Dependent Genes in Skin. *J. Cell Biol.* 147, 1365–1370.
- Tuckermann, J.P., Kleiman, A., McPherson, K.G., and Reichardt, H.M. (2005). Molecular mechanisms of glucocorticoids in the control of inflammation and lymphocyte apoptosis. *Crit. Rev. Clin. Lab. Sci.* 42, 71–104.
- Tuckermann, J.P., Kleiman, A., Moriggl, R., Spanbroek, R., Neumann, A., Illing, A., Clausen, B.E., Stride, B., Förster, I., Habenicht, A.J.R., et al. (2007). Macrophages and neutrophils are the targets for immune suppression by glucocorticoids in contact allergy. *J. Clin. Invest.* 117, 1381–1390.
- Utsunomiya, A. (2019). Progress in Allogeneic Hematopoietic Cell Transplantation in Adult T-Cell Leukemia-Lymphoma. *Front. Microbiol.* 10, 1–16.
- Vaishnava, S., Yamamoto, M., Severson, K.M., Ruhn, K.A., Yu, X., Koren, O., Ley, R., Wakeland, E.K., and Hooper, L. V. (2011). The Antibacterial Lectin RegIII Promotes the

- Spatial Segregation of Microbiota and Host in the Intestine. *Science* (80-.). 334, 255–258.
- Vandevyver, S., Dejager, L., Tuckermann, J., and Libert, C. (2013). New Insights into the Anti-inflammatory Mechanisms of Glucocorticoids: An Emerging Role for Glucocorticoid-Receptor-Mediated Transactivation. *Endocrinology* 154, 993–1007.
- Varga, G., Ehrchen, J., Tsianakas, A., Tenbrock, K., Rattenholl, A., Seeliger, S., Mack, M., Roth, J., and Sunderkoetter, C. (2008). Glucocorticoids induce an activated, anti-inflammatory monocyte subset in mice that resembles myeloid-derived suppressor cells. *J. Leukoc. Biol.* 84, 644–650.
- Wagner, J., Steinbuch, M., Kernan, N., Broxmayer, H., and Gluckman, E. (1995). Allogeneic sibling umbilical-cord-blood transplantation in children with malignant and non-malignant disease. *Lancet* 346, 214–219.
- Wahl, D.R., Byersdorfer, C.A., Ferrara, J.L.M., Jr, A.W.O., and Glick, G.D. (2012). Distinct metabolic programs in activated T cells: opportunities for selective immunomodulation. 249, 104–115.
- Wang, H., Asavaroengchai, W., Yong Yeap, B., Wang, M.-G., Wang, S., Sykes, M., and Yang, Y.-G. (2009). Paradoxical effects of IFN- γ in graft-versus-host disease reflect promotion of lymphohematopoietic graft-versus-host reactions and inhibition of epithelial tissue injury. *Blood* 113, 3612–3619.
- Warnke, R.A., Slavin, S., Coffman, R.L., Butcher, E.C., Knapp, M.R., Strober, S., and Weissman, I.L. (1979). The pathology and homing of a transplantable murine B cell leukemia (BCL 1). *J. Immunol.*
- Webster, J.C., Oakley, R.H., Jewell, C.M., and Cidlowski, J.A. (2001). Proinflammatory cytokines regulate human glucocorticoid receptor gene expression and lead to the accumulation of the dominant negative isoform: A mechanism for the generation of glucocorticoid resistance. *Proc. Natl. Acad. Sci.* 98, 6865–6870.
- Weiden, P.L., Flournoy, N., Thomas, E.D., Prentice, R., Fefer, A., Buckner, C.D., and Storb, R. (1979). Antileukemic Effect of Graft-versus-Host Disease in Human Recipients of Allogeneic-Marrow Grafts. *N. Engl. J. Med.*
- Wüst, S., van den Brandt, J., Tischner, D., Kleiman, A., Tuckermann, J.P., Gold, R.,

Lühder, F., and Reichardt, H.M. (2008). Peripheral T Cells Are the Therapeutic Targets of Glucocorticoids in Experimental Autoimmune Encephalomyelitis. *J. Immunol.* *180*, 8434–8443.

Yamamoto, H., Saito, M., Goto, T., Ueshima, K., Ishida, M., Hayashi, S., Ikoma, K., Mazda, O., and Kubo, T. (2019). Heme oxygenase-1 prevents glucocorticoid and hypoxia-induced apoptosis and necrosis of osteocyte-like cells. *Med. Mol. Morphol.* *52*, 173–180.

Yang, S., and Zhang, L. (2004). Glucocorticoids and Vascular Reactivity. *Curr. Vasc. Pharmacol.* *2*, 1–12.

Yi, T., Chen, Y., Wang, L., Du, G., Huang, D., Zhao, D., Johnston, H., Young, J., Todorov, I., Umetsu, D.T., et al. (2009). Reciprocal differentiation and tissue-specific pathogenesis of Th1, Th2, and Th17 cells in graft-versus-host disease. *Blood*.

Yu, M., Wang, J., Fang, Q., Liu, P., Chen, S., Zhe, N., Lin, X., Zhang, Y., Zhao, J., and Zhou, Z. (2016). High expression of heme oxygenase-1 in target organs may attenuate acute graft-versus-host disease through regulation of immune balance of TH17/Treg. *Transpl. Immunol.* *37*, 10–17.

Zeiser, R., and Blazar, B.R. (2017). Acute Graft-versus-Host Disease — Biologic Process, Prevention, and Therapy. *N. Engl. J. Med.* *377*, 2167–2179.

Zeiser, R., Socié, G., and Blazar, B.R. (2016). Pathogenesis of acute graft-versus-host disease: from intestinal microbiota alterations to donor T cell activation. *Br. J. Haematol.* *175*, 191–207.

6. Appendix

6.1 Acknowledgements

First I would like to thank my supervisor Prof. Dr. Holger Reichardt for giving me the opportunity to finish my thesis in our laboratory and his guidance, patience and always being supportive during my Ph.D. study. His scientific thoughts and ways of conceiving a trial and analyzing experimental data have greatly inspired me.

I also would like to express my thanks to my thesis committee members: Prof. Dr. Lutz Walter and Prof. Dr. Ralf Dressel for their scientific suggestions and advice proposed at the thesis academy meetings and their interest in my project. Many thanks go to Prof. Dr. Lutz Walter for providing methods and a platform for me to carry out the gene CHIP analysis and Prof. Dr. Ralf Dressel for helping me with cytotoxic ability analysis, Dr. Bohnenberger for histological analysis as well. Also thank Nico, Leslie, and Jennifer for their excellent technical support.

I would like to thank Sybille and Amina. They give me much much assistance not only in my scientific but also daily life; they are always being very kind and help me go through stressful and tough days in the lab. Many thanks go to my lovely colleagues, Tina, Elena, Norika, Eric, Chiara, and Agathe. Working and sharing with you guys make scientific life so wonderful and enjoyable. I would also like to thank the rest of the Department of Cellular and Molecular Immunology for their kind help.

In the end, I want to thank my family and all my friends for their support and for always getting my back during my four years in Göttingen.